COSMOLOGY IN MODIFIED GRAVITIES WITH HOLOGRAPHIC CUTOFFS

AMORNTHEP TITA

A Dissertation Submitted to Graduate School of Naresuan University
in Partial Fulfillment of the Requirements
for the Doctor of Philosophy Degree in Theoretical Physics
March 2025

Dissertation entitled "Cosmology in modified gravities with holographic cutoffs"
by Amornthep Tita
has been approved by the Graduate School as partial fulfillment of
the requirement for the Doctor of Philosophy in Theoretical Physics of
Naresuan University

Oral Defense Committee

Piyabut Burikham ..... Chair

(Associate Professor Piyabut Burikham, Ph.D.)

Pornrad Srisawad ..... Advisor

(Associate Professor Pornrad Srisawad, Ph.D.)

Burin Gumjudpai ..... Committee

(Professor Burin Gumjudpai, Ph.D.)

..... Committee

(Associate Professor Pichet Vanichchapongjaroen, Ph.D.)

..... Committee

(Associate Professor Pitayuth Wongjun, Ph.D.)

Approved

Krongkarn Chootip .....

(Associate Professor Krongkarn Chootip, Ph.D.)

Dean of the Graduate School

14 MAR 2025

ACKNOWLEDGMENTS

First, I would like to thank my supervisor, Associate Professor Dr.Pornrad Srisawad, for giving me the opportunity to work on this project. Her support helped me to complete this dissertation. Additionally, she offered me a full scholarship under the Royal Golden Jubilee Ph.D. Programme (RGJ Ph.D. scholarship), formerly funded by the Thailand Research Fund (TRF) and now administered by the National Research Council of Thailand (NRCT).

I am very thankful to Professor Dr.Burin Gumjudpai, for his continuous support, guidance, and patience throughout my research. His patience and advice helped me to understand many difficult concepts in theoretical physics. Without his help, this work would not be possible.

I also would like to thank Associate Professor Dr.Pichet Vanichchapongjaroen for his valuable comments and suggestions. His insights helped improve the quality of my research.

I appreciate the support and warm atmosphere at The Institute for Fundamental Study, Naresuan University, where I have been fortunate to pursue my academic journey. Additionally, I would like to thank the Centre for Theoretical Physics and Natural Philosophy, Mahidol University Nakhonsawan Campus, where I have been conducting my research. The facilities and environment have been crucial in helping me focus on my work.

Lastly, I would like to thank my family, friends, and colleagues for their encouragement and support, which kept me motivated throughout this journey.

Amornthep Tita

Title	COSMOLOGY IN MODIFIED GRAVITIES WITH HOLOGRAPHIC CUTOFFS
Author	Amornthep Tita
Advisor	Associate Professor Pornrad Srisawad, Ph.D.
Academic Paper	Ph.D. Dissertation in Theoretical Physics, Naresuan University, 2024
Keywords	Non-minimal derivative coupling, Holographic dark energy

ABSTRACT

This dissertation investigates the cosmological evolution of a universe composed of non-relativistic matter (dust), a scalar field with non-minimal coupling (NMC) and derivative coupling (NMDC) to gravity, and vacuum energy based on holographic principles. Understanding the interplay between dark energy, scalar fields, and spacetime curvature is essential for explaining the accelerated expansion of the universe.

The study focuses on two models: (1) a scalar field coupled to the Einstein curvature tensor (NMDC model) and (2) a scalar field coupled to the Ricci scalar (NMC model). In both models, the dynamics of the universe at late times are emphasized. In modern cosmology, NMDC provides a mechanism for generating inflation without relying on the slow-roll approximation for scalar fields in the early universe. However, NMDC models are generally disfavored by observational data. Consequently, the focus shifts to the NMC theory, which aligns more closely with inflationary observational constraints.

This dissertation examines these models during the late stages of cosmic evolution. Specifically, it explores the NMDC and NMC models in conjunction with holographic vacuum energy, which depends on the cosmological horizon. The

observable universe is bounded by the apparent horizon, a trapped-null surface analogous to a black hole's event horizon.

To account for the complexity of the models, the evolution of the universe is analyzed using dynamical system techniques and numerical integration.

LIST OF CONTENTS

Chapter Page

LIST OF CONTENTS (CONT.)

Chapter Page

LIST OF FIGURES

Figure **Page**

LIST OF TABLES

Table **Page**

CHAPTER I

INTRODUCTION

1.1 Overview

Understanding the current accelerated expansion of the Universe remains a challenge in cosmology. This acceleration could be driven either by dark energy, an exotic form of energy with negative pressure, or modifications to the theory of general relativity [1, 2, 3, 4, 5, 6, 7]. It corresponds to a negative equation of state parameter less than $-1/3$, with observational evidence suggesting a value close to -1 [8, 9, 10, 11]. Dark energy can be described as either a dynamic scalar field or a cosmological constant. This exotic energy can be modeled as an additional dynamical component that modifies the matter sector within the Lagrangian. Alternatively, late-time acceleration could be attributed to modifications in the gravitational sector of Einstein's field equations. Modified gravity theories offer various approaches, such as replacing the Einstein-Hilbert Lagrangian, $\mathcal{L} = R$, with a function of the Ricci scalar, $\mathcal{L} = f(R)$, [12, 13]. Other models involve interactions between barotropic fluids, scalar fields, and gravity, leading to complex behaviors within the framework of scalar-tensor theories [1, 14, 15]. This dissertation explores a gravity model where a coupling between the scalar field's kinetic term and the Einstein tensor leads to the non-minimal derivative coupling gravity model (NMDC). Previous research has demonstrated that this model can lead to an accelerated expansion of the Universe, as indicated in various studies [16, 17, 18, 19, 20, 21]. The NMDC model provides second-order equations of motion, representing a subclass of the most general scalar-tensor theory with second-order equation of motion, known as Horndeski theory [22, 23]. The second-order equation of motion for the field ensures that it avoids energy that is unbounded from below, a condition known as

Ostrogradsky instability [24, 25]. The NMDC action is given by

$$S = \int \mathrm{d}^4x\sqrt{-g}\left[\frac{R}{16\pi G} - \frac{1}{2}g_{\mu\nu}\nabla^\mu\phi\nabla^\nu\phi - \frac{\kappa}{2}G_{\mu\nu}\nabla^\mu\phi\nabla^\nu\phi - V(\phi)\right] + S_\mathrm{m} + S_\Lambda\,, \tag{1.1}$$

where S_m and S_Λ are the actions of the matter fields, including dark matter and baryonic fields, and the cosmological vacuum energy, respectively. The third term on the right-hand side represents the NMDC interaction between the kinetic term, $\nabla^\mu\phi$, and the Einstein tensor, $G_{\mu\nu}$, with κ denoting the coupling constant, which characterizes the strength of the coupling. At late times, for a power-law potential of the form $V(\phi) = V_0\phi^n$ with $n = 2$, the model predicts accelerated expansion, with the equation of state parameter matching observational data [20, 26, 27]. For potential exponents $n < 2$, the scale factor exhibits oscillatory behavior, while for exponents $n > 2$, the model predicts a Big Rip singularity [28]. The NMDC coupling plays a crucial role at early times, as it can drive inflation without the need for fine-tuning the potential [26]. However, at late times, the NMDC coupling is unable to drive acceleration due to the very small value of the coupling constant [29]. Hence, it behaves like quintessence, as it is driven by the potential.

The most successful model, which is highly compatible with observational data, is the ΛCDM model, with the cosmological constant, Λ, driving late-time accelerated expansion. This naturally leads to the inclusion of a cosmological constant term in the action. Traditionally, the cosmological constant is interpreted as vacuum energy. However, the well-known cosmological constant problem remains due to a large discrepancy between the cosmological constant energy density and the UV cutoff of quantum zero-point vacuum energy [30]. It is possible that the cosmological constant does not represent vacuum energy.

The cosmological constant problem motivates the replacement of the cosmological constant with holographic dark energy as a candidate for cosmological vacuum energy density. Holographic dark energy (HDE), sometimes referred to

as holographic vacuum energy, is a form of vacuum energy derived from applying the holographic principle to cosmology. The energy density of holographic vacuum energy can be expressed as

$$\rho_\Lambda = \frac{3c^2}{8\pi GL}, \tag{1.2}$$

where L is a cosmological horizon cutoff or IR cutoff, and the parameter $0 \leq c < 1$ is a numerical constant [31]. HDE explains the evolution of the universe, influenced by the cosmological horizon cutoff. It can be interpreted as the vacuum energy with an IR cutoff. Considering either the Hubble horizon, $L \sim H^{-1}$, for flat spacetime or the apparent horizon, $L \sim 1/\sqrt{H^2 + k/a^2}$, for non-flat spacetime as the cosmological cutoff leads to a HDE equation of state parameter $w_\Lambda = 0$. This behavior is dust-like, which is inconsistent with observational data [32]. To achieve an accelerating expansion, the concept of a future event horizon has been proposed [31]. However, this approach requires information from future states, which is incompatible with the principle of causality. Furthermore, HDE with the future event horizon encounters the cosmic age problem, predicting a Universe that is younger than what is observed from high-redshift objects [33].

We employ the apparent horizon as the cosmological cutoff because it is expected to exhibit properties similar to a black hole event horizon. It should enclose a cosmic volume bounded by a trapped null surface from which no light signal can reach. In a non-flat accelerating Universe, a trapped null surface exists when using the apparent horizon as a cutoff scale. This horizon alleviates the cosmological constant problem, as the energy density of HDE with the apparent horizon can be compatible with the density of the cosmological constant [34]. Moreover, the Friedmann equation can be derived from the first law of thermodynamics when applying the apparent horizon to Cai-Kim temperature $T = 1/(2\pi R_A)$ [35]. Using the apparent horizon as the cosmological cutoff provides a strong motivation; however, the dust-like behavior problem still remains. To address this issue, several

models involving modified black hole entropy have been proposed. Due to the non-extensive nature of black hole entropy, characterized by Bekenstein entropy, Tsallis entropy has been introduced as a non-extensive version of Bekenstein entropy. By applying Tsallis entropy to a cosmological context, Tsallis holographic dark energy has been proposed [36]. Rényi entropy is also considered in cosmology, leading to the development of Rényi holographic dark energy [37, 38]. Additionally, Kaniadakis entropy has been developed into Kaniadakis holographic dark energy [39]. Sharma-Mittal entropy is also considered, resulting in Sharma-Mittal holographic dark Energy [40].

This dissertation investigates non-flat spacetime cosmological models of HDE with the apparent horizon cutoff in combination with the NMDC model. The matter content consists of the NMDC scalar field, dust field, and holographic vacuum energy. We perform a dynamical system analysis to explore the interplay between HDE, the NMDC field, and spatial curvature, focusing on their implications for the kinematic properties of late-time cosmic expansion. Additionally, we compare our results to the observed expansion history derived from Type Ia supernovae data.

1.2 Outline of the Dissertation

In Chapter 2, we introduce the basic concepts of dark energy. This chapter provides an overview of cosmology based on General Relativity, with the cosmological constant as the simplest dark energy model. Additionally, the chapter examines the well-known cosmological constant problem, which addresses the discrepancy between the observed energy density of the cosmological constant and the theoretical prediction from quantum zero-point energy. In Chapter 3, we provide a brief review of the NMDC theory. The historical development of the theory is outlined in this chapter. We begin by reviewing the first NMDC model introduced by Amen-

dola [16], followed by subsequent developments by Capozziello, Lambiase, Schmidt [17], as well as Granda [19], and Sushkov [20]. Chapter 4 discusses the concept of HDE. This chapter provides a brief review of the application of the holographic principle to cosmology, including the construction of the UV/IR correspondence based on black hole physics. We also review HDE models that incorporate various cosmological horizon cutoffs, such as the Hubble horizon, particle horizon, future event horizon, and Ricci dark energy. In Chapter 5, we investigate the interplay between the NMDC scalar field and holographic dark energy within a non-flat universe. We derive the corresponding field equations and the Friedmann equation in the context of the FLRW universe. Furthermore, we construct an autonomous system to analyze the dynamical stability of the model. The qualitative behavior of the universe is discussed, and numerical integration are performed to study the kinematic behavior of the Hubble parameter and the equation of state parameter. Given that the inflationary NMDC model has been ruled out as inconsistent with observational data from the cosmic microwave background (CMB) radiation [41, 42, 43], We investigate a new model that is viable in both the early Universe and late-time accelerated expansion. In chapter 6, we investigate the non-minimal coupling (NMC) between the scalar field and the Ricci scalar model. Additionally, we construct an autonomous system to examine the dynamical stability of the model. We discuss the qualitative behavior of the universe and perform numerical integration to analyze the evolution of the density parameters and the equation of state parameter. The conclusions and discussions are presented in Chapter 7.

CHAPTER II

BASIC KNOWLEDGE OF DARK ENERGY

In this chapter, we review the basic knowledge foundation of dark energy. In modern cosmology, the accelerated expansion of the Universe has been confirmed by observational data from Type Ia Supernovae. In 1998, two independent research teams reported this discovery: Riess *et al.* [11] from the Supernova Search Team, and Perlmutter *et al.* [9] from the Supernova Cosmology Project Team. One proposed explanation for this acceleration is dark energy, a mysterious form of exotic energy exhibiting repulsive pressure. Observations of supernovae suggest that approximately 70% of the current Universe consists dark energy. Although the nature of dark energy remains unknown, its origin is one of the biggest questions in modern cosmology. Additional evidence supporting the existence of dark energy comes from measurements of the cosmic microwave background (CMB) radiation [44, 45, 46], large-scale structure (LSS) surveys [47] and baryon acoustic oscillations (BAO) [48].

Theoretically, General Relativity, when combined with the cosmological principle, can account for the accelerated expansion of the Universe. There are two main approaches to studying dark energy. The first approach modifies the matter component by introducing an exotic energy-momentum tensor with negative pressure into Einstein's field equations. The second approach involves modifying the gravitational sector of the equations by replacing the Einstein-Hilbert Lagrangian with a function of the Ricci scalar, known as $f(R)$ gravity. Among the various dark energy models, the simplest and most successful explanation for the accelerated expansion is the cosmological constant, which was originally introduced by Einstein in his field equations.

In the next section, we review the basic concepts of cosmology and explore

how they describe the behavior of dark energy. We then introduce the cosmological constant model and discuss its related theoretical problem, commonly known as the cosmological constant problem.

2.1 Cosmology based on General Relativity

General Relativity is a geometric theory of gravity, in which gravity arises as a consequence of the curvature of spacetime caused by the distribution of mass and energy. Mathematically, the relationship between spacetime curvature and the distribution of matter and energy is described by Einstein's field equations[1],

$$G_{\mu\nu} = 8\pi G T_{\mu\nu}\,, \tag{2.1}$$

where $G_{\mu\nu}$ represents the Einstein tensor, which encodes the geometric curvature of spacetime, and $T_{\mu\nu}$ denotes the energy-momentum tensor, which quantifies the distribution of matter and energy within the spacetime. In General Relativity, the Einstein tensor is constructed using the contracted Bianchi identities, given by $\nabla^\mu G_{\mu\nu} = \nabla^\mu(R_{\mu\nu} - g_{\mu\nu}R/2) = 0$, where $R_{\mu\nu}$, R and $g_{\mu\nu}$ represent the Ricci tensor, Ricci scalar and metric tensor, respectively. These identities are linked to the conservation of energy and momentum, expressed by the vanishing divergence of the energy-momentum tensor, $\nabla^\mu T_{\mu\nu} = 0$. This condition ensures consistency between left-hand and right-hand sides of Einstein's field equations.

Modern cosmology is based on the cosmological principle, which states that the universe is homogeneous and isotropic on extremely large scales. A homogeneous universe is translationally invariant, meaning its properties remain consistent at all location. An isotropic universe is rotationally invariant, indicating that its properties are the same in all directions. Mathematically, the line element describ-

---

[1]Throughout this dissertation, we adopt units where the speed of light is $c = 1$ and the metric signature is $(-,+,+,+)$.

ing a homogeneous and isotropic universe is given by the Friedmann-Lemaître-Robertson-Walker (FLRW) metric, which is expressed as

$$\mathrm{d}s^2 = -\mathrm{d}t^2 + a^2(t)\left(\frac{\mathrm{d}r^2}{1-kr^2} + r^2\mathrm{d}\theta^2 + r^2\sin^2\theta\mathrm{d}\phi^2\right), \tag{2.2}$$

where $a(t)$ is the scale factor, a time-dependent function that determines the expansion of the Universe. The constant k specifies the spatial curvature of the Universe, with values $k = 0, -1$ and $+1$ corresponding to flat, open, and closed spacetime geometries, respectively. In accordance with the cosmological principle, the energy-momentum tensor in Einstein's field equation (2.1) can be modeled as a perfect fluid. A perfect fluid is an idealized fluid with no viscosity, no heat conduction, and isotropic pressure. It is characterized only by its energy density and pressure. The energy-momentum tensor for a perfect fluid is given by

$$T_{\mu\nu} = (\rho + P)u_\mu u_\nu + P g_{\mu\nu}, \tag{2.3}$$

where $\rho = \rho(t)$ and $P = P(t)$ are time-dependent energy density and pressure, respectively. The four-velocity in comoving coordinates is $u^\mu = (-1, 0, 0, 0)$.

Within the context of the FLRW universe (2.2), solving Einstein's field equations (2.1) together with the perfect fluid energy-momentum tensor (2.3) yields the Friedmann equations,

$$3H^2 + \frac{3k}{a^2} = 8\pi G\rho, \tag{2.4}$$

$$3H^2 + 2\dot{H} + \frac{k}{a^2} = -8\pi G P, \tag{2.5}$$

where $H = \dot{a}/a$ is the Hubble parameter, which quantifies the expansion rate of the Universe with respect to cosmic time, driven by the energy density and pressure of the matter components. By substituting equation (2.4) into (2.5), we can derive the acceleration equation for the scale factor, given by

$$\frac{\ddot{a}}{a} = -\frac{4\pi G}{3}(\rho + 3P). \tag{2.6}$$

Equation (2.6) reveals the conditions for the expansion of the Universe based on pressure as follows:

- $P < -\rho/3$, the Universe experiences acceleration $(\ddot{a}/a > 0)$,
- $P > -\rho/3$, the Universe experiences deceleration $(\ddot{a}/a < 0)$,
- $P = -\rho/3$, the expansion rate remains constant $(\ddot{a}/a = 0)$.

Since the energy density is always positive, negative pressure is required to drive accelerated expansion.

The conservation of energy and momentum is encoded in the vanishing divergence of the energy-momentum tensor, $\nabla_\mu T^\mu_\nu = 0$. In a homogeneous and isotropic universe, the continuity equation can be derived by focusing on the time component (i.e., $\nabla_\mu T^\mu_0 = 0$) of the divergence-free energy-momentum tensor. This leads to the energy conservation equation,

$$\dot{\rho} + 3H(\rho + P) = 0. \tag{2.7}$$

This equation expresses the relationship between the energy density and pressure of a perfect fluid in an expanding universe, describing how the energy density evolves over cosmic time. The spatial component of the divergence-free equation, $\nabla_\mu T^\mu_i = 0$, provides the momentum conservation equation, or Euler equations, in fluid dynamics, which describe how momentum evolves in space. However, in a homogeneous and isotropic universe, there are no spatial variations in energy density and pressure, meaning the spatial components do not contribute to the dynamics. Mathematically, this gives trivial solution for the spatial component of the divergence-free energy-momentum tensor. In fact, the continuity equation (2.7) is not independent of the Friedmann equations. It can be derived by taking the time derivative of the first Friedmann equation (2.4) and then using the second Friedmann equation (2.5). Consequently, the system of Friedmann equations cannot be completely solved for all three variables, i.e., $a(t)$, $\rho(t)$ and $P(t)$. This is because we have two independent equations and three unknowns. To resolve the issue, an

equation of state (EoS) for the matter components is introduced. The EoS relates energy density and pressure through a linear relationship,

$$P = w\rho, \tag{2.8}$$

where w is EoS parameter. This additional equation allows us to express one variable in terms of another, reducing the system to two independent equations and two unknowns. The EoS parameter plays a crucial role in determining the evolution of matter energy density as the Universe expands. This evolution is governed by the continuity equation (2.7). By applying the EoS equation (2.8) to the continuity equation (2.7), the evolution of the energy density with respect to the scale factor can be expressed as

$$\rho(a) \propto a^{-3(1+w)}. \tag{2.9}$$

However, equation (2.9) is only valid when the EoS parameter w remains constant.

Suppose the universe is filled with a single component. Different matter components in the Universe correspond to different values of the EoS parameter. Non-relativistic matter, which includes baryonic and dark matter, is pressureless ($P_{\rm m} = 0$), leading to an EoS parameter of $w_{\rm m} = 0$. Here, the subscript "m" denotes the non-relativistic matter component. According to equation (2.9), the solution is given by

$$\rho_{\rm m} \propto \frac{1}{a^3}. \tag{2.10}$$

During the matter-dominated epoch, this equation implies that the energy density scales inversely with the volume, a^3. As the Universe expands, the energy density of non-relativistic matter decreases.

For radiation, including photon and relativistic particles, the EoS parameter is $w_{\rm r} = 1/3$. Here, the subscript "r" represents the radiation component. According to equation (2.9), the energy density of radiation evolves as

$$\rho_{\rm r} \propto \frac{1}{a^4}. \tag{2.11}$$

This relationship implies that during the radiation-dominated era, the energy density of radiation decreases faster than the volume of the Universe. This is due to the additional factor of a in the denominator. Physically, besides the effect of expanding volume, radiation is also influenced by redshift. The redshift, z, is inversely proportional to the scale factor ($z \approx -1 + 1/a$).

According to the conditions for accelerated expansion, the corresponding EoS parameter must satisfies: $w < -1/3$ for accelerated expansion, $w > -1/3$ for decelerated expansion, and $w = -1/3$ for a constant expansion rate. This indicates that both non-relativistic matter and radiation lead to a decelerated expansion of the Universe. The condition for accelerated expansion requires the EoS parameter

$$w_{\text{de}} < -\frac{1}{3}. \tag{2.12}$$

This implies that the mysterious component driving the accelerated expansion must have negative pressure, a property not exhibited by ordinary matter. This exotic form of matter is called dark energy, denoted by the subscript "de". The EoS parameter of dark energy can either be constant or a function of the scale factor. A constant EoS parameter simplifies the model, while a function EoS parameter offers more flexibility to accommodate different cosmological scenarios and observational data. The continuity equation for dark energy is given by

$$\dot{\rho}_{\text{de}} + 3H\rho_{\text{de}}(1 + w_{\text{de}}) = 0\,, \tag{2.13}$$

This equation can be integrated. Ingeneral, the energy density of dark energy can be expressed as

$$\rho_{\text{de}} \propto \exp\left[-3\int \frac{\mathrm{d}a}{a}(1 + w_{\text{de}}(a))\right]. \tag{2.14}$$

Suppose the Universe is filled with multiple components, including radiation, non-relativistic matter, and dark energy. To account for these different components, the Friedmann equation (2.4) can be written as

$$3H^2 + \frac{3k}{a^2} = 8\pi G\left[\frac{\rho_{\text{r},0}}{a^4} + \frac{\rho_{\text{m},0}}{a^3} + \rho_{\text{de},0}\exp\left(-3\int \frac{\mathrm{d}a}{a}(1 + w_{\text{de}})\right)\right], \tag{2.15}$$

where $\rho_{\mathrm{m}0}$, $\rho_{\mathrm{r}0}$, and $\rho_{\mathrm{de}0}$ represent the current energy density of radiation, dust, and dark energy, respectively. The equation becomes a first-order differential equation in terms of $H = \dot{a}/a$. If w_{de} is known, this equation can be integrated to obtain the scale factor as a function of cosmic time. The expansion history of the Universe can be qualitatively divided into distinct epoch: a radiation-dominated period, followed by a dust matter-dominated period, and finally a dark energy-dominated epoch. To compare with observational data, the Friedmann equation is often expressed in terms of the dimensionless density parameter as

$$1 \;=\; \Omega_{\mathrm{r}} + \Omega_{\mathrm{m}} + \Omega_{\mathrm{de}} + \Omega_k \,, \tag{2.16}$$

where the density parameter, Ω_i, is defined as $\Omega_i = 8\pi G\rho_i/3H^2$, with " i " representing r(radiation), m(dust), de(dark energy) for each cosmic component. These parameters quantify the relative contributions of each component to the total energy density of the universe, sometimes referred to as the constraint equation. Additionally, equation (2.16) includes the curvature parameter $\Omega_k = -k/(a^2H^2)$, which characterizes the geometry of the Universe. This equation imposes a constraint on the total matter density of the Universe. The current value of each density parameter is obtained by setting $H = H_0$ and the present scale factor $a_0 = 1$, resulting in the relation

$$1 \;=\; \Omega_{\mathrm{r},0} + \Omega_{\mathrm{m},0} + \Omega_{\mathrm{de},0} + \Omega_{k,0} \,. \tag{2.17}$$

The Friedmann equation (2.15) can be expressed in terms of the current values of the density parameters, which are constrained by observational data.

$$H^2 \;=\; H_0^2 \left[\frac{\Omega_{\mathrm{r},0}}{a^4} + \frac{\Omega_{\mathrm{m},0}}{a^3} + \Omega_{\mathrm{de},0} \exp\left(-3 \int \frac{\mathrm{d}a}{a} (1 + w_{\mathrm{de}}) \right) + \frac{\Omega_{k,0}}{a^2} \right] . \tag{2.18}$$

Here, H_0 represents the present-day Hubble parameter, commonly referred to as the Hubble constant.

In the present-day Universe, the contribution of radiation to the total energy density is negligible. As a result, the Friedmann equation can be simplified to focus

on the interplay between matter, dark energy, and spatial curvature. Observational analysis of the cosmic microwave background (CMB) data from the WMAP 9-year mission [45] strongly constraints the spatial curvature of the present Universe to be very close to flat, with $\Omega_{k,0} = -0.0027^{+0.0039}_{-0.0038}$. The WMAP data also provides constraints on the density parameter of other components, $\Omega_{\mathrm{m},0} = 0.2865^{+0.0095}_{-0.0096}$ for non-relativistic matter (including baryons and cold dark matter) and $\Omega_{\mathrm{de},0} = 0.7135^{+0.0095}_{-0.0096}$ for dark energy. Recently, analysis of Planck 2018 data [46] constraints the spacial curvature to be even closer to zero $\Omega_{k,0} = 0.0007 \pm 0.0019$ compared to WMAP, further supporting a flat Universe. The density parameter for non-relativistic matter, $\Omega_{\mathrm{m},0} = 0.315 \pm 0.007$, and dark energy, $\Omega_{\mathrm{de},0} = 0.6847 \pm 0.0073$, are also determined with higher precision by Plank data. Additionally, Plank data provides a constraint on the dark energy EoS parameter, $w_{\mathrm{de}} = -1.03 \pm 0.03$.

Moreover, the current value of Hubble constant, H_0, derived from local measurement of Cepheid variables and Type Ia Supernovae reported by the Supernovae and H_0 for the Equation of State (SH0ES) project [49], is $H_0 = 73 \pm 1.04$ km/s/Mpc. In contrast, the Dark Energy Spectroscopic Instrument 2024 (DESI) [50] reports a current value of $H_0 = 67.97 \pm 0.38$ km/s/Mpc based on baryon acoustic oscillation measurements. The Hubble constant observed from DESI corresponds to the Planck 2018 data [46], which measures the early universe from the CMB, yielding a value of $H_0 = 67.36 \pm 0.54$ km/s/Mpc. These values highlight a slight tension between measurements at low redshift and high redshift, known as the Hubble tension.

Cosmological observations provide constraints on the composition of the present-day Universe. Dark energy is the dominant component, contributing roughly 70% of the total energy density, while non-relativistic matter constitutes 30%. The current density of radiation is negligible ($\Omega_{\mathrm{r},0} \approx 10^{-4}$) and can be ignored for late-Universe considerations. However, the nature of dark energy remains a mystery,

and its properties are a subject of active and ongoing research.

2.2 Cosmological constant model

Among the various models proposed for dark energy, the cosmological constant is the simplest. It manifests as a uniform energy density throughout space and remains constant over time, acting as a source term in the Einstein's field equations. The ΛCDM model, which incorporates the cosmological constant along with cold dark matter, is the most successful model for explaining the universe's history and exhibits strong compatibility with observational data. Historically, to maintain a static universe, Einstein introduced the cosmological constant in his field equations as follows

$$G_{\mu\nu} + \Lambda g_{\mu\nu} = 8\pi G T_{\mu\nu} \,. \tag{2.19}$$

In this context, the term $\Lambda g_{\mu\nu}$ can be interpreted as the energy-momentum tensor of the cosmological constant,

$$T^{(\Lambda)}_{\mu\nu} = \frac{\Lambda}{8\pi G} g_{\mu\nu} \,. \tag{2.20}$$

In the FLRW universe, the energy-momentum tensor can be represented by a perfect fluid as described in equation (2.3). For the cosmological constant, this leads to the expressions for energy density and pressure as follows

$$\rho_\Lambda = \frac{\Lambda}{8\pi G}, \quad P_\Lambda = -\frac{\Lambda}{8\pi G} \,. \tag{2.21}$$

According to EoS equation (2.8), the pressure and energy density are related by

$$P_\Lambda = -\rho_\Lambda \,. \tag{2.22}$$

Consequently, the equation of state parameter for the cosmological constant is given by

$$w_\Lambda = -1 \,. \tag{2.23}$$

The cosmological constant satisfies the condition for accelerated expansion, as its EoS parameter, w_Λ, is less than $-1/3$. The EoS parameter of the cosmological constant is consistently supported by observational data from the Planck 2018 mission. In the FLRW universe, applying the Einstein field equation (2.19) yields the following Friedmann equation

$$H^2 = \frac{8\pi G}{3}\rho_i - \frac{k}{a^2} + \frac{\Lambda}{3}, \tag{2.24}$$

where ρ_i represent the energy density of non-relativistic matter (dust and dark matter) and radiation component of the Universe. Assuming a flat universe ($k = 0$), which is consistent with WMAP and Plank mission data, The Universe filled solely with a cosmological constant at late time ($\rho_i = 0$) leads to the following Friedmann equation

$$H^2 = \frac{\Lambda}{3}. \tag{2.25}$$

This can be simplified to yield the Hubble parameter

$$H = \sqrt{\frac{\Lambda}{3}}. \tag{2.26}$$

The equation can be integrated directly to determine the evolution of the scale factor $a(t)$ as a function of cosmic time. This gives

$$a(t) = a_0 e^{\sqrt{\Lambda/3}t}. \tag{2.27}$$

The solution is known as the de Sitter solution. In this scenario, the scale factor exhibits exponential growth with respect to cosmic time, leading to the accelerated expansion of the universe.

2.3 Cosmological constant problem

To estimate the current value of the cosmological constant, we consider the Friedmann equation (2.24) in a flat universe ($k = 0$). The current Universe is

assumed to be dominated by dark energy, we can approximate it by neglecting other components. From this, we find that the current value of cosmological constant is of the order H_0^2. Due to Hubble tension, we take a rough average of the two different reported Hubble parameter values, yielding approximately $H_0 \approx 70$ km/s/Mpc. Therefore, the current value of the cosmological constant can be expressed as

$$\Lambda \approx H_0^2 = (1.49 \times 10^{-42}\text{GeV})^2 . \tag{2.28}$$

The corresponding energy density is given by

$$\rho_\Lambda = \frac{\Lambda}{8\pi G} \approx 10^{-47}\text{GeV}^4 , \tag{2.29}$$

which represents an extremely small energy density.

Suppose the energy is the zero-point vacuum energy from empty space. According to quantum field theory, the Hamiltonian operator for a field with mass m in momentum space is given by

$$\hat{H} = \frac{1}{4}\int \frac{d^3\vec{k}}{(2\pi)^3}\left(a_{\vec{k}}a_{\vec{k}}^\dagger + a_{\vec{k}}^\dagger a_{\vec{k}}\right), \tag{2.30}$$

where $a_{\vec{k}}$ and $a_{\vec{k}}^\dagger$ are the annihilation and creation operators respectively. The commutation relation between the annihilation and creation operators is given by

$$[a_{\vec{k}}, a_{\vec{k}'}^\dagger] = 2E_{\vec{k}}(2\pi)^3\delta^{(3)}(\vec{k}-\vec{k}') , \tag{2.31}$$

where the energy is $E_{\vec{k}} = \sqrt{\vec{k}^2 + m^2}$. Using this commutation relation, we obtain the following expression

$$\begin{aligned} a_{\vec{k}}a_{\vec{k}}^\dagger &= [a_{\vec{k}}, a_{\vec{k}}^\dagger] + a_{\vec{k}}^\dagger a_{\vec{k}} \\ &= 2E_k(2\pi)^3\delta^{(3)}(0) + a_{\vec{k}}^\dagger a_{\vec{k}}. \end{aligned} \tag{2.32}$$

Substituting the relation into the Hamiltonian operator (2.30) yields

$$\hat{H} = \frac{1}{2}\int \frac{d^3\vec{k}}{(2\pi)^3}a_{\vec{k}}^\dagger a_{\vec{k}} + \frac{1}{2}\int d^3\vec{k}E_{\vec{k}}\delta^{(3)}(0) . \tag{2.33}$$

The zero-point energy, E_0, of the ground state can be expressed as

$$\hat{H}|0\rangle \equiv E_0|0\rangle = \left[\frac{1}{2}\int \frac{d^3\vec{k}}{(2\pi)^3} a^\dagger_{\vec{k}} a_{\vec{k}} + \frac{1}{2}\int d^3\vec{k} E_{\vec{k}} \delta^{(3)}(0)\right]|0\rangle = \infty|0\rangle . \tag{2.34}$$

This integral represents the vacuum energy contribution form the quantum field ground state due to the non-zero energy of each mode $E_{\vec{k}}$. The factor of $\delta^{(3)}(0)$ indicates the infinite vacuum energy density. For more details, there are two distinct types of infinities appearing in the expression (2.34). The first arises from the infinite volume of space (infrared divergence). Second, there is a high-frequency (or short-distance) infinity known as ultraviolet divergence. To address the first infinity, we consider the theory within a box of sides length L with periodic boundary conditions. This length L is referred to as the Infrared cutoff (IR cutoff). Applying the Fourier transformation to the delta function, we get

$$\delta^{(3)}(0) = \int_{-L/2}^{L/2} \frac{d^3x}{(2\pi)^3} e^{i\vec{k}\cdot\vec{x}}|_{\vec{k}=0} = \int_{-L/2}^{L/2} \frac{d^3x}{(2\pi)^3} = \frac{V}{(2\pi)^3} , \tag{2.35}$$

where V represents the volume of the theory. Thus, the Hamiltonian operator becomes

$$\hat{H} = \frac{1}{2}\int \frac{d^3\vec{k}}{(2\pi)^3} a^\dagger_{\vec{k}} a_{\vec{k}} + \frac{1}{2}\int \frac{d^3\vec{k}}{(2\pi)^3} E_{\vec{k}} V . \tag{2.36}$$

The second infinity can be addressed by introducing a cutoff scale at high momenta, summing the zero-point energies up to this limit. This cutoff is known as the ultraviolet cutoff (UV cutoff), denoted by $k_{\max}$. With the modification, The Hamiltonian operator from equation (2.36) becomes

$$\hat{H} = \frac{1}{2}\int^{k_{\max}} \frac{d^3\vec{k}}{(2\pi)^3} \left(a^\dagger_{\vec{k}} a_{\vec{k}} + E_{\vec{k}} V\right) . \tag{2.37}$$

Hence, the vacuum energy density is given by

$$\frac{\hat{H}}{V}|0\rangle = \left(\frac{1}{2}\int^{k_{\max}} \frac{d^3\vec{k}}{(2\pi)^3} \sqrt{\vec{k}^2 + m^2}\right)|0\rangle = \rho_0|0\rangle , \tag{2.38}$$

where the annihilation operator defined by the property $a_{\vec{k}}|0\rangle = 0$. The zero-point vacuum energy density from quantum field theory can be obtained as

$$\rho_0 = \frac{1}{2}\int^{k_{\max}} \frac{d^3\vec{k}}{(2\pi)^3}\sqrt{\vec{k}^2 + m^2}\,. \tag{2.39}$$

Summing the field energy up to the Planck length cutoff, k_{Planck}, the vacuum energy density becomes

$$\begin{aligned}\rho_0 &= \frac{1}{2}\int^{k_{\text{Plank}}} \frac{d^3\vec{k}}{(2\pi)^3}\sqrt{\vec{k}^2 + m^2}, \\ &\approx \frac{k^4_{\text{Plank}}}{16\pi^2} \\ &= 10^{74}\,\text{Gev}^4\,.\end{aligned} \tag{2.40}$$

This represents an extremely large energy density when compared to the cosmological constant energy density calculated in Equation (2.29).

This leads to a discrepancy of approximately 121 orders of magnitude between the cosmological constant energy density and the zero-point energy density, which constitutes one of the most significant challenges in modern cosmology and particle physics. If the cosmological constant problem remains unsolved, we need to explore alternative models of dark energy. In the next chapter, we provide a brief review of scalar-tensor theory as one of the representative modified matter models, which involves non-minimal coupling between scalar field and curvature. Another model that we need to explore is holographic dark energy, which serves as an alternative to vacuum energy.

CHAPTER III

NON-MINIMAL DERIVATIVE COUPLING THEORY

In this chapter, we provide a brief review of the cosmological model in which the derivative of scalar field non-minimally couples (NMDC) to gravity. In NMDC models, the Lagrangian includes a kinetic term for the scalar field, a potential term, and a non-minimal coupling term. The altered coupling introduces new terms into the gravitational field equations, influencing the expansion of the universe.

3.1 Amendola's model

The first NMDC model was proposed by Luca Amendola in 1993 [16]. In this model, the NMDC coupling function depends not only on the scalar field, but also on its derivatives, expressed as $f = f(\phi, \nabla_\mu\phi, \nabla_\mu\nabla_\nu\phi, ...)$. This type of interaction is inspired by various theories, such as scalar electrodynamics, a field theory that requires invariance under local $U(1)$ symmetry. In scalar electrodynamics, the Lagrangian includes a coupling between the derivative of the scalar field, ϕ, and the electromagnetic vector potential, A_μ. Non-minimal derivative coupling terms often appear as low-energy manifestations of higher-dimensional theories, allowing for the perturbative study of quantum gravity. They also appear in the Weyl anomaly in $\mathcal{N} = 4$ conformal supergravity [51, 52]. Moreover, the coupling terms between the curvature and the energy-momentum tensor of matter, i.e., TR and $T_{\mu\nu}R^{\mu\nu}$, in some modified gravity theories actually include non-minimal derivative coupling. The NMDC coupling also appears in inflationary models based on Kaluza-Klein and superstring theories [53]. However, a conformal transformation cannot convert the NMDC theory into the standard field equations in the Einstein frame. The conformal transformation needs to be generalized to a Legendre transformation in order to recover the Einstein frame [16, 54], often referred to as a disformal

transformation.

The most general form of NMDC in the Einstein-Hilbert Lagrangian, where the Lagrangian is linear in curvature scalar, R, and quadratic in the scalar field, can be written as follows

$$\begin{aligned} \mathcal{L}_1 &= \kappa_1(\nabla_\mu\phi)(\nabla^\mu\phi)R, \quad \mathcal{L}_2 = \kappa_2(\nabla^\mu\phi)(\nabla^\nu\phi)R_{\mu\nu}, \quad \mathcal{L}_3 = \kappa_3\phi(\nabla_\mu\nabla^\mu\phi)R, \\ \mathcal{L}_4 &= \kappa_4\phi(\nabla^\mu\nabla^\nu\phi)R_{\mu\nu}, \quad \mathcal{L}_5 = \kappa_5\phi(\nabla_\mu\phi)R^\mu, \quad \mathcal{L}_6 = \kappa_6\phi^2\nabla_\mu\nabla^\mu R, \end{aligned} \tag{3.1}$$

where $\kappa_1, ..., \kappa_6$ are coupling constants with dimensions of inverse mass squared, $mass^{-2}$. Due to the divergence-free boundary condition, there exists constraint equation where three of the six terms can be expressed in terms of the others. Amendola keeps only $\mathcal{L}_1$ term together with free scalar field and NMC term in the Lagrangian to consider influence of NMDC coupling in the context of inflation,

$$\mathcal{L} = -R + \xi f(\phi)R + \kappa(\nabla_\mu\phi)(\nabla^\mu\phi)R + (\nabla_\mu\phi)(\nabla^\mu\phi) - 2V(\phi)\,. \tag{3.2}$$

3.2 Capozziello, Lambiase & Schmidt model

In 1999, Capozziello, Lambiase, and Schmidt [17] showed that among the six terms in the Lagrangian (3.1), without losing its generality, four of them i.e., $\mathcal{L}_3, \mathcal{L}_4, \mathcal{L}_5$ and $\mathcal{L}_6$ are not necessary to be considered. Thus, the NMDC action, which includes only $\mathcal{L}_1$ and $\mathcal{L}_2$ terms, can be expressed as follows

$$S = \int \mathrm{d}^4x\sqrt{-g}\left(-\frac{R}{2} + \frac{1}{2}g^{\mu\nu}\nabla_\mu\phi\nabla_\nu\phi + \zeta R^{\mu\nu}\nabla_\mu\phi\nabla_\nu\phi + \xi R g^{\mu\nu}\nabla_\mu\phi\nabla_\nu\phi\right). \tag{3.3}$$

In the FLRW universe, the results indicate the existence of a cosmological constant solution that can be derived from NMDC parameters, i.e., ζ and ξ, without requiring the introduction of a scalar field potential [55]. The late-time de Sitter expansion, driven by the cosmological constant, represents an attractor solution

[17]. In the absence of the parameter ξ, constraints on the coupling parameter ζ have been explored through precision tests of General Relativity [56].

3.3 Granda's model

Another NMDC modification model was studied by Granda in 2010 [19]. In this model, the action includes the Einstein-Hilbert term, a free kinetic term, a potential term, and NMDC coupling term, with the coupling parameters scaled by the square of the scalar field, $1/\phi^2$. The NMDC action, incorporating a barotropic matter component, is given by

$$S = \int \mathrm{d}^4x\sqrt{-g}\left(\frac{R}{16\pi G} - \frac{1}{2}\nabla_\mu\phi\nabla^\mu\phi - V - \frac{\xi}{2\phi^2}R\nabla_\mu\phi\nabla^\mu\phi - \frac{\eta}{2\phi^2}R_{\mu\nu}\nabla^\mu\phi\nabla^\nu\phi\right) + S_\mathrm{m}\,. \tag{3.4}$$

For simplicity, the coupling parameters ξ and η are restricted by the relation $\eta + 2\xi = 0$. Asymptotic de Sitter behavior is exhibited when the Hubble parameter approaches a constant value, $H = \kappa\sqrt{V_0/3}$, where κ and V_0 are constants. Considering only the NMDC contribution, the model exhibits a power-law solution consistent with dark matter behavior. For $\eta = -\xi - 1$, in the interval $0 < \xi < 1/3$, the Friedmann equation leads to a solution with accelerated expansion. A general function of the term $1/\phi^2$ in the action equation (3.4), i.e., $F(\phi)$, was also studied by Granda [18, 57, 58]. Moreover, the NMDC general function has also been investigated in its coupling to Gauss-Bonnet theory [59, 60, 61] or in context of Chaplygin gas [62].

3.4 Sushkov's model

In 2009, Sushkov [20] considered NMDC theory with coupling terms of the form $\kappa_1 R\nabla_\mu\phi\nabla^\mu\phi$ and $\kappa_2 R_{\mu\nu}\nabla^\mu\phi\nabla^\nu\phi$, where the coupling parameters are related by $-2\kappa_1 = \kappa_2 \equiv \kappa$. This type of derivative coupling includes the Einstein tensor

as a term in the Lagrangian, given by

$$\begin{aligned} \kappa R_{\mu\nu}\nabla^{\mu}\phi\nabla^{\nu}\phi - \frac{\kappa}{2}Rg_{\mu\nu}\nabla^{\mu}\phi\nabla^{\nu}\phi &= \kappa(R_{\mu\nu} - \frac{1}{2}g_{\mu\nu}R)\nabla^{\mu}\phi\nabla^{\nu}\phi\,, \\ &= \kappa G_{\mu\nu}\nabla^{\mu}\phi\nabla^{\nu}\phi\,. \end{aligned} \tag{3.5}$$

The Einstein-Hilbert action, incorporating a free scalar kinetic term, a scalar potential, NMDC coupling term, and a matter action, is given by

$$S = \int \mathrm{d}^4x\sqrt{-g}\left(\frac{R}{16\pi G} - \frac{\varepsilon}{2}g_{\mu\nu}\nabla^{\mu}\phi\nabla^{\mu}\phi - V(\phi) - \frac{\kappa}{2}G_{\mu\nu}\nabla^{\mu}\phi\nabla^{\nu}\phi\right) + S_{\mathrm{m}}\,, \tag{3.6}$$

where $\varepsilon = 1, -1$ represents a numerical constant for the canonical and phantom scalar field, respectively.

This coupling term indeed appears in a subclass of the Horndeski action, which represents the most general scalar-tensor theory that yields second-order equations of motion for the involved fields. Further details can be found in [63]. The Horndeski Lagrangian is given by

$$\begin{aligned} \mathcal{L} = {} & G_2(\phi, X) - G_3(\phi, X)\Box\phi + G_4(\phi, X)R + G_{4X}\left[(\Box\phi)^2 - \phi^{\mu\nu}\phi_{\mu\nu}\right] \\ & + G_5(\phi, X)G^{\mu\nu}\phi_{\mu\nu} - \frac{G_{5X}}{6}\left[(\Box\phi)^3 - 3\Box\phi\phi^{\mu\nu} + 2\phi_{\mu\nu}\phi^{\nu\lambda}\phi^{\mu}_{\lambda}\right]\,, \end{aligned} \tag{3.7}$$

where $\phi_{\mu\nu} \equiv \nabla_{\mu}\nabla_{\nu}\phi$, $X \equiv g^{\mu\nu}\nabla_{\mu}\phi\nabla_{\nu}\phi$, and $\Box \equiv \nabla_{\mu}\nabla^{\mu}$. The term G_{4X} and G_{5X} represent the derivative of G_4 and G_5 with respect to X, respectively. Due to the divergence-free nature of the Einstein tensor ($\nabla_{\mu}G^{\mu\nu} = 0$), the Horndeski Lagrangian reduces to the NMDC form when the specific Horndeski terms are chosen as: $G_2 = -(\varepsilon/2)g_{\mu\nu}\nabla^{\mu}\phi\nabla^{\nu}\phi - V(\phi)$, $G_3 = 0$, $G_4 = (16\pi G)^{-1}$, $G_{4X} = 0$, $G_5 = \kappa\phi/2$, $G_{5X} = 0$. Equation (3.6) for the action guarantees second-order equation of motion for the dynamical fields. This avoids the higher-order time derivative ghost-like instability, commonly referred to as the Ostrogradski instability [25].

Varying the action in equation (3.6) with respect to the metric tensor yields the gravitational field equations

$$G_{\mu\nu} = 8\pi G(T^{(\mathrm{m})}_{\mu\nu} + T^{(\phi)}_{\mu\nu} + \kappa\Theta_{\mu\nu})\,, \tag{3.8}$$

where $T^{(\mathrm{m})}_{\mu\nu}, T^{(\phi)}_{\mu\nu}$ are energy-momentum tensor for dust matter and the free scalar field, respectively. The NMDC modification term to the Einstein field equation is given by $\kappa\Theta_{\mu\nu}$ where

$$\begin{aligned}\Theta_{\mu\nu} &= -\frac{1}{2}(\nabla_\mu\phi)(\nabla_\nu\phi)R + 2(\nabla_\alpha\phi)\nabla_{(\mu}\phi R^\alpha{}_{\nu)} + (\nabla^\alpha\phi)(\nabla^\beta\phi)R_{\mu\alpha\nu\beta} \\ &\quad +(\nabla_\mu\nabla^\alpha\phi)(\nabla_\nu\nabla_\alpha\phi) - (\nabla_\mu\nabla_\nu\phi)\Box\phi - \frac{1}{2}(\nabla\phi)^2 G_{\mu\nu} \\ &\quad +g_{\mu\nu}\left[-\frac{1}{2}(\nabla^\alpha\nabla^\beta\phi)(\nabla_\alpha\nabla_\beta\phi) + \frac{1}{2}(\Box\phi)^2 - (\nabla_\alpha\phi)(\nabla_\beta\phi)R^{\alpha\beta}\right] . \quad (3.9)\end{aligned}$$

Varying the action in equation (3.6) with respect to the scalar field yields the modified Klein-Gordon equation

$$\left[\varepsilon g^{\mu\nu} + \kappa G^{\mu\nu}\right]\nabla_\mu\nabla_\nu\phi = -V_\phi\,. \quad (3.10)$$

Cosmological studies are conducted within a spatially flat FLRW universe, characterized by the line element

$$\mathrm{d}s^2 = -\mathrm{d}t^2 + a^2(t)\mathrm{d}x^2\,, \quad (3.11)$$

where $\mathrm{d}x^2$ represents the Euclidean metric. Using the FLRW line element in the gravitational field equations (3.8), the $(0,0)$ component of the Friedmann equation is given by

$$3H^2 = 8\pi G\frac{\dot\phi^2}{2}\left(\varepsilon - 9\kappa H^2\right) + 8\pi G V(\phi) + 8\pi G\rho_{\mathrm{m}}\,, \quad (3.12)$$

and the (i,j) component of the Friedmann equation is expressed as

$$2\dot H + 3H^2 = -8\pi G\frac{\dot\phi^2}{2}\left[\varepsilon + \kappa(2\dot H + 3H^2 + 4H\ddot\phi\dot\phi^{-1})\right] + 8\pi G V(\phi) - 8\pi G P_{\mathrm{m}}\,. \quad (3.13)$$

According to the Friedmann equations, the NMDC effect modifies the kinetic term of both field equations. Applying the Klein-Gordon equation (3.10) to the FLRW metric yields the equation of motion for the scalar field, which is given by

$$\varepsilon(\ddot\phi + 3H\dot\phi) - 3\kappa(H^2\ddot\phi + 2H\dot H\dot\phi - 3\kappa H^3\dot\phi) = -V_{,\phi}\,. \quad (3.14)$$

3.4.1 No potential case

In the absence of a potential term and dust matter field, cosmological studies within a spatially flat FLRW universe governed by the model equation (3.12) yield the following asymptotic results [20]:

- For $\kappa > 0$, the model exhibits a early universe quasi-de Sitter phase without the need for a fine-tuned potential. The inflationary behavior of the model is influenced only by the NMDC coupling parameter.
- For $\kappa < 0$, the model predicts an initial singularity at early universe.

However, regardless of the sign of κ, the universe transitions to a non-acceleration phase at very late times, where the scale factor scales as $a(t) \propto t^{1/3}$.

3.4.2 Constant potential case

To achieve late-time accelerated expansion in the absence of dust matter, Sushkov and Saridakis (2010) [21] proposed a NMDC model incorporating a constant potential term for both quintessence ($\varepsilon > 0$) and phantom fields ($\varepsilon < 0$). The model exhibits a transition between two asymptotically de Sitter solutions i.e., inflation and late time de Sitter, which is a pure effect of the NMDC coupling. Moreover, it allows for various cosmological scenarios, including a Big Bang, cosmological turnaround, Big Crunch, or cosmological bounce, depending on the specific values of the coupling constant [21]. When a matter component is included in the NMDC model with $\kappa > 0$, it successfully describes several cosmological epochs. These include an inflation phase without any fine-tuned potential, the matter-dominated epoch, and the accelerated phase [26]. The accelerated expansion is driven by the constant potential term, which can be interpreted as a cosmological constant.

3.4.3 Potential without free kinetic term

The dynamics of the scalar field in the NMDC model were investigated by Gao [64]. In the absence of scalar kinetic and potential terms, as well as matter fields (radiation, dust, dark energy), Gao's analysis indicates that the NMDC scalar field tracks pressureless dark matter during the matter-dominated epoch. When including matter fields, the equation of state parameter for the NMDC scalar demonstrates that during the radiation-dominated, matter-dominated, and dark energy-dominated epochs, the NMDC scalar field behaves as curvature ($w = -1/3$), dark matter ($w = 0$), and stiff fluid ($w = 1$), respectively. With an exponential potential of the form $V(\phi) = e^{-\zeta\phi}$, the scalar field could serve as a candidate for both dark matter and dark energy, where the equation of state parameter satisfies $-1 \leq w \leq 0$. However, the dynamics of the scalar field field can lead it to cross into the phantom regime, which is physically unrealistic as it implies a superluminal sound speed. The work by Feng et al. [65] also studied the model without a free kinetic term, in conjunction with a curvaton model.

3.4.4 Free scalar field without potential term

In 2011, Gubitosi and Linder [66] showed that not only can a scalar field potential drive an accelerating universe, but a kinetic coupling gravity term can also lead to an accelerated universe. They propose the most general form of a purely kinetic coupling to gravity action that obeys a shift symmetry (Galileon symmetry),

$$S = \int \mathrm{d}^4x\sqrt{-g}\left[\left(\frac{c_1}{M_p^2}\nabla_\mu\phi\nabla_\nu\phi g^{\mu\nu} + \frac{c_2}{M_p^2}\Box\phi\right)R + \frac{c_3}{M_p^2}R^{\mu\nu}\nabla_\mu\phi\nabla_\nu\phi + \frac{c_4}{M_p^2}R^{\alpha\beta\gamma\delta}\Phi_{\alpha\beta\gamma\delta}\right], \tag{3.15}$$

where the c_i are dimensionless coefficients. This final form, which satisfies second-order equation of motion, yields the sum of the canonical kinetic term and the coupling to Einstein tensor, without potential term. The model achieve wide range

of w from stiff ($w = 1$) to phantom crossing ($w < -1$). Only a positive coupling constant can result in phantom crossing; however, it also leads to non-causal scalar and tensor perturbations, making the purely kinetic model unsuitable for inflation [27].

3.4.5 Power-law potential with matter field

The NMDC gravity model with a power-law potential, $V(\phi) = V_0\phi^N$, was analyzed using dynamical system techniques by Sushkov (2013) [28]. To achieve early inflation in the Universe, the potential exponent must satisfy $0 < N < 2$. In this scenario, NMDC inflation does not depend on the potential but is only determined by the coupling parameter κ. For $N > 2$, NMDC inflation becomes impossible. For the quadratic potential $N = 2$, two exponential asymptotic solutions exist, depending on the value of κ. One asymptotic solution corresponds to an inflationary regime, while the other represents late-time inflation. During strong coupling in inflation, fewer gravitational particles are produced [67]. Using the combined WMAP9, Plank+WP, and Plank *TT, TE, EE*+lowP+Lensing+ext datasets, the model gives a constant potential in the same order as cosmological constant. The model predicts a constant potential of the same order as the cosmological constant. The model results in a negative cosmological constant for power-law expansion, whereas phantom expansion leads to a positive cosmological constant [68]. The perturbation behavior of the NMDC model with a constant potential was further explored in [69] to confront observational data.

CHAPTER IV

HOLOGRAPHIC DARK ENERGY

4.1 Holographic principle

In cosmology, the concept of holographic dark energy arises from applying the holographic principle to the dark energy problem. The holographic principle has its origins in the study of black hole thermodynamics. One key issue with black holes is that when a system falls into one, it seems to be lost forever. This implies that the entropy of the system might decrease, which would violate the second law of thermodynamics. One states that the total entropy of an isolated system must always increase or remain constant, $\Delta S_{\text{system}} \geq 0$. To address this, Jacob Bekenstein proposed that black hole possess entropy and introduced the generalized second law of thermodynamics $\Delta S_{\text{system}} + \Delta S_{\text{BH}} \geq 0$ [70]. Later, Stephen Hawking applied semi-classical approach of quantum field theory in curved spacetime to black holes, leading to two important conclusions. First, black holes can radiate. Second, the entropy of a black hole is proportional to the area of its event horizon, as given by [71, 72],

$$S_{\text{BH}} = \frac{A}{4G}, \tag{4.1}$$

where natural units are adopted, with $c = \hbar = k_B = 1$.

One of the outstanding mysteries in black hole physics is the information paradox. Quantum mechanics dictates that information cannot be destroyed, while general relativity implies that anything falling into a black hole is lost to our observable Universe. This apparent contradiction gives rise the information paradox. Leonard Susskind addressed this issue by proposing the idea of black hole complementarity [73, 74]. According to this theory, information falling into a black hole

exists in two complementary states, depending on the observer's reference frame. For an outside observer, the information appears to be frozen at the event horizon and is eventually released as Hawking radiation. For an infalling observer, the information crosses the event horizon and continues towards the singularity. This suggests a way for information to be preserved, even though it seem to vanish from the outside observer's perspective. Black hole complementarity implies that the three-dimensional information falling into a black hole, quantified by its entropy, is somehow encoded on the two-dimensional surface of the event horizon, in accordance with the Beckenstein-Hawking entropy. This connection leads to the holographic principle, which proposes that the interplay between quantum mechanics and gravity requires the three-dimensional Universe to be encoded on a two-dimensional boundary, similar to a hologram [75]. Susskind later explored the string theory interpretation of this principle [76]. For a more detailed discussion, see the review paper by Bousso [77].

4.2 UV/IR Correspondence

Effective field theory (EFT) is highly effective at describing particle physics at low energies. However, it begins to break down at very high energies. This breakdown occurs because EFT works by integrating out high-energy degrees of freedom, imposing an ultraviolet (UV) cutoff, which acts as the maximum energy scale for its validity. Furthermore, EFT faces challenges in describing systems with large volumes due to the non-extensive scaling behavior of black hole entropy.

In EFT, the entropy S of a system typically increases with the size L of the system, with a UV cutoff Λ. This represents an extensive relationship between entropy and system size. However, based on black hole thermodynamics, Bekenstein proposed that the maximum entropy within a fixed volume does not increase indefinitely. Instead, it is proportional to the surface area of the region, not its vol-

ume. This is called Bekenstein bound. Later, 't Hooft and Susskind demonstrated that the Bekenstein bound could still be satisfied in EFT, but only if the size of the system is limited by the following equation

$$L^3\Lambda^3 \lesssim S_{\rm BH} \equiv \pi L^2 M_p^2, \tag{4.2}$$

where πL^2 represents the area of the system, and $S_{\rm BH}$ is the entropy of a black hole with Schwarzschild radius L. Here, L can be interpreted as the IR cutoff, representing a lower energy limit below which the EFT description also breaks down.

However, when considering the system in terms of temperature (T), the Schwarzschild radius will be larger than the box size. This occurs because the thermal energy can be expressed as $M \sim L^3T^4$, and entropy $S \sim L^3T^3$. If the Bekenstein bound (4.2) is saturates(i.e., hold with equality), we obtain $T \sim (M_p^2/L)^{1/3}$. The Schwarzschild radius ($L_s = 2GM$) then scales as $L_s \sim L(M_pL)^{2/3} > L$. This demonstrates that according to the bound, the Schwarzschild radius is indeed larger than the box size.

To resolve this issue, Cohen, Kaplan, and Nelson (CKN) [78] proposed a new constraint connecting the UV and IR cutoffs. They considered the maximum energy density Λ^4 within a system of size L. Their suggestion was that the energy density of the quantum field should not exceed the mass of a black hole of the same size. This leads to the constraint

$$L^3\Lambda^4 \lesssim LM_p^2. \tag{4.3}$$

This constraint is more stringent than the Bekenstein bound (4.2). When the inequality (4.3) approaches saturation, the maximum entropy of the effective field is given by

$$S_{\rm max} \simeq S_{\rm BH}^{3/4}, \tag{4.4}$$

and this implies that the maximum size of the system is equivalent to the Schwarzschild radius, $L_s \sim L$. Equation (4.3) suggests that in all effective field theories, the UV cutoff is correlated with the IR cutoff due to the constraints imposed by the formation of black holes. This relationship is known as the UV/IR correspondence.

4.3 Holographic dark energy model

Let E_Λ represents the quantum zero-point energy cut off by the UV cutoff. According to the CKN conjecture, the maximum energy within a box of size L should not exceed the mass of a black hole of the same size. To explore this further, consider the energy of a field theory with a UV cutoff

$$E_\Lambda = \rho_\Lambda L^3 , \tag{4.5}$$

where ρ_Λ is the corresponding energy density within the box of size L. The Schwarzschild mass is given by $M_s = L_s/(2G) \sim L_s M_p^2$. This leads to the following constraint

$$\rho_\Lambda L^3 \lesssim L_s M_p^2 , \tag{4.6}$$

The maximum allowed energy density satisfies

$$\rho_\Lambda \sim M_p^2 L_s^{-2} . \tag{4.7}$$

Equation (4.7) suggests that the maximum energy density with UV cutoff inside the box is determined by the Schwarzschid radius, L_s, which acts as the IR cutoff.

The dependence of energy density on the length scale L motivated Miao Li (2004) [31] to explore its application in the context of dark energy. Consider a universe with a cosmological length scale L. According to the holographic principle, the energy density of dark energy could be described by quantities on the surface boundary. This implies that the energy density can be constructed using only two fundamental physical quantities: the Planck mass M_p and the cosmological length

scale L. Using dimensional analysis, we obtain the following equation

$$\rho_\Lambda = c_1 M_p^4 + c_2 M_p^2 L^{-2} + c_3 L^{-4} + \dots, \tag{4.8}$$

where c_1, c_2, c_3 are numerical constants. The first term of the equation (4.8) represents the cosmological constant. However, this term is disfavor because it predicts a vacuum energy discrepancy that is about 10^{120} times larger than observed, which is one of the central issues in the cosmological constant problem. The second term in equation (4.8) aligns with the CKN bound in equation (4.7). Therefore, we can neglect the other terms, leading to the following expression for ρ_Λ

$$\rho_\Lambda = \frac{3c^2}{8\pi G L^2}, \tag{4.9}$$

where we set $c_2 = 3c^2$ for convenience, and use the relationship $M_p^2 = 1/(8\pi G)$. Equation (4.9) suggests a connection between the density of dark energy and the area of the cosmological horizon. This model is known as the holographic dark energy (HDE) model.

This form of dark energy can be interpreted as a type of cosmological constant arising from vacuum energy within an effective field theory. However, it differs from Einstein's cosmological constant. In contrast to the constant term in Einstein's theory, this dark energy density (4.9) depends on the cosmological length scale L. It's important to note that the HDE model also differs from other dark energy models. While other models introduce additional terms into the Lagrangian, HDE is derived from the holographic principle and dimensional analysis.

Next, we will explore the cosmological behavior associated with different choices of the cosmological cutoff L.

4.3.1 Hubble horizon cutoff

The simplest choice for the cosmological length scale is the Hubble radius,

defined as

$$L = \frac{1}{H}. \tag{4.10}$$

Substituting this length scale into the holographic dark energy equation (4.9), the energy density of HDE becomes

$$\rho_\Lambda = \frac{3c^2H^2}{8\pi G}. \tag{4.11}$$

This equation relates the energy density of dark energy to the Hubble parameter H, where c is a dimensionless constant.

Considering the current size of the Universe, $L = 1/H_0 \sim 10^{28}$ cm (where H_0 is the present Hubble constant), setting $c = 1$ for entirely HDE domination, this leads to an energy density compatible with the observed value of dark energy, which is around $\rho_\Lambda \sim 10^{-47}\text{GeV}^4$ [79, 80].

However, Hsu(2004) [32] points out that EoS parameter of HDE is dust-like behavior. In a flat FLRW universe with a combination of barotropic matter and HDE, the Friedmann equation is $3H^2 = 8\pi G(\rho_\text{m} + \rho_\Lambda)$. Given the HDE energy density in equation (4.11), the density of barotropic matter can be expressed as

$$\rho_\text{m} = \frac{3(1-c^2)}{8\pi G}H^2. \tag{4.12}$$

This indicates that the energy density of dut matter and HDE both scale with H^2. As the energy density of dust ρ_m scales with scale factor as $\rho_\text{m} \sim a^{-3}$, the evolution of HDE would similarly scale as $\rho_\Lambda \sim a^{-3}$. This suggests that the EoS for HDE would be $w_\Lambda = 0$. This implies that the HDE behaves like dust, with no acceleration phase for the Universe.

4.3.2 Particle horizon cutoff

Since the Hubble horizon cutoff leads to an incorrect EoS, Fischler and Susskind [81] investigated a particle horizon cutoff as an alternative cosmological

length scale. Let us consider the particle horizon, defined as follows

$$L = R_p = a\int_0^t \frac{d\tilde{t}}{a} = a\int_0^a \frac{d\tilde{a}}{H\tilde{a}^2}. \tag{4.13}$$

With this definition, the HDE energy density equation (4.9) can be rewritten as

$$\rho_\Lambda = \frac{3c^2}{8\pi G R_p^2}. \tag{4.14}$$

In a flat FLRW universe where the HDE-dominated epoch, the Friedmann equation can be expressed as

$$H^2 = \frac{8\pi G}{3}\rho_\Lambda = \frac{c^2}{R_p^2}. \tag{4.15}$$

Using the definition of R_p, we obtain

$$\int_0^a \frac{d\tilde{a}}{H\tilde{a}^2} = \frac{c}{Ha}. \tag{4.16}$$

For simplicity, let us introduce $X = 1/(Ha)$ and differentiate it with respect to the scale factor. This yields

$$\begin{aligned} \frac{d}{da}\int_0^a \frac{d\tilde{a}}{H\tilde{a}^2} &= c\frac{dX}{da}, \\ \frac{1}{Ha^2} &= c\frac{dX}{da}, \\ \frac{X}{a} &= c\frac{dX}{da}, \\ \int \frac{da}{a} &= c\int \frac{dX}{X}. \end{aligned} \tag{4.17}$$

Following these steps, we arrive at the solution

$$\begin{aligned} X &= \alpha a^{1/c}, \\ \frac{1}{Ha} &= \alpha a^{\frac{1}{c}}, \\ H^{-1} &= \alpha a^{1+\frac{1}{c}}, \end{aligned} \tag{4.18}$$

where α is a constant. Equation (4.18) describes the evolution of the scale factor for HDE with a particle horizon cutoff. Substituting equation (4.18) into equation (4.13), the particle horizon becomes

$$R_H = \alpha a\int_0^a \frac{d\tilde{a}}{\tilde{a}^2}\tilde{a}^{1+\frac{1}{c}} = \alpha c a^{\frac{1}{c}+1}.$$

Therefore, the HDE energy density equation (4.14) can be written as

$$\rho_\Lambda = \frac{3}{8\pi G\alpha^2} a^{-2(\frac{1}{c}+1)}. \tag{4.19}$$

Assuming the HDE does not interact with other components, it will satisfy the following conservation equation

$$\dot{\rho}_\Lambda + 3H(1+\omega_\Lambda)\rho_\Lambda = 0. \tag{4.20}$$

Substituting equation (4.19) into the conservation equation (4.20), we obtain the EoS for HDE with a particle horizon cutoff

$$\begin{aligned} -2(\frac{1}{c}+1) &= -3(1+\omega_\Lambda), \\ \omega_\Lambda &= -\frac{1}{3} + \frac{2}{3c}. \end{aligned} \tag{4.21}$$

According to equation (4.15), $c = HR_H$, and since both H and R_H are positive, the constant c is always positive. This implies that the HDE EoS, ω_Λ, is always greater than $-1/3$. As a result, the particle horizon cutoff scenario does not predict an accelerating phase for the Universe.

4.3.3 Future event horizon cutoff

According to the EoS for the particle horizon, equation (4.21), the EoS is always greater than $-1/3$. This leads Li (2004) [31] to propose replacing the particle horizon with the future event horizon cutoff. The future event horizon cutoff is defined by the integrals

$$R_h = a\int_t^\infty \frac{d\tilde{t}}{a} = a\int_a^\infty \frac{d\tilde{a}}{H\tilde{a}^2}. \tag{4.22}$$

Again, considering a flat FLRW universe dominated by HDE, the Friedmann equation becomes

$$\int_a^\infty \frac{d\tilde{a}}{H\tilde{a}^2} = \frac{c}{Ha}. \tag{4.23}$$

Setting $X = 1/(Ha)$ and differentiating equation (4.23) with respect to the scale factor a, we obtain

$$\begin{aligned} -\frac{X}{a} &= c\frac{dX}{da}, \\ \int \frac{da}{a} &= -c\int \frac{dX}{X}. \end{aligned} \tag{4.24}$$

Following these steps, we arrive at the solution

$$H^{-1} = \alpha a^{1-\frac{1}{c}}. \tag{4.25}$$

The future event horizon is then given by

$$R_H = \alpha c a^{1-\frac{1}{c}}. \tag{4.26}$$

The corresponding HDE energy density can be expressed as

$$\rho_\Lambda = \frac{3}{8\pi G\alpha^2} a^{-2(1-\frac{1}{c})}. \tag{4.27}$$

According to the HDE conservation equation (4.20), the EoS for HDE with future event horizon cutoff is

$$\begin{aligned} -2(1-\frac{1}{c}) &= -3(1+\omega_\Lambda), \\ \omega_\Lambda &= -\frac{1}{3} - \frac{2}{3c}. \end{aligned} \tag{4.28}$$

In the special case of $c = 1$, the behavior of HDE is similar to a cosmological constant, with $w_\Lambda = -1$. For any value of $c > 0$, this implies an accelerating expansion of the Universe because the HDE EoS is always less than $-1/3$. However, the future event horizon cutoff faces a causality problem [82, 83]. Since the horizon lies in the future, it cannot be used to predict the current behavior of the Universe.

4.3.4 Ricci dark energy

Due to the causality issues associated with the future event horizon cutoff, Gao et al.(2009) [84] proposed a new approach that uses the Ricci scalar curvature,

R, as the cosmological cutoff. The Ricci scalar is related to the cutoff by the expression

$$L \propto \frac{1}{R^{1/2}}. \tag{4.29}$$

Consequently, the HDE density equation (4.9) is modified to

$$\rho_\Lambda = -\frac{\alpha}{16\pi G}R = \frac{3\alpha}{8\pi G}\left(\dot{H}+2H^2+\frac{k}{a^2}\right), \tag{4.30}$$

where α is a numerical constant. A more generalized version of the flat Ricci cutoff was also proposed by Granda and Oliveros (2009) [85], given by

$$\rho_\Lambda = \frac{3}{8\pi G}\left(\alpha H^2+\beta\dot{H}\right). \tag{4.31}$$

In flat FLRW cosmology, the Friedmann equation can be expressed as

$$H^2 = \frac{8\pi G}{3}\left(\rho_{\rm m}+\rho_{\rm r}\right)+\alpha(\dot{H}+2H^2). \tag{4.32}$$

A general solution of this equation is given by

$$h^2 = \Omega_{\rm m0}e^{-3N}+\Omega_{\rm r0}e^{-4N}-\left(\frac{\alpha}{\alpha-2}\right)\Omega_{\rm m0}e^{-3N}+f_0e^{\left(\frac{2}{\alpha}-4\right)N}, \tag{4.33}$$

where $h = H/H_0$ is the normalized Hubble parameter and $N = \ln a$ is the e-folding number. According to the solution equation (4.33), the last two terms represent the Ricci dark energy component. This gives the energy density of Ricci dark energy as

$$\rho_\Lambda = \frac{\alpha}{2-\alpha}\Omega_{\rm m0}e^{-3N}+f_0e^{\left(-4+\frac{2}{\alpha}\right)N}, \tag{4.34}$$

where

$$f_0 = \frac{3w_{\Lambda0}\Omega_{\Lambda0}^2}{3w_{\Lambda0}\Omega_{\Lambda0}-\Omega_{\rm m0}}, \quad \alpha = \frac{2\Omega_{\Lambda0}}{\Omega_{\rm m0}+\Omega_{\Lambda0}-3w_{\Lambda0}\Omega_{\Lambda0}}. \tag{4.35}$$

Assuming energy conservation, the pressure of Ricci dark energy can be obtained from the conservation equation as

$$p_\Lambda = -\left(\frac{2}{3\alpha}-\frac{1}{3}\right)f_0e^{\left(-4+\frac{2}{\alpha}\right)N}. \tag{4.36}$$

Using equation (4.34) and (4.36), the EoS for Ricci dark energy at the present time can be expressed as

$$\omega_{\Lambda 0} = -\left(\frac{2}{3\alpha} - \frac{1}{3}\right)\frac{f_0}{\Omega_{\Lambda 0}}. \tag{4.37}$$

Based on current observations, with $\Omega_{\Lambda 0} = 0.73, \Omega_{\mathrm{m}0} = 0.27, f_0 = 0.65$ and $\alpha = 0.46$, the current EoS of Ricci dark energy is $w_{\Lambda 0} = -1$. This Ricci dark energy model is phenomenologically viable and avoid the causality problem encountered with the future event horizon cutoff. However, a deeper understanding of the Ricci scalar as a cosmological length scale remains elusive. The observational constraint for the parameter α in the Ricci dark energy model, obtained from a joint analysis of the SNIa, CMB, and BAO data, is $\alpha = 0.359^{+0.024}_{-0.025}$ [86]. This suggests that Ricci dark energy exhibits behavior similar to a quintom model, starting in a quintessence-like phase and evolving to become phantom-like.

CHAPTER V

COSMOLOGY DYNAMICS OF NON-MINIMAL DERIVATIVE COUPLING WITH HOLOGRAPHIC CUTOFF

As discussed in Chapter IV, the behavior of HDE is influenced by the choices of cosmological cutoff, such as the Hubble horizon cutoff, particle horizon cutoff, future particle horizon cutoff, or Ricci HDE. Among these different choices, the Hubble horizon emerges as a natural candidate. The HDE energy density is constructed based on the maximum energy bound, which corresponds to the formation of a black hole, where the infrared (IR) cutoff L is chosen as the black hole's event horizon. In this context, the cosmological horizon should exhibit similar characteristics to the event horizon of a black hole. Cosmic volume should be enclosed by a trapped-null surface, whose horizon is inaccessible to light signals. In an accelerating Universe, a trapped-null surface exists when the apparent horizon cutoff is used in a spatially curved Universe such that light signals can never reach the horizon. The apparent horizon cutoff given by

$$r_{\mathrm{A}} = \frac{1}{\sqrt{H^2 + k/a^2}}, \tag{5.1}$$

where k represents the spatial curvature, and a is the scale factor. Furthermore, the apparent horizon plays a crucial role in the thermodynamic description of the Universe. Cai & Kim (2005) [87] demonstrated that the Friedmann equation can be derived by applying the apparent horizon to the Hawking temperature, $T = 1/(2\pi r_{\mathrm{A}})$, along with Bekenstein entropy, $S = A/G$, within the framework of the first law of thermodynamics $(-dE = TdS)$.

This strongly motivates retaining the Hubble horizon, or the apparent horizon in spatially curved spacetime, within HDE theory. However, the limitations of the Hubble cutoff, particularly its tendency to produce dust-like behavior, lead us

to explore HDE within the context of Non-minimal Derivative Coupling (NMDC) theories in spatially curved spacetimes.

5.1 NMDC with HDE action and field equations

The Einstein-Hilbert action, together with a NMDC scalar field, dust matter, and holographic vacuum energy, is given by

$$S = \int \mathrm{d}^4x\sqrt{-g}\left[\frac{R}{16\pi G} - \frac{(\varepsilon g_{\mu\nu} + \kappa G_{\mu\nu})}{2}(\nabla^\mu\phi)(\nabla^\nu\phi) - V(\phi)\right] + S_{\mathrm{m},\Lambda}\,, \tag{5.2}$$

where ε is $+1$ for a canonical scalar field and -1 for a phantom scalar field. κ is the NMDC coupling constant with the dimension of $mass^{-2}$. The first term in brackets in the action (5.2) contains the curvature information of spacetime, while the second term represents the NMDC field. The terms S_{m} and S_Λ denote the actions of dust matter and holographic vacuum energy, respectively. It is important to note that HDE is constructed based on the holographic principle. However, it may also be derived from an action principle, as suggested by [88, 89, 90], similar to other dark energy models. Therefore, it is reasonable to formulate HDE within an action in a general form.

Taking the variation on the action (5.2) with respect to the metric tensor $g^{\mu\nu}$ leads to the Einstein field equation [2]

$$G_{\mu\nu} = 8\pi G\left(T^{(\mathrm{m})}_{\mu\nu} + T^{(\phi)}_{\mu\nu} + \kappa\Theta_{\mu\nu} + T^{(\Lambda)}_{\mu\nu}\right)\,, \tag{5.3}$$

where $T^{(\mathrm{m})}_{\mu\nu}, T^{(\phi)}_{\mu\nu},, \Theta_{\mu\nu}$, and $T^{(\Lambda)}_{\mu\nu}$ represent the energy-momentum tensors of dust, the scalar field, and the NMDC coupling, and HDE, respectively. The expressions for the energy-momentum tensors of dust, scalar field and NMDC coupling are

[2]The detailed calculations are presented in the Appendix A.

given by

$$T^{(\mathrm{m})}_{\mu\nu} = g_{\mu\nu}\mathcal{L}_{\mathrm{m}} - \frac{\delta\mathcal{L}_{\mathrm{m}}}{\delta g^{\mu\nu}}\,, \tag{5.4}$$

$$T^{(\phi)}_{\mu\nu} = \varepsilon(\nabla_\mu\phi)(\nabla_\nu\phi) - \frac{\varepsilon}{2}g_{\mu\nu}(\nabla_\sigma\phi)(\nabla^\sigma\phi) - V(\phi)g_{\mu\nu}\,, \tag{5.5}$$

$$\begin{aligned}\Theta_{\mu\nu} = {} & -\frac{1}{2}(\nabla_\mu\phi)(\nabla_\nu\phi)R + 2(\nabla_\sigma\phi)\nabla_{(\nu}\phi R^\sigma_{\mu)} + (\nabla^\sigma\phi)(\nabla^\lambda\phi)R_{\nu\lambda\mu\sigma} \\ & + (\nabla_\mu\nabla_\sigma\phi)(\nabla_\nu\nabla^\sigma\phi) - (\nabla_\mu\nabla_\nu\phi)\Box\phi - \frac{1}{2}(\nabla_\sigma\phi)(\nabla^\sigma\phi)G_{\mu\nu} \\ & + g_{\mu\nu}\left(\frac{1}{2}(\Box\phi)^2 - (\nabla^\sigma\phi)(\nabla^\rho\phi)R_{\sigma\rho} - \frac{1}{2}(\nabla_\rho\nabla_\sigma\phi)(\nabla^\rho\nabla^\sigma\phi)\right)\,,\end{aligned} \tag{5.6}$$

where D'Alembertian operator is defined as $\Box \equiv \nabla_\sigma\nabla^\sigma$. However, the exact form of the energy-momentum tensor for HDE remains unknown.

Taking the variation of the action in equation (5.2) with respect to the scalar field yields the modified Klein-Gordon equation

$$\varepsilon\nabla_\mu\nabla^\mu\phi + \kappa G_{\mu\nu}\nabla^\mu\nabla^\nu\phi - V_{,\phi} = 0\,, \tag{5.7}$$

where $V_{,\phi} \equiv \mathrm{d}V(\phi)/\mathrm{d}\phi$. The equation provides the equation of motion for the scalar field. Due to Bianchi identity $\nabla^\mu G_{\mu\nu} = 0$, the modified energy-momentum tensor must satisfy the conservation law

$$\nabla^\mu[T^{(\phi)}_{\mu\nu} + \kappa\Theta_{\mu\nu}] = 0\,. \tag{5.8}$$

5.2 Cosmological dynamics: Flat case

Let us consider the NMDC model in a flat FLRW universe. The Friedmann equation can be interpreted in two ways as follows:

$$H^2 = \frac{8\pi G}{3}\left[\frac{\dot\phi^2}{2}\left(\varepsilon - 9\kappa H^2\right) + V(\phi) + \rho_m + \rho_\Lambda\right]\,, \tag{5.9}$$

or

$$H^2 = \frac{8\pi G_{\mathrm{eff}}}{3}\left[\frac{\varepsilon\dot\phi^2}{2} + V(\phi) + \rho_m + \rho_\Lambda\right]\,. \tag{5.10}$$

Although equations (5.9) and (5.10) are mathematically equivalent, they offer two distinct interpretations of the Universe's behavior. In the first interpretation, equation (5.9) describes an FLRW universe with a standard gravitational constant, G. Here, the Universe is filled with dust matter, holographic vacuum energy, and a scalar field with a modified kinetic term due to the NMDC field, $(1/2)\dot{\phi}^2(\varepsilon - 9\kappa H^2)$. In the second interpretation, equation (5.10) describes a Universe with an effective gravitational constant, G_{eff}, which is modified by the kinetic term of the scalar field. The effective gravitational constant is given by the relation

$$G_{\text{eff}}(\dot{\phi}) \equiv \frac{G}{1 + 12\pi G\kappa\dot{\phi}^2}. \tag{5.11}$$

In this picture, the Universe is filled with dust matter, holographic vacuum energy, and a canonical ($\varepsilon = 1$), or phantom ($\varepsilon = -1$), scalar field. We consider only the case of a canonical scalar field. These two interpretations lead to different values for the gravitational constant when defining the holographic vacuum energy density. Depending on which picture we choose, the HDE energy density equation (4.9) will take on a corresponding form.

In the context of a flat Universe, the apparent horizon coincides with the Hubble horizon, $L = H^{-1}$. This implies that the holographic energy density can be expressed in either of the following ways

$$\rho_\Lambda = \frac{3c^2H^2}{8\pi G}, \tag{5.12}$$

or

$$\rho_\Lambda = \frac{3c^2H^2}{8\pi G_{\text{eff}}} = \frac{3c^2H^2}{8\pi G}(1 + 12\pi G\kappa\dot{\phi}^2). \tag{5.13}$$

The second Friedmann equation, which corresponds to the (i, j) components of the field equation (5.3) in a flat FLRW universe, can be expressed as

$$2\dot{H} + 3H^2 = -8\pi G\left\{\frac{\dot{\phi}^2}{2}\left[1 + \kappa\left(2\dot{H} + 3H^2 + 4H\ddot{\phi}\dot{\phi}^{-1}\right)\right] - V(\phi) + P_{\text{m}} + P_\Lambda\right\}, \tag{5.14}$$

or, in terms of G_{eff}, we obtain

$$2\dot{H}+3H^2 \;=\; -8\pi G_{\text{eff}}\left\{\frac{\dot{\phi}^2}{2}\left[1-\kappa\left(4\dot{H}+6H^2-4H\ddot{\phi}\dot{\phi}^{-1}\right)\right]-V(\phi)+P_{\text{m}}+P_{\Lambda}\right\}. \tag{5.15}$$

The equation (5.7) in a flat FLRW universe gives the Klein-Gordon equation,

$$\ddot{\phi}+3H\dot{\phi} \;=\; -\frac{V_{\phi}}{\varepsilon-3\kappa H^2}+\frac{6\kappa H\dot{H}\dot{\phi}}{\varepsilon-3\kappa H^2}, \tag{5.16}$$

where V_{ϕ} denotes the derivative of the potential with respect to the scalar field. This equation describes how the scalar field evolves in the context of a Universe that is expanding, incorporating the effects of both the potential energy associated with the scalar field and the additional modifications due to the NMDC coupling.

Equation (5.13) has been previously explored in flat FLRW spacetime [91, 41]. To avoid redundancy, we will focus on the first interpretation (5.12) alongside the corresponding Friedmann equation (5.9). There is another reason to concentrate on the first interpretation (5.12). In curved spacetime, the NMDC term that modifies curvature cannot be entirely captured within the effective gravitational constant, $G_{\text{eff}}(\dot{\phi})$. This is because, in NMDC theory, an effective gravitational constant cannot be expressed at the Lagrangian level. While $G_{\text{eff}}(\dot{\phi})$ can be incorporated at the Friedmann equation level in the flat case, this approach becomes problematic when dealing with more general scenarios involving curved spacetime. In other words, the concept of an effective gravitational constant breaks down at the Friedmann equation level when non-zero curvature is introduced.

To explore cosmological dynamics, an autonomous system is constructed using equations (5.9), (5.12), and (5.16). The dimensionless dynamical variables are defined as follows

$$x \;\equiv\; \frac{8\pi G\dot{\phi}^2}{6H^2},\quad y \;\equiv\; \frac{8\pi GV(\phi)}{3H^2},\quad r \;\equiv\; -12\pi G\kappa\dot{\phi}^2,\quad \Omega_m \;\equiv\; \frac{8\pi G\rho_m}{3H^2}, \tag{5.17}$$

The variables x, y, r and $\Omega_{\rm m}$ represent the kinetic term, potential, NMDC coupling, and dust density parameter, respectively. The Friedmann equation (5.9) can be expressed as

$$1 \;=\; x+y+r+\Omega_{\rm m}+c^2\,, \tag{5.18}$$

where $c^2 = 8\pi G\rho_\Lambda/(3H^2)$ represents the density parameter of HDE. Therefore, the Friedmann constraint becomes

$$\Omega_{\rm m} \;=\; 1-x-y-r-c^2\,. \tag{5.19}$$

We can represent the dust density parameter, $\Omega_{\rm m}$, as a function of the dynamical variables $\{x, y, r\}$. We consider a power-law potential given by

$$V(\phi) \;=\; V_0\phi^n\,. \tag{5.20}$$

The autonomous system of these variables is given by [3]

$$\begin{aligned} x' &= 2x\,(\epsilon-\delta)\,,\\ y' &= 2y\left(\frac{nu}{2}+\epsilon\right),\\ r' &= -2r\delta\,,\\ u' &= u\,(\epsilon-\delta)\,, \end{aligned} \tag{5.21}$$

where prime " $'$ " denotes differentiation with respect to e-folding number, $N = \ln a$. We define the following quantities

$$\delta \;\equiv\; -\frac{\ddot{\phi}}{H\dot{\phi}},\quad \epsilon \;\equiv\; -\frac{\dot{H}}{H^2},\quad \text{and,}\quad u \;\equiv\; \frac{\dot{\phi}}{H\phi}\,. \tag{5.22}$$

The autonomous system is closed since the parameters ϵ and δ are determined by the other dynamical variables:

$$\delta \;=\; \frac{6x(2r-3+3c^2)-3nuy(1-c^2)-ry(6-nu)}{-2r^2-6x(1-c^2)+2r(x-1+c^2)}\,, \tag{5.23}$$

[3]The detailed calculations are presented in the Appendix E.

$$\epsilon = \frac{-3r^2 + 9x(-1 + c^2 - x + y) + r(-3 + 3c^2 - 12x + 3y - 2nuy)}{-2r^2 - 6x(1 - c^2) + 2r(x - 1 + c^2)}. \quad (5.24)$$

Considering the Friedmann equation (5.9), which can be interpreted as $3H^2 = 8\pi G\rho_{\text{tot}}$, along with equation (5.14), interpreted as $2\dot{H} + 3H^2 = -8\pi G P_{\text{tot}}$, the effective equation of state parameter, defined as $w_{\text{eff}} = P_{\text{tot}}/\rho_{\text{tot}}$, is given by

$$w_{\text{eff}} = -1 - \frac{2\dot{H}}{3H^2} = -1 + \frac{2\epsilon}{3}. \quad (5.25)$$

5.2.1 Numerical solution

To simplify the comparison of our solution with observational data, we transform the argument of the derivative from the e-folding number, $N = \ln a$, to the redshift parameter, z, as follows:

$$\frac{\mathrm{d}x}{\mathrm{d}z} = \frac{\mathrm{d}x}{\mathrm{d}N} \cdot \frac{\mathrm{d}N}{\mathrm{d}z} = \frac{\mathrm{d}x}{\mathrm{d}N} \cdot \frac{\mathrm{d}\ln a}{\mathrm{d}a} \cdot \frac{\mathrm{d}a}{\mathrm{d}z}. \quad (5.26)$$

Using the connection between the scale factor, a, and the redshift, z, we obtain

$$a = \frac{1}{1+z}, \quad (5.27)$$

and

$$\frac{\mathrm{d}a}{\mathrm{d}z} = -\frac{1}{(1+z)^2}. \quad (5.28)$$

The expression for the derivative of the dynamical variable with respect to redshift is given by

$$\frac{\mathrm{d}x}{\mathrm{d}z} = \frac{-1}{(1+z)}\frac{\mathrm{d}x}{\mathrm{d}N} = \frac{-1}{(1+z)}x'. \quad (5.29)$$

Hence, the autonomous system becomes

$$\begin{aligned}
\frac{\mathrm{d}x}{\mathrm{d}z} &= -\frac{2x(\epsilon - \delta)}{(1+z)}, \\
\frac{\mathrm{d}y}{\mathrm{d}z} &= -\frac{2y(nu/2 + \epsilon)}{(1+z)}, \\
\frac{\mathrm{d}r}{\mathrm{d}z} &= \frac{2r\delta}{(1+z)},
\end{aligned}$$

$$\frac{du}{dz} = -\frac{u(\epsilon - \delta)}{(1+z)}. \tag{5.30}$$

The autonomous system can be integrated numerically. Figure 1 presents the solutions for the effective equation of state parameter, $w_{\text{eff}}(z)$, and the Hubble parameter, $H(z)$. Here, we consider a power-law potential with $n = 2$, corresponding to a potential of the form $V(\phi) = V_0\phi^2$. The parameter c takes on values of $0, 0.1, 0.5, 0.7$ and 0.9.

The numerical solutions are compared with the observed $H(z)$ error bar at low redshift, as reported in [92]. Figure 1 indicates that a positive coupling constant ($\kappa > 0$) does not yields acceptable results for either $w_{\text{eff}}(z)$ or $H(z)$. The data favor a negative coupling constant ($\kappa < 0$), particularly with a large magnitude (e.g., $\kappa = -200$ in the units of $8\pi G = 1$) to match the observed $H(z)$ data.

A larger value of the parameter c corresponds to a higher holographic vacuum energy density, which increases both the slope and magnitude of $w_{\text{eff}}(z)$ and $H(z)$. A large negative NMDC coupling constant, combined with a significant fraction of holographic vacuum density, can enhance the phantom effect. In fact, if the negative NMDC coupling is sufficiently strong, w_{eff} can enter the phantom region, as illustrated in Figure 1.

5.3 Cosmological dynamics: Non-flat case

The introduction of non-zero curvature in holographic NMDC cosmology significantly alters cosmological dynamics by incorporating the curvature term,k. The apparent horizon, defined by equation (5.1), is selected as the cosmological length scale. As a result, the holographic vacuum energy density, expressed by equation (4.9), becomes

$$\rho_\Lambda = \frac{3c^2}{8\pi G}\left(H^2 + \frac{k}{a^2}\right). \tag{5.31}$$

This leads to a modified Friedmann equation derived from the field equations (5.3),

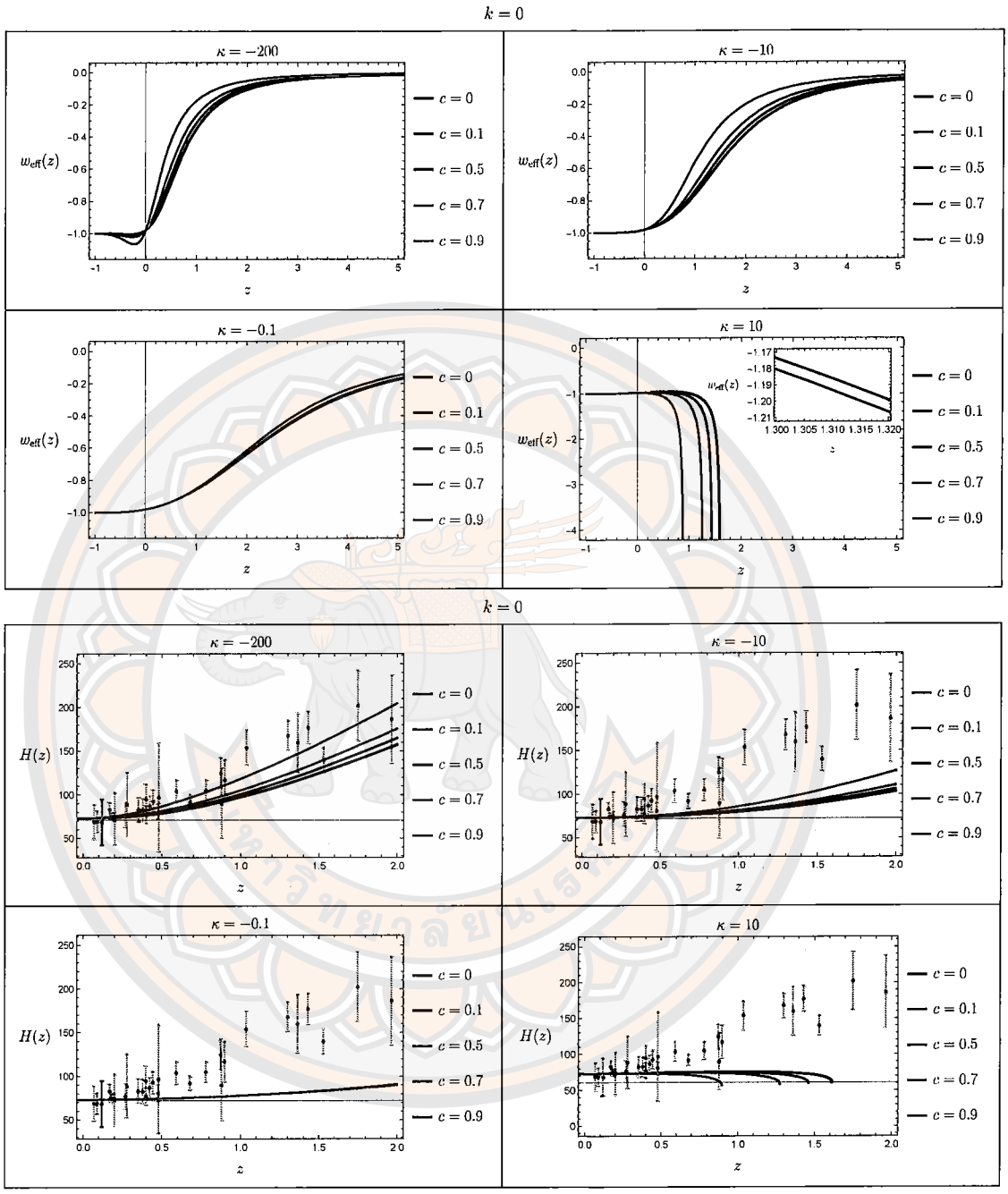

Figure 1 **Numerical solutions of $w_{\text{eff}}(z)$ and $H(z)$ for flat universe case**

which takes the form[4],

$$3H^2 + \frac{3k}{a^2} = 8\pi G \left\{ \frac{\dot{\phi}^2}{2} \left[1 - \kappa \left(9H^2 + \frac{3k}{a^2} \right) \right] + V(\phi) + \rho_m + \rho_\Lambda \right\} . \quad (5.32)$$

By factoring the Friedmann equation in terms of the effective gravitational con-

[4]The detailed calculations are presented in the Appendix B

stant, G_{eff}, it can be written as

$$3H^2 + \frac{3k}{a^2} = 8\pi G_{\text{eff}} \left[\frac{\dot{\phi}^2}{2} + V(\phi) + \frac{3\kappa k \dot{\phi}^2}{a^2} + \rho_{\text{m}} + \rho_{\Lambda} \right], \tag{5.33}$$

indicating how the curvature term influences the modified Friedmann dynamics in this context.

According to equation (5.33), a crucial term is the NMDC-curvature coupling term, $3\kappa k\dot{\phi}^2/a^2$. Unlike the flat case (equation (5.10)), this term reveals that the NMDC effect cannot be fully captured within G_{eff}. As previously mentioned, the effective gravitational constant cannot be formulated at the Lagrangian level. Consequently, using G_{eff} within the holographic vacuum energy density expression, $\rho_{\Lambda} = 3c^2/8\pi G_{\text{eff}} L^2$, is not plausible. Therefore, we will focus only on the scenario where the HDE energy density is given by $\rho_{\Lambda} = 3c^2/8\pi G L^2$.

Considering a power-law potential of the form $V(\phi) = V_0\phi^n$, where $V_0 \geq 0$ and n is an even positive integer, we define the following dimensionless dynamical variables to simplify the analysis of the system

$$x \equiv \frac{8\pi G\dot{\phi}^2}{6H^2}, \quad y \equiv \frac{8\pi G V_0 \phi^n}{3H^2}, \quad r \equiv -12\pi G\kappa\dot{\phi}^2, \quad s \equiv -\frac{4\pi G\kappa k\dot{\phi}^2}{a^2H^2},$$
$$\Omega_m \equiv \frac{8\pi G\rho_m}{3H^2}, \quad \Omega_{\Lambda} \equiv c^2\left(1 + \frac{k}{a^2H^2}\right), \quad \Omega_k \equiv -\frac{k}{a^2H^2}. \tag{5.34}$$

The variables $x, y, r, s, \Omega_{\text{m}}, \Omega_{\Lambda}$ and Ω_k represent kinetic term, potential term, NMDC contribution, NMDC-curvature coupling term, dust field density parameter, HDE density parameter and curvature density parameter, respectively. The corresponding Friedmann equation (5.32), written using these dimensionless variables, takes the form

$$1 = x + y + r + s + \Omega_m + \Omega_{\Lambda} + \Omega_k. \tag{5.35}$$

This equation expresses the constraint on the total energy density. However, the dynamical variables are not independent of each other. Constraint equations exist

between these variables, as follows

$$\Omega_\Lambda = c^2(1-\Omega_k), \quad s = -\frac{r\Omega_k}{3}. \tag{5.36}$$

The two constraint equations help reduce the number of independent variables. The first constraint relates the HDE density parameter Ω_Λ to the curvature density parameter Ω_k through the constant c^2, representing the fraction of HDE. The second constraint relates the NMDC-curvature coupling term s to the pure NMDC contribution r and the curvature density parameter Ω_k. Given the Friedmann equation (5.35), we can derive the Friedmann constraint for the matter density parameter Ω_m

$$\Omega_\mathrm{m} = 1 - x - y - r + \frac{r\Omega_k}{3} - c^2(1-\Omega_k) - \Omega_k\,. \tag{5.37}$$

The autonomous system of these variables is therefore

$$\begin{aligned} x' &= 2x\,(\epsilon-\delta)\,, \\ y' &= 2y\left(\frac{1}{2}nu+\epsilon\right), \\ r' &= -2r\delta\,, \\ u' &= u(\epsilon-\delta-u)\,, \\ \Omega_k' &= 2\Omega_k(\epsilon-1)\,, \end{aligned} \tag{5.38}$$

where we define

$$\delta \equiv -\frac{\ddot{\phi}}{H\dot{\phi}}, \quad \epsilon \equiv -\frac{\dot{H}}{H^2}, \quad \text{and} \quad u \equiv \frac{\dot{\phi}}{H\phi}. \tag{5.39}$$

More importantly, as noted in [28], the variables u, r, x and y are not independent. This is because there exist a relation between them:

$$ryu^n + 3\kappa V_0 6^{\frac{n}{2}}(8\pi G)^{\frac{2-n}{2}} x^{\frac{n+2}{2}} = 0\,, \tag{5.40}$$

where n, κ, V_0, c are numerical parameters. This constraint makes finding solutions more complex. Therefore, we will solve the autonomous system directly and then exclude any solutions that do not satisfy the constraint equation (5.40).

However, the autonomous system given by equation (5.38) is not closed. This is because it includes additional dynamical variables, δ and ϵ, that are not present in our analysis. To obtain a closed autonomous system, we need to express ϵ and δ in terms of the other dynamical variables, i.e., $\epsilon = \epsilon(x, y, r, u, \Omega_k)$ and $\delta = \delta(x, y, r, u, \Omega_k)$. By using second Friedmann equation,

$$\begin{aligned} 2\dot{H} + 3H^2 + \frac{k}{a^2} &= -8\pi G\left[\frac{\dot{\phi}^2}{2} + \frac{\kappa\dot{\phi}^2}{2}\left(2\dot{H} + 3H^2 + 4H\ddot{\phi}\dot{\phi}^{-1} - \frac{k}{a^2}\right)\right. \\ &\quad \left. -V(\phi) + P_m + P_\Lambda\right], \end{aligned} \tag{5.41}$$

together with Klein-Gordon equation,

$$\ddot{\phi} + 3H\dot{\phi} = \frac{-V_{,\phi} + 6\kappa H\dot{H}\dot{\phi} - 6\kappa H\dot{\phi}k/a^2}{1 - 3\kappa(H^2 + k/a^2)}, \tag{5.42}$$

we can obtain ϵ and δ, expressed as

$$\begin{aligned} \epsilon &= \left\{ -3r\left[c^2(\Omega_k^2 - 4\Omega_k + 3) - 2nuy + 4x(\Omega_k - 3) - 3y\Omega_k + 3y - \Omega_k^2 + 4\Omega_k - 3\right]\right. \\ &\quad \left. + 9x\left[c^2(\Omega_k - 3) + 3x - 3y - \Omega_k + 3\right] + r^2(\Omega_k^2 - 2\Omega_k + 9)\right\} \Big/ \\ &\quad \left\{ -18x(c^2 - 1) + 2r^2(3 + \Omega_k) + 6r\left[c^2(\Omega_k - 1) - x - \Omega_k + 1\right]\right\}, \end{aligned} \tag{5.43}$$

and

$$\delta = \frac{-18x(3c^2 + 2r - 3) + 18ry + 4r^2\Omega_k - 3nuy(3c^2 + r - 3)}{-18x(c^2 - 1) + 2r^2(3 + \Omega_k) + 6r\left[c^2(\Omega_k - 1) - x - \Omega_k + 1\right]}. \tag{5.44}$$

According to the Friedmann equations, $3H^2 + 3k/a^2 = 8\pi G\rho_{\text{tot}}$ and $2\dot{H} + 3H^2 + k/a = -8\pi G P_{\text{tot}}$, the effective equation of state parameter, w_{eff}, is given by

$$w_{\text{eff}} = \frac{-3H^2 - 2\dot{H} - k/a}{3H^2 + 3k/a^2} = \frac{-1 + (2\epsilon/3) + (\Omega_k/3)}{1 - \Omega_k}. \tag{5.45}$$

Table 1 Fixed points of all dynamical variables and theirs effective equation of state parameters

Names	Fixed points								w_{eff}
	x_c	y_c	r_c	s_c	u_c	Ω_{kc}	$\Omega_{\Lambda c}$	Ω_{mc}	
(a)	0	0	r	0	0	0	c^2	$1-c^2-r$	0
(b)	0	$1-c^2$	0	0	0	0	c^2	0	-1
(c)	$(-1+c^2)/2$	0	$[3(1-c^2)]/2$	0	0	0	c^2	0	-1
(d)	$1-c^2$	0	0	0	0	0	c^2	0	1

5.3.1 Dynamical systems analysis

The system (5.38) is difficult to solve for an exact solution of all dynamical variables. To better understand the evolution of the Universe, we will employ techniques from dynamical systems theory to analyze the qualitative behavior of the solutions.

This subsection explores a dynamical systems approach to the cosmological model. For an introduction and more mathematical details, please refer to [93, 94]. Considering the autonomous system (5.38), we can search for fixed points. These fixed points, denoted by $(x_c, y_c, r_c, u_c, \Omega_{kc})$, are solutions of the system where we set the derivatives to zero. Mathematically, we denote the set of dynamical variables as $\mathbf{x} = (x, y, r, u, \Omega_k)$. A dynamical system can be expressed in the form $\dot{\mathbf{x}} = \mathrm{f}(\mathbf{x})$, where $\mathrm{f}(\mathbf{x})$ represents a set of functions, given by $\mathrm{f}(\mathbf{x}) = \mathrm{f}\left(f_x(\mathbf{x}), f_y(\mathbf{x}), ..., f_{\Omega_k}(\mathbf{x})\right)$. A fixed point, denoted by $\mathbf{x}_c$, is a solution of the system $\dot{\mathbf{x}} = \mathrm{f}(\mathbf{x}_c) = 0$.

Table 1 summarizes the characteristics of all fixed points of the dynamical variables in the autonomous system (5.38). Additionally, the table displays the behavior of the universe at each fixed point, as indicated by the equation of state parameter w_{eff}, which is determined by equation (5.45). We analyze the Stability of the fixed points by considering linear perturbations around them, expressed as

$x = x_c + \delta x$, $y = y_c + \delta y$, $r = r_c + \delta r$, $u = u_c + \delta u$ and $\Omega_k = \Omega_{kc} + \delta\Omega_k$, where δx, δy, δr, δu, $\delta\Omega_k$ represent the deviations from the fixed point. Substituting these perturbations into the autonomous system (5.38) and keeping only first-order terms, we can express the perturbation equations in matrix form. This leads to a linearized system given by

$$\frac{d}{dN}\begin{pmatrix} \delta x \\ \delta y \\ \delta r \\ \delta u \\ \delta\Omega_k \end{pmatrix} = \mathcal{M}\begin{pmatrix} \delta x \\ \delta y \\ \delta r \\ \delta u \\ \delta\Omega_k \end{pmatrix}, \tag{5.46}$$

where $\mathcal{M}$ is the Jacobian matrix evaluated at the fixed point $(x_c, y_c, r_c, u_c, \Omega_{kc})$. The Jacobian matrix is expressed as

$$\mathcal{M} = \begin{pmatrix} \partial_x x' & \partial_y x' & \partial_r x' & \partial_u x' & \partial_{\Omega_k} x' \\ \partial_x y' & \partial_y y' & \partial_r y' & \partial_u y' & \partial_{\Omega_k} y' \\ \partial_x r' & \partial_y r' & \partial_r r' & \partial_u r' & \partial_{\Omega_k} r' \\ \partial_x u' & \partial_y u' & \partial_r u' & \partial_u u' & \partial_{\Omega_k} u' \\ \partial_x \Omega_k' & \partial_y \Omega_k' & \partial_r \Omega_k' & \partial_u \Omega_k' & \partial_{\Omega_k} \Omega_k' \end{pmatrix}_{\text{at fixed points}} \tag{5.47}$$

where, for example, $\partial_x x', \partial_y x', \partial_r x', \partial_u x', \partial_{\Omega_k} x'$ denote the differentiation of x' with respect to x, y, r, u, and Ω_k, respectively. The eigenvalues of this Jacobian matrix determine the stability of the fixed points. The Jacobian matrix is a 5×5 matrix, resulting in five eigenvalues. The stability of a fixed point can be classified as follows:

- **stable point**: All eigenvalues are negative.
- **unstable point**: All eigenvalues are positive.
- **saddle point**: The fixed point has at least one positive eigenvalue.

Linear stability analysis cannot determine stability when all eigenvalues are zero or when there is a mix of zero and negative or positive eigenvalues. In such cases,

alternative methods like Lyapunov's method or center manifold theory may be required. For our analysis, we will use numerical integration by varying initial conditions around the fixed points. The eigenvalues and stability conditions for each fixed point are summarized in Table (2).

Table 2 Eigenvalues, stability, and existence condition for each fixed points

Names	Eigenvalues	stability	existence
(a)	0, 1, 3/2, 3, 3	saddle	case (1): $r = 0$ with $\kappa \neq 0$, case (2): $0 < r \leq 1 - c^2$ with $\kappa < 0$
(b)	0, 0, −3, −3, −2	stable	for $\forall\kappa$
(c)	−3, −3, −2, 0, 0	-	unphysical fixed point
(d)	−6, 6, 4, 3, 0	saddle	$V_0 = 0$ and $\kappa = 0$

5.3.1.1 Fixed Point (a).

At this fixed point, the eigenvalues are both zero and positive, indicating non-hyperbolic behavior. Consequently, linear perturbation analysis fails to determine the stability of point (a). To investigate stability, we perform numerical integration of the autonomous system by slightly varying the initial conditions near the fixed point. However, it is important to ensure that these initial conditions satisfy the constraint (5.39); otherwise, the results regarding divergent and convergent behavior may be misleading. Figure 2 shows that the fixed point (a) represents a saddle fixed point. By substituting the fixed points into the constraint equations (5.37) and (5.36), we obtain the dust density parameter $\Omega_{mc} = 1 - c^2 - r$ and the holographic dark energy density $\Omega_\Lambda = c^2$. Substituting the fixed points into equation (5.43), we find that $\epsilon = -\dot{H}/H^2 = 3/2$. This confirms that this point

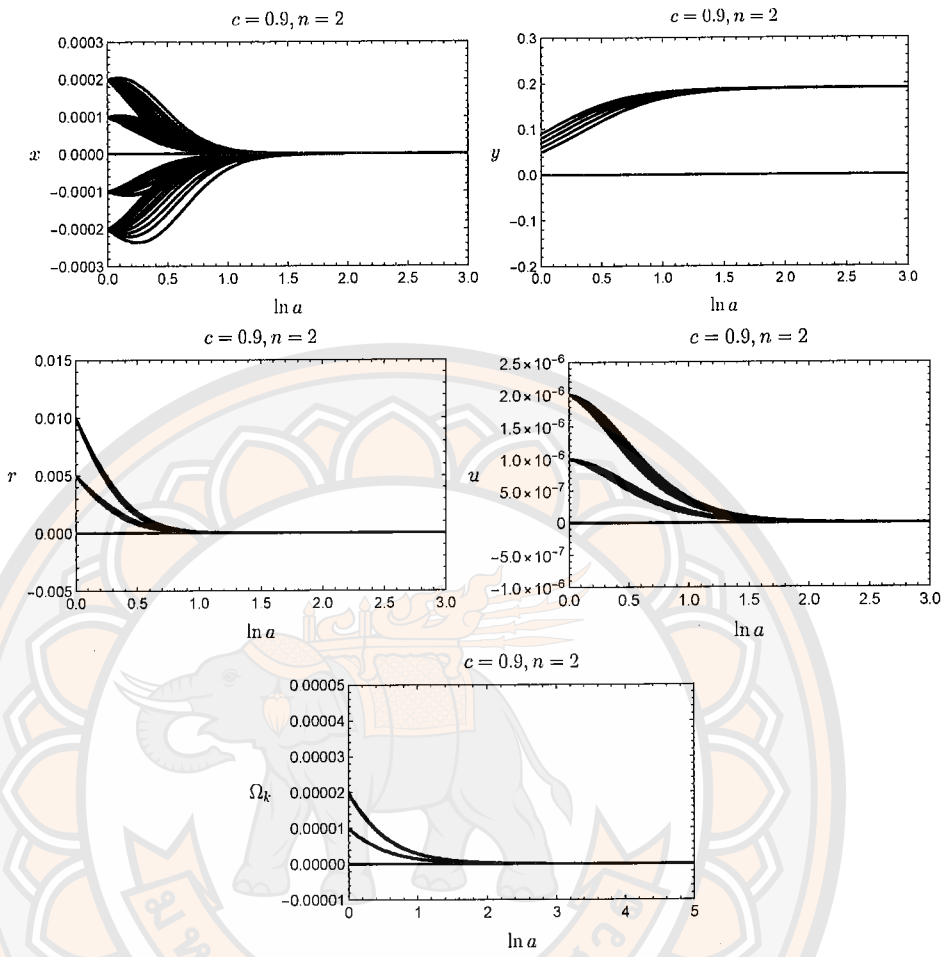

Figure 2 **Numerical integration of an autonomous system near the fixed point (a), where $n = 2$ and $c = 0.9$. The fixed point is shown by the orange lines, while the blue lines indicate the numerical evolution from various initial conditions.**

corresponds to a dust-dominated solution, given by

$$H(t) = \frac{2}{3(t - t_0)}, \tag{5.48}$$

where the scale factor is obtained by integrating the equation $H = \dot{a}/a$,

$$\begin{aligned} \int \left(\frac{\mathrm{d}a}{a}\right) &= \int \frac{2}{3(t - t_0)} \mathrm{d}t, \\ \ln \frac{a(t)}{a_0}, &= \ln(t - t_0)^{2/3}, \\ a(t) &= a_0(t - t_0)^{2/3}, \end{aligned} \tag{5.49}$$

where a_0 and t_0 represent the initial values of the scale factor and time, respectively.

Integrating $r = r_c = -12\pi G\kappa\dot{\phi}^2$, we find a solution for the scalar field

$$\phi(t) = \sqrt{\frac{r_c}{-12\pi G\kappa}}(t - t_0) + \phi_0\,, \tag{5.50}$$

where ϕ_0 represents the initial value of the scalar field. As shown in Table 1, the dynamical parameter r is arbitrary. Its existence depends on scalar field solution being real. For the fixed point with $r = 0$ (i.e., $\dot{\phi} = 0$), the solution exists for all value of κ. In this case, we have a constant scalar field solution ϕ_0. However, for $0 < r \leq 1 - c^2$, the solution exists only when $\kappa < 0$. Note that the parameter c is constrained to the range $0 \leq c \leq 1$. In this scenario, the scalar field solution is $\phi \propto t$, recovering the NMDC result reported earlier [28]. For a positive curvature case ($k > 0$), the fixed point $r = r_c$ does not exist. This is because the solution for the scalar field would become imaginary. This fixed point corresponds to an effective dust-dominated Universe, characterized by an equation of state parameter $w_{\text{eff}} = 0$, where there are two components: dust matter Ω_{m} and holographic vacuum energy Ω_Λ, driving evolution of the Universe. If there are no holographic effect ($\Omega_\Lambda = 0$), this fixed point becomes purely matter-dominated with $\Omega_{\text{mc}} = 1$. Alternatively, if there is only pure holographic vacuum energy, this case corresponds to $\Omega_{\Lambda c} = 1$, which behaves like dust, as mentioned by Hsu [32].

5.3.1.2 Fixed Point (b).

According to Table 2, the eigenvalues of this fixed point are zero and negative. This fixed point has non-hyperbolic eigenvalues, therefore, linear perturbation analysis fails to determine its stability. To investigate the stability of the fixed point, we use a numerical perturbation method on the autonomous system. This involves slightly changing the initial conditions around the fixed point and plotting the evolution of all dynamical variables with respect to the e-folding number $N = \ln a$, as shown in Figure 3. The numerical solutions indicate that this is a stable fixed point because the evolution of all dynamical variables converges toward the fixed point as the scale factor increases. This fixed point exists for all values of

n, κ and V_0. It corresponds to a cosmological constant-dominated point, with the EoS parameter for the point being $w_{\text{eff}} = -1$. Substituting fixed point (b) into the constraint equations (5.40) and (5.37), we obtain the dynamical variables $\Omega_{\text{mc}} = 0$ and $\Omega_{\Lambda c} = c^2$, respectively. Hence, according to this fixed point, the potential term and holographic vacuum energy together act like an effective cosmological constant in the late-time regime, as $t \to \infty$, leading to an asymptotically flat universe where $\Omega_k \to 0$.

To investigate the asymptotic solutions of the scale factor and scalar field for $n = 2$ and $c = 0.9$, we substitute the fixed points and their constraints into equation (5.43), we obtain $\dot{H}/H^2 = 0$. Integrating this equation gives

$$H = \pm\sqrt{\lambda_1}\,. \tag{5.51}$$

Alternatively, we can write

$$\begin{aligned} \int \frac{\mathrm{d}a}{a} &= \int \pm\sqrt{\lambda_1}\mathrm{d}t\,, \\ \ln\left(\frac{a}{a_0}\right) &= \pm\sqrt{\lambda_1}(t-t_0)\,, \\ a(t) &= a_0 e^{\pm\sqrt{\lambda_1}(t-t_0)}\,, \end{aligned} \tag{5.52}$$

where $\lambda_1 > 0$ is a constant. Using the definition $y = 8\pi G V_0 \phi^n/(3H^2) = y_c$, the solution for the scalar field is a constant function, given by

$$\begin{aligned} \frac{8\pi G V_0 \phi^n}{3H^2} &= 1 - c^2\,, \\ \frac{8\pi G V_0 \phi^n}{3\lambda_1^2} &= 1 - c^2\,, \\ \phi &= \left(\frac{3\lambda_1(1-c^2)}{8\pi G V_0}\right)^{\frac{1}{n}} = \phi_0\,, \end{aligned} \tag{5.53}$$

where $\lambda_1 \equiv 8\pi G V_0 \phi_0^n/[3(1-c^2)]$. In this case, we see that the scale factor solution depends on the initial value of the scalar field and scales with the holographic effect.

5.3.1.3 Fixed Point (c).

In equation (5.45), point (c), where $w_{\text{eff}} = -1$, corresponds to a Universe dominated by a cosmological constant. As shown in Table 1, the interplay between

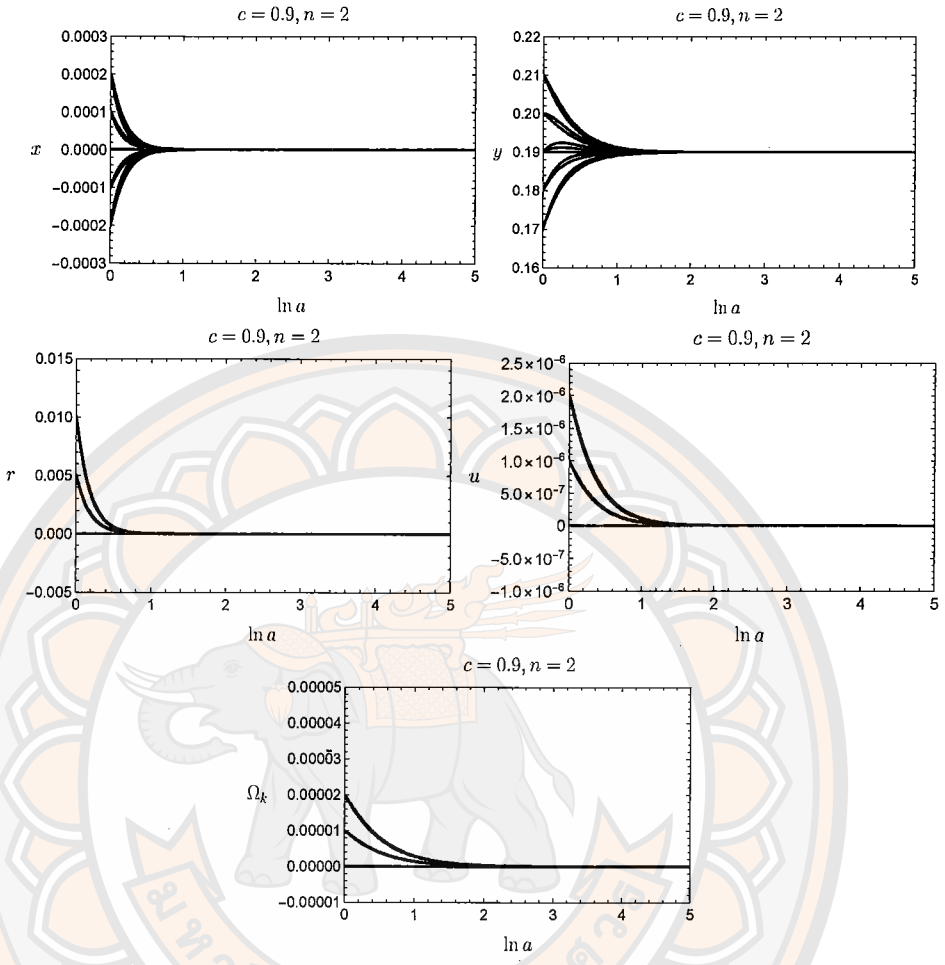

Figure 3 **Numerical integration of an autonomous system near the fixed point (b), where $n = 2$ and $c = 0.9$. The fixed point is shown by the orange lines, while the blue lines indicate the numerical evolution from various initial conditions.**

the kinetic term, $x = 8\pi G\dot{\phi}^2/(6H^2)$, the NMDC coupling term, $r = -12\pi G\kappa\dot{\phi}^2$, and the holographic effect parameter c can contribute to the accelerated expansion of the Universe. Analyzing the fixed point of the autonomous system, we find that fixed point (c) occurs at $x_c = (-1 + c^2)/2$ and $r_c = 3(1 - c^2)/2$. Substituting these fixed point values into the constraint equations (5.36), (5.37), and (5.43), we obtain $\Omega_{\rm mc} = 0$, $\Omega_{\Lambda c} = c^2$ and $\epsilon = -\dot{H}/H^2 = 0$. Using $r = r_c$, we can find the scalar field solution

$$\dot{\phi}^2 = -\frac{(1 - c^2)}{8\pi G\kappa},$$

$$\int \mathrm{d}\phi = \int \sqrt{-\frac{(1-c^2)}{8\pi G\kappa}}\mathrm{d}t\,,$$
$$\phi(t) = \sqrt{-\frac{(1-c^2)}{8\pi G\kappa}}(t-t_0)+\phi_0\,. \tag{5.54}$$

which is real if $\kappa < 0$. At point (c), integrating the equation $\epsilon = -\dot{H}/H^2 = 0$, we obtain the solution,

$$H = \pm\sqrt{\lambda_2}\,, \quad \text{or} \quad a(t) = a_0 e^{\pm\sqrt{\lambda_2}t}\,, \tag{5.55}$$

where λ_2 is a numerical constant. To explore the asymptotic behavior near fixed point (c), we consider the relationship between x_c and r_c, which is $x_c/r_c = -1/3$. Using the definitions of x and r, as given before, we obtain $x/r = -(9\kappa H^2)^{-1}$. Evaluating this expression at fixed point (c) yields

$$H = \frac{1}{\sqrt{3\kappa}}\,. \tag{5.56}$$

Comparing equation (5.55) and (5.56), the expression for λ_2 is

$$\lambda_2 = \frac{1}{3\kappa}\,. \tag{5.57}$$

Since $\kappa < 0$ is required for the scalar field to be real, we have $\lambda_2 = (3\kappa)^{-1} < 0$, meaning $\sqrt{\lambda_2}$ is imaginary. Therefore, the Hubble parameter $H = \pm i\sqrt{|\lambda_2|}$ corresponds to an imaginary function, which results in an imaginary scale factor. This fixed point (c) leads to an unphysical behavior for the Universe.

5.3.1.4 Fixed Point (d).

As shown in Table (2), the Eigenvalues associated with fixed point (d) exhibit a mixed character, with one eigenvalue being positive and the other negative. This signature identifies fixed point (d) as a saddle point. According to equation (5.45), the corresponding value of the effective equation of state parameter is $w_{\text{eff}} = 1$, which represents a stiff fluid, where the kinetic term of the scalar field dominates. At this point, equation (5.43) gives $\epsilon = -\dot{H}/H^2 = 3$. Integrating this equation, the asymptotic solution for the Hubble parameter is

$$H(t) = \frac{1}{3(t-t_0)}\,. \tag{5.58}$$

Integrating both sides of the Hubble parameter equation, we obtain the solution for the scale factor

$$\begin{aligned} \int \frac{\mathrm{d}a}{a} &= \int \frac{1}{3(t-t_0)}\mathrm{d}t\,, \\ \ln\left(\frac{a}{a_0}\right) &= \ln(t-t_0)^{1/3}\,, \\ a(t) &= a_0(t-t_0)^{1/3}\,. \end{aligned} \tag{5.59}$$

From Table 1, fixed points (d) is determined by the kinetic term, with $x_c = 1 - c^2$, and the holographic effect, $\Omega_{\Lambda c} = c^2$. To obtain the asymptotic behavior of the scalar field near this fixed point, we use the definition of the kinetic dimensionless parameter from equation (5.34). We have

$$\begin{aligned} \frac{8\pi G\dot{\phi}^2}{6H^2} &= 1 - c^2\,, \\ \dot{\phi} &= \sqrt{\frac{1-c^2}{12\pi G}}\frac{1}{(t-t_0)}\,, \\ \int \mathrm{d}\phi &= \int \sqrt{\frac{1-c^2}{12\pi G}}\frac{1}{(t-t_0)}\mathrm{d}t\,, \\ \phi(t) &= \sqrt{\frac{1-c^2}{12\pi G}}\ln(t-t_0) + \phi_0\,. \end{aligned} \tag{5.60}$$

At the fixed point y_c, where the solutions for $H(t)$ and $\phi(t)$ are non-zero, the condition $y_c = 8\pi G V_0 \phi^n (t - t_0) = 0$ is satisfied. However, this condition is valid only if $V_0 = 0$. Similarly, the fixed point condition $r_c = -12\pi G\kappa\dot{\phi}^2 = 0$ holds only when $\kappa = 0$.

5.3.2 Numerical solution

The autonomous system equation (5.38) can be numerically integrated to obtain the evolution of the Hubble parameter, $H(z)$, and the effective equation of state parameter, w_{eff}. Figure 5 presents these numerical solutions. In particular, the curve for $H(z)$ is plotted alongside observed data points, including error bars, at low redshifts as presented in [92]. The comparison reveals that the solutions for the non-flat case differ slightly from those of the flat case, making it difficult to

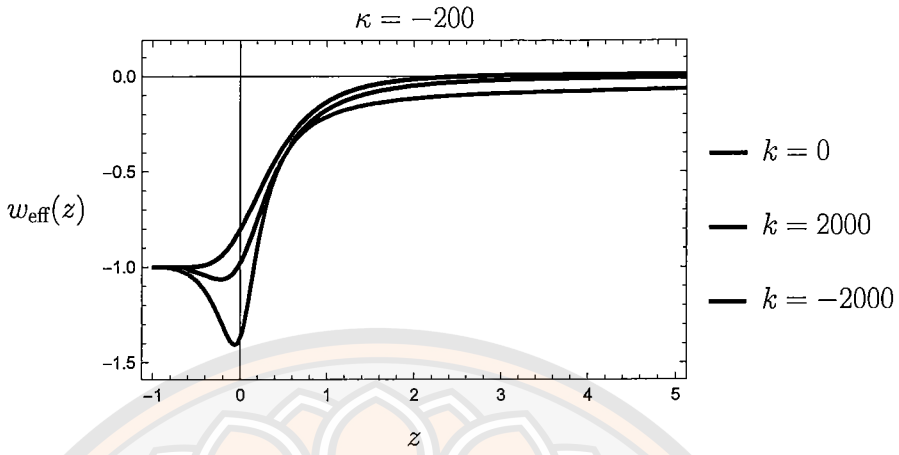

Figure 4 **Numerical solutions for the equation of state parameter $w_{\text{eff}}(z)$ in both flat and non-flat geometries for $n = 2$ (with a potential $V = V_0\phi^2$ where $V_0 = 1/2$). The parameter c is 0.9 and the NMDC coupling is $\kappa = -200$. The spatial curvature values are $k = 0$ and ± 2000.**

distinguish between the two scenarios based on these results. To better understand the qualitative impact of spatial curvature, we analyze the system by selecting an exaggerated value for the curvature parameter, $k = \pm 2000$. This large value significantly amplifies the contribution of the curvature term in the equations, allowing us to investigate more pronounced effects on the evolution of both $w_{\text{eff}}(z)$ and $H(z)$. This approach highlights the role of curvature, particularly in distinguishing the behavior of the non-flat case from the flat case over a range of redshifts.

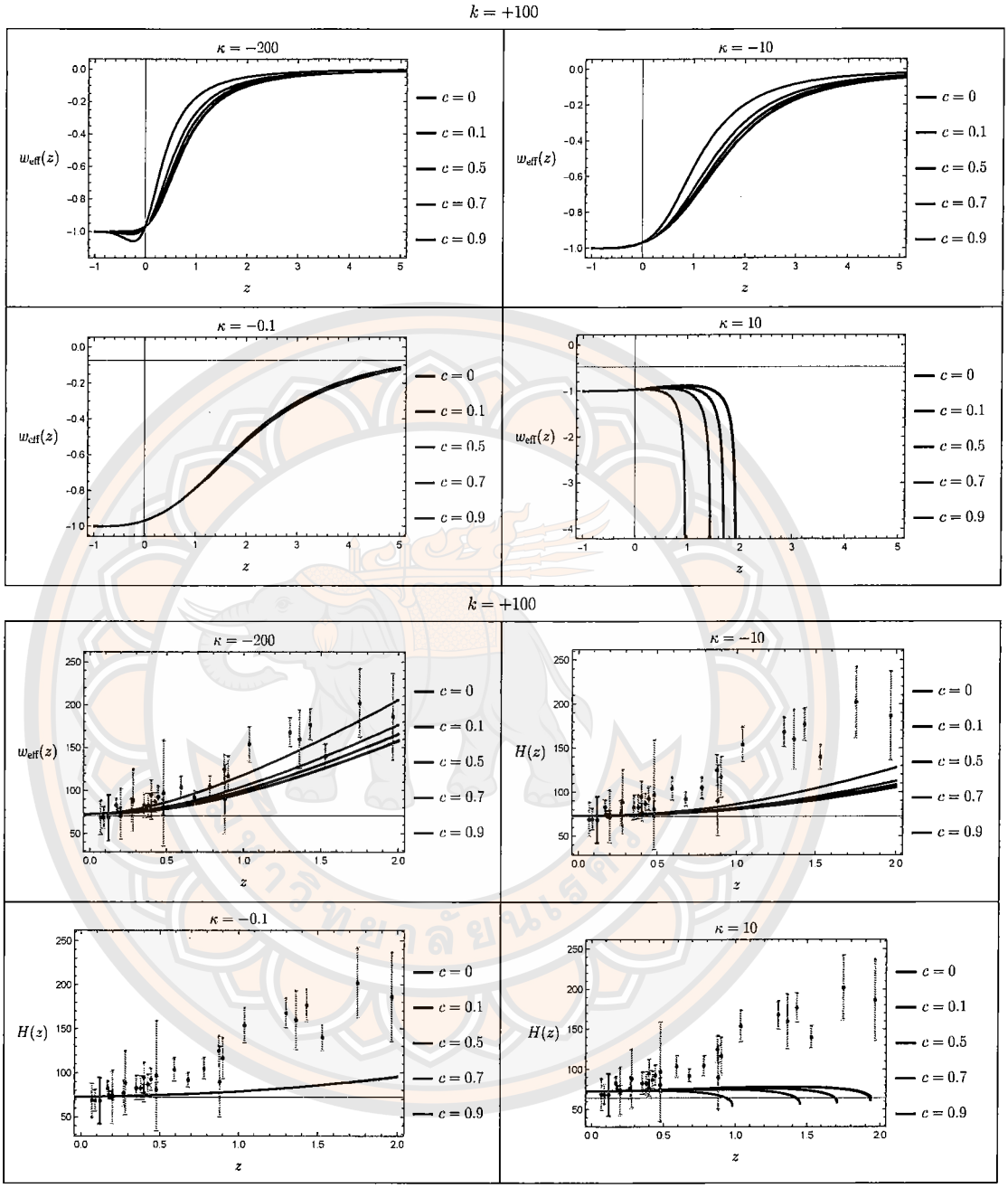

Figure 5 Numerical solutions for $w_{\text{eff}}(z)$ and $H(z)$ in a non-flat universe show slight differences compared to those in a flat universe.

CHAPTER VI

COSMOLOGICAL DYNAMICS OF HOLOGRAPHIC DARK ENERGY WITH NON-MINIMAL COUPLED SCALAR FIELD

In this chapter, we explore a scalar field non-minimally coupled to gravity (NMC), incorporating holographic vacuum energy. The NMC theory considers the coupling between scalar field and Ricci scalar in the form $(1/2)\xi\phi^2 R$, where ξ is the coupling constant.

6.1 NMC with HDE action and field equations

The NMC theory is a subset of the generalized scalar-tensor theory, the Horndeski theory, with the action (3.7), which takes the form

$$G_2 = -(1/2)g_{\mu\nu}(\nabla^\mu\phi)(\nabla^\nu\phi) - V(\phi),\ G_3 = 0,\ G_4 = (16\pi G)^{-1} - \xi\phi^2/2,$$
$$G_{4X} = 0,\ G_5 = 0, G_{5X} = 0. \tag{6.1}$$

This formulation leads to second-order equations of motion, avoiding the higher-order derivatives that can lead to unphysical solutions. The action for the NMC theory in the Jordan frame with matter and vacuum energy is

$$S = \int \mathrm{d}^4x\sqrt{-g}\left[\frac{R}{16\pi G} - \frac{1}{2}g^{\mu\nu}\nabla_\mu\phi\nabla_\nu\phi + V(\phi) - \frac{1}{2}\xi\phi^2 R + \mathcal{L}_\mathrm{m}\right] + S_\Lambda\,. \tag{6.2}$$

Varying the NMC action with respect to metric tensor $g_{\mu\nu}$ yields the Einstein field equations[5]

[5]Detailed calculations are provided in the Appendix C

$$G_{\mu\nu} = \frac{8\pi G}{1-8\pi G\xi\phi^2}\Bigg[\nabla_\mu\phi\nabla_\nu\phi - \frac{1}{2}g_{\mu\nu}\nabla^\rho\phi\nabla_\rho\phi - V(\phi)g_{\mu\nu} - \xi\left(\nabla_\mu\nabla_\nu\phi^2 - g_{\mu\nu}\nabla_\rho\nabla^\rho\phi^2\right) + T^{(\mathrm{m})}_{\mu\nu} + T^{(\Lambda)}_{\mu\nu}\Bigg], \tag{6.3}$$

where $T^{(\mathrm{m})}_{\mu\nu}$ and $T^{(\Lambda)}_{\mu\nu}$ are the energy-momentum tensors for matter and holographic vacuum energy, respectively. One can view the theory with effective gravitational constant in the Einstein field equation as

$$G_{\mathrm{eff}}(\phi) = \frac{G}{1-8\pi G\xi\phi^2}. \tag{6.4}$$

The gravitational constant is field-dependent. It reduces to G when the scalar field is absent or when the non-minimal coupling constant vanishes ($\xi = 0$). It is natural to express the model in terms of the effective gravitational constant, as it naturally emerges at the action level. To make this clearly, we factorize the action in equation (6.2), this gives

$$\begin{aligned} S &= \int \mathrm{d}^4x\sqrt{-g}\left[\left(1-8\pi G\xi\phi^2\right)\frac{R}{16\pi G} - \frac{1}{2}g^{\mu\nu}\nabla_\mu\phi\nabla_\nu\phi - V(\phi) + \mathcal{L}_{\mathrm{m}}\right] + S_\Lambda, \\ &= \int \mathrm{d}^4x\sqrt{-g}\left[\frac{R}{16\pi G_{\mathrm{eff}}(\phi)} - \frac{1}{2}g^{\mu\nu}\nabla_\mu\phi\nabla_\nu\phi - V(\phi) + \mathcal{L}_{\mathrm{m}}\right] + S_\Lambda. \end{aligned} \tag{6.5}$$

The action reduces to standard quintessence matter but with a modified gravitational constant due to NMC. By varying the action (6.2) with respect to the scalar field ϕ, we obtain the Klein-Gordon equation for the NMC action as[6]

$$\nabla_\mu(\nabla^\mu\phi) - V_{,\phi} - \xi R\phi = 0, \tag{6.6}$$

which describes the dynamics of the scalar field, incorporating the non-minimal coupling between scalar field ϕ and the Ricci scalar R. These modified equations emphasize the influence of the non-minimal coupling on both the Einstein field equation and the Klein-Gordon equation.

[6]Detailed calculations are provided in the Appendix C

In the spatial curved FLRW universe, $(0,0)$ and (i,j) components of the Einstein field equations (6.3) gives the Friedmann equations as follows[7]:

$$3H^2 + \frac{3k}{a^2} = 8\pi G_{\text{eff}} \left[\frac{\dot{\phi}^2}{2} + V(\phi) + 6\xi H\phi\dot{\phi} + \rho_{\text{m}} + \rho_{\Lambda} \right], \tag{6.7}$$

$$2\dot{H} + 3H^2 + \frac{k}{a^2} = -8\pi G_{\text{eff}} \left[\frac{\dot{\phi}^2}{2} - V(\phi) - 2\xi \left(\phi\ddot{\phi} + \dot{\phi}^2 + 2H\phi\dot{\phi} \right) + P_{\text{m}} + P_{\Lambda} \right].$$

The term ρ_{m} represents the dust matter density, ρ_{Λ} denotes the holographic vacuum energy density, and P_{Λ} is its pressure. Dust matter is pressureless, with $P_{\text{m}} = 0$. This introduces a field-dependent gravitational constant. The dependence of gravity on the scalar field has significant implications for the cosmological behavior of the model. In NMC theory, , the holographic vacuum energy density is determined by considering the apparent horizon as the cosmological cutoff, giving

$$\rho_{\Lambda} = \frac{3c^2}{8\pi G_{\text{eff}} R_A^2}, \tag{6.8}$$

where $R_A = 1/\left(\sqrt{H^2 + k/a^2}\right)$ is the apparent horizon radius and $0 \leq c < 1$. Substituting for G_{eff}, we obtain

$$\rho_{\Lambda} = \frac{3c^2 \left(1 - 8\pi G\xi\phi^2\right) \left(H^2 + \frac{k}{a^2} \right)}{8\pi G}. \tag{6.9}$$

This equation describes the holographic vacuum energy density as a function of the scalar field, the Hubble parameter, and the spatial curvature. In the holographic scenario, a cosmological bulk region should be enclosed by trapped null surface, similar in concept to a black hole event horizon, where light never reaches the horizon. The apparent horizon, which is a trapped null surface in an accelerating expansion, is a natural choice for the holographic cutoff.

If there is no interaction between the dust matter field and the holographic vacuum energy, the energy densities for both components follow the conservation

[7]Detailed calculations are provided in the Appendix D

equations,

$$\dot{\rho}_{\rm m} + 3H\rho_{\rm m} = 0\,, \tag{6.10}$$

$$\dot{\rho}_{\Lambda} + 3H\rho_{\Lambda}(1+w_{\Lambda}) = 0\,, \tag{6.11}$$

where $w_{\rm m} = 0$ for dust matter, and w_{Λ} is the equation of state parameter for the holographic vacuum energy.

The evolution of the scalar field in the FLRW background is governed by the Klein-Gordon equation,

$$\ddot{\phi} = -3H\dot{\phi} - V_{,\phi} - 6\xi\phi(2H^2 + \dot{H} + \frac{k}{a^2})\,, \tag{6.12}$$

where $V_{,\phi}$ denotes the derivative with repect to ϕ.

Together, equations (6.7), (6.9), (6.10), (6.11), and (6.12) fully describe the evolution of the Hubble parameter, the scalar field, and the holographic vacuum energy in the context of an FLRW universe with non-minimal coupling. The method we use to explore the dynamics of the universe is dynamical systems analysis.

6.2 Dynamics of the holographic NMC model

6.2.1 Dynamical variables

It is convenient to express the dynamical fields such as the scalar field, kinetic term, matter field, and holographic vacuum energy, in terms of dimensionless variables. Considering power-law potential given by $V(\phi) = V_0\phi^n$, we define dimensionless dynamical variables as follows:

$$x \equiv \frac{8\pi G_{\rm eff}\dot{\phi}^2}{6H^2},\; y \equiv \frac{8\pi G_{\rm eff}V_0\phi^n}{3H^2},\; s \equiv \frac{16\pi G_{\rm eff}\xi\phi\dot{\phi}}{H},\; A \equiv 8\pi G_{\rm eff}\xi\phi^2$$
$$\Omega_{\rm m} \equiv \frac{8\pi G_{\rm eff}\rho_{\rm m}}{3H^2},\; \Omega_{\Lambda} \equiv \frac{8\pi G_{\rm eff}\rho_{\Lambda}}{3H^2},\; \Omega_k \equiv -\frac{k}{a^2H^2}\,. \tag{6.13}$$

where $\Omega_{\rm m}, \Omega_{\Lambda}$, and Ω_k denote the density parameters for dust matter, holographic vacuum energy, and spatial curvature, respectively. To make the dynamical system

autonomous, we introduce an additional parameter, A. The parameter x represents the scalar field's kinetic term, and y denotes the power-law potential term. The variable s represents the NMC coupling term; notably, $s = 0$ implies $\xi = 0$ and this changes G_{eff} back to G, restoring the model's non-NMC limit. On the other hand $c = 0$ indicates the absence of holographic vacuum energy. Effectively, NMC effect is within G_{eff} in almost all dynamical variables. The first Friedmann equation (6.7) can be written in terms of dynamical parameters and expressed as a constraint equation, normalizing the density parameters of all components,

$$1 = \Omega_\phi + \Omega_{\text{m}} + \Omega_\Lambda + \Omega_k \,. \tag{6.14}$$

The density parameter of the scalar field, which is non-minimally coupled to the Ricci scalar, can be expressed as

$$\Omega_\phi = x + y + s \,. \tag{6.15}$$

From equation (6.14), both the holographic vacuum energy and the scalar field drive the acceleration such that dark energy density parameter is

$$\Omega_{\text{de}} \equiv \Omega_\phi + \Omega_\Lambda \,. \tag{6.16}$$

According to the energy density of HDE in equation (6.9), there exists a relationship between the HDE density parameter and the spatial curvature term, leading to the constraint

$$\Omega_\Lambda = c^2(1 - \Omega_k) \,. \tag{6.17}$$

Additionally, another constraint arises from the relationship between x, s, and A, expressed as

$$x = \frac{s^2}{24\xi A} \,, \tag{6.18}$$

where $\xi \neq 0$, otherwise indeterminate. Hence, the Friedmann constraint provides an expression for the dust density parameter in terms of y, s, A and Ω_k, as

$$\Omega_{\text{m}} = 1 - \frac{s^2}{24\xi A} - y - s - c^2(1 - \Omega_k) - \Omega_k \,. \tag{6.19}$$

Equation of state parameter for a NMC scalar field is given by its energy density and pressure. According to definition of Friedmann equations (6.7), we obtain

$$\rho_\phi = \frac{\dot{\phi}^2}{2} + V(\phi) + 6\xi H\phi\dot{\phi}, \tag{6.20}$$

$$P_\phi = \frac{\dot{\phi}^2}{2} - V(\phi) - 2\xi\left(\dot{\phi}^2 + \phi\ddot{\phi} + 2\phi H\dot{\phi}\right), \tag{6.21}$$

$$w_\phi = \frac{P_\phi}{\rho_\phi} = \frac{s + 3[x - 4x\xi + y(2n\xi - 1) - 4A\xi(\epsilon + \Omega_k - 2)]}{3(x + y + s)}, \tag{6.22}$$

where $\epsilon \equiv -\dot{H}/H^2$. Using equation (6.9) together with the continuity equation of holographic vacuum energy, $\dot{\rho}_\Lambda + 3H\rho_\Lambda(1 + w_\Lambda) = 0$,equation of state parameter for the holographic vacuum energy is

$$w_\Lambda = \frac{-1 + 2\epsilon/3 + \Omega_k/3 + s(1 - \Omega_k)/3}{1 - \Omega_k}. \tag{6.23}$$

Equation of state parameter for dark energy is then defined as

$$w_{\text{de}} = \frac{w_\phi\Omega_\phi + w_\Lambda\Omega_\Lambda}{\Omega_\phi + \Omega_\Lambda}. \tag{6.24}$$

Using Friedmann equations (6.7), expressed in the form $3H^2 + 3k/a^2 = 8\pi G_{\text{eff}}\rho_{\text{tot}}$ and $2\dot{H} + 3H^2 + k/a^2 = -8\pi G_{\text{eff}}P_{\text{tot}}$, the effective equation of state parameter can be obtained through the definition $w_{\text{eff}} = P_{\text{tot}}/\rho_{\text{tot}}$. This gives

$$w_{\text{eff}} = -\frac{2\dot{H} + 3H^2 + k/a^2}{3H^2 + 3k/a^2} = \frac{-1 + 2\epsilon/3 + \Omega_k/3}{1 - \Omega_k}. \tag{6.25}$$

According to equations (6.13), (6.17), (6.18), and (6.19), we have seven dynamical variables and three constraint equations. Consequently, the dynamical system can be constructed using only four independent variables: y, s, A, and Ω_k. The autonomous system is constructed by taking the derivative of the dynamical parameters with respect to the e-folding number, $N \equiv \ln a$. This is[8]

$$y' = sy + \frac{nsy}{2A} + 2y\epsilon,$$

$$s' = s^2 + \frac{s^2}{2A} + s(\epsilon - 3) - 6ny\xi + 12A\xi(\epsilon - 2 + \Omega_k),$$

[8]Detailed calculations are provided in the Appendix F

$$
\begin{aligned}
A' &= s(1+A)\,, \\
\Omega_k' &= -2\Omega_k(1-\epsilon)\,.
\end{aligned}
\tag{6.26}
$$

Here, " $'$ " denotes derivative with respect to N. The parameter $\epsilon \equiv -\dot{H}/H^2$ is expressed in terms of the dynamical variables to obtain the autonomous system. Using equation (6.7) together with the NMC Klein-Gordon equation (6.12) and the equation of state parameter of holographic vacuum energy equation (6.23), the parameter ϵ is expressed as

$$
\begin{aligned}
\epsilon &= s^2\,(1-4\xi) + 8As\xi\left[1+c^2(1-\Omega_k)\right] - 8A\xi\big[-3+3y-24A\xi-6ny\xi \\
&\quad +c^2(3-\Omega_k)+\Omega_k+12A\xi\Omega_k\big]\Big/16A\xi(1-c^2+6A\xi)\,.
\end{aligned}
$$

6.2.2 Fixed points and stabilities

Fixed points of the autonomous system are found by setting the system of equation (6.26) to zero. The fixed points for all dynamical variables are listed in Table 3. To determine stability of each fixed point, we analyze the system using linear perturbations about each fixed points, i.e., $y = y_c + \delta y$, $s = s_c + \delta s$, $A = A_c + \delta A$, $\Omega_k = \Omega_{kc} + \delta\Omega_k$, and examining the eigenvalues of the resulting Jacobian matrix, $\mathcal{M}$. The first-order perturbation system is expressed as

$$
\frac{\mathrm{d}}{\mathrm{d}N}\begin{pmatrix}\delta y\\ \delta s\\ \delta A\\ \delta\Omega_k\end{pmatrix} = \mathcal{M}\begin{pmatrix}\delta y\\ \delta s\\ \delta A\\ \delta\Omega_k\end{pmatrix}\,,
\tag{6.27}
$$

where $y_c, s_c, A_c, \Omega_{kc}$ denote fixed points and $\delta y, \delta s, \delta A, \delta\Omega_k$ represent linear perturbations. The Jacobian matrix $\mathcal{M}$ is defined as

$$
\mathcal{M} = \begin{pmatrix}
\partial_y y' & \partial_s y' & \partial_A y' & \partial_{\Omega_k} y' \\
\partial_y s' & \partial_s s' & \partial_A s' & \partial_{\Omega_k} s' \\
\partial_y A' & \partial_s A' & \partial_A A' & \partial_{\Omega_k} A' \\
\partial_y \Omega_k' & \partial_s \Omega_k' & \partial_A \Omega_k' & \partial_{\Omega_k} \Omega_k'
\end{pmatrix}_{\text{at fixed points}}\,,
\tag{6.28}
$$

where, for example, $\partial_y y', \partial_s y', \partial_A y', \partial_{\Omega_k} y'$ denote derivatives of y' with respect to y, s, A and Ω_k, respectively. The eigenvalues of the Jacobian matrix indicate the stability characteristics of each fixed point. Since the autonomous system has four degrees of freedom, the Jacobian matrix has four eigenvalues. A fixed point is stable if all eigenvalues are negative, and it is unstable if all are positive. If at least one eigenvalue is positive, the fixed point is classified as a saddle point. When some eigenvalues are zero while others are negative or positive, linear stability analysis fails, and numerical integration is required to determine stability.

The eigenvalues of the Jacobian matrix, derived from equation (6.28), and the stability characteristics of each fixed point, are presented in Table 4. Additionally, the corresponding equation of state parameters for each fixed point are listed in Table 5.

Based on the fixed points listed in Table 3, the system yields nine fixed points, as follows:

6.2.2.1 Fixed point 1.

Fixed point 1 represents a state completely dominated by spatial curvature, characterized by $\Omega_{kc} = 1$. The effective equation of state parameter at this point is indeterminate due to the zero denominator in equation (6.25). Since the eigenvalues contain both positive and negative components, the stability of this point corresponds to a saddle line for all ξ and $0 \leq c < 1$, with the parameter $A_c \in (-\infty, \infty)$. However, because w_{eff}, is indeterminate, this fixed point is considered non-physical.

6.2.2.2 Fixed point 2.

Fixed point 2 represents a state dominated by spatial curvature, with an effective equation of state parameter given by $w_{\text{eff}} = -1/3$. The stability of this point depends on the parameter ξ: for $\xi < 0$ and $\xi > (4 - 3c^2)/24$, the eigenvalues consist of both positive and negative values, indicating a saddle point. In contrast, for $0 < \xi < (4 - 3c^2)/24$ all eigenvalues are positive, making the point unstable.

Table 3 Fixed points of all dynamical variables for $n = 2$ case, where $B \equiv -1 + c^2 + 6\xi$.

Name	Fixed points						
	x_c	y_c	s_c	A_c	Ω_{kc}	$\Omega_{\Lambda c}$	Ω_{mc}
1	0	0	0	A_c	1	0	0
2	$-\frac{1}{24\xi}$	0	1	-1	$1-\frac{1}{8\xi}$	$\frac{c^2}{8\xi}$	$-1+\frac{1}{6\xi}-\frac{c^2}{8\xi}$
3	$-\frac{2B^2}{3c^4\xi}$	0	$\frac{4B}{c^2}$	-1	$\left[2(1-6\xi)^2 +3c^4\xi-2c^2 +12c^2\xi\right]/3c^4\xi$	$-\frac{2(-1+6\xi)B}{3c^2\xi}$	0
4	$-\frac{3}{8\xi}$	$2-\frac{3}{8\xi}$	3	-1	0	c^2	$-4-c^2+\frac{3}{4\xi}$
5	$-\frac{2\xi}{3(1-4\xi)^2}$	0	$\frac{4\xi}{1-4\xi}$	-1	0	c^2	$-c^2+\left[3 -34\xi+96\xi^2\right]/ 3(1-4\xi)^2$
6	$-\frac{2\xi(1+c^2)^2}{3(1-4\xi)^2}$	$\left[3-34\xi +2c^4\xi+96\xi^2 +c^2(-3+16\xi)\right]/ 3(1-4\xi)^2$	$-\frac{4\xi(1+c^2)}{-1+4\xi}$	-1	0	c^2	0
7	$1-c^2-12\xi +2\sqrt{6\xi B}$	0	$12\xi-2\sqrt{6\xi B}$	-1	0	c^2	0
8	$1-c^2-12\xi -2\sqrt{6\xi B}$	0	$12\xi+2\sqrt{6\xi B}$	-1	0	c^2	0
9	0	$1-c^2$	0	$\frac{-1+c^2}{2}$	0	c^2	0

Singularities occur at $\xi = 0$ and $\xi = (1 - c^2)/6$. The condition for a positive holographic density parameter requires $\xi > 0$, but this leads to $x_c < 0$ which is not physical. On the other hand, choosing $\xi < 0$ makes $x_c > 0$, but this makes $\Omega_{\Lambda c} < 0$, which is also non-physical. Therefore, although this fixed point formally exists, it remains non-physical for all values of ξ.

6.2.2.3 Fixed point 3.

Fixed point 3 represents a phase dominated by spatial curvature, characterized by $\Omega_{kc} = 1$, which occurs when $\xi = (1 - c^2)/6$. The effective equation of state parameter at this point remains constant at $w_{\text{eff}} = -1/3$ for all values of ξ. Based

Table 4 **Eigenvalues and their stabilities of all fixed points for $n = 2$, $B = -1+c^2+6\xi$, $\Delta = c^4[8\xi(194\xi-23)+1]+32c^2\xi(6\xi-1)(116\xi-13)+256\xi(9\xi-1)(1-6\xi)^2$, and $\Theta = 3\xi[c^4\xi(48\xi^2+104\xi-21)+6c^2(128\xi^3+40\xi^2-28\xi+3)+2(6\xi-1)(3-16\xi)^2]$**

Fixed points	eigenvalues	stability	existence conditions for $0 \le c < 1$
1	$0,\ -1,\ -2,\ 2$	saddle	$\forall\xi,\ \xi \neq 0$
2	$1,\ 2,\ \frac{-[4\xi(c^2-4)+c^2+96\xi^2]-\sqrt{\Delta}}{32\xi B},$ $\frac{-[4\xi(c^2-4)+c^2+96\xi^2]+\sqrt{\Delta}}{32\xi B}$	saddle, unstable	if $\xi < 0$, or $(4-3c^2)/24 < \xi$, for $\xi \neq 0$ and $\xi \neq (1-c^2)/6$, if $0 < \xi < (4-3c^2)/24$, for $\xi \neq 0$ and $\xi \neq (1-c^2)/6$
3	$2,\ \frac{4B}{c^2},\ \frac{3c^2+24\xi-4}{c^2},\ \frac{6c^4\xi+4c^2(6\xi-1)+4(1-6\xi)^2}{3c^4\xi}$	saddle, unstable	if $\xi < (8-c^4-4c^2+c^3\sqrt{8+c^2})/48,\ \xi \neq 0, c \neq 0$ if $(8-c^4-4c^2+c^3\sqrt{8+c^2})/48 \le \xi,\ \xi \neq 0, c \neq 0$
4	$-2,\ 3,\ \frac{3c^2(4\xi-1)-\sqrt{\Theta}}{4B},\ \frac{3c^2(4\xi-1)+\sqrt{\Theta}}{4B}$	saddle	$\xi \neq (1-c^2)/6,\ \xi \neq 0$
5	$\frac{4\xi}{1-4\xi},\ \frac{1-8\xi}{1-4\xi},\ \frac{3-16\xi}{1-4\xi},\ \frac{3c^2(1-4\xi)^2-96\xi^2+34\xi-3}{2(4\xi-1)B}$	saddle	$\xi \neq 1/4,\ \xi \neq 0$ $\xi \neq (1-c^2)/6$
6	$\frac{-4\xi(1+c^2)}{4\xi-1},\ -2,\ \frac{3-4\xi(4+c^2)}{4\xi-1},$ $\frac{3c^2-2c^2\xi(8+c^2)-96\xi^2+34\xi-3}{(4\xi-1)B}$	stable, saddle	if $\xi < 0$ or $1/4 < \xi,\ \xi \neq 0$, if $0 < \xi < 1/4,\ \xi \neq 0$,
7	$12\xi-2\sqrt{6\xi B},\ [c^2(3-12\xi)+(6\xi-1)(2\sqrt{6\xi B}-12\xi+3)]/B,$ $[2c^2(\sqrt{6\xi B}-12\xi+2)+2(6\xi-1)(2\sqrt{6\xi B}-12\xi+2)]/B,$ $[2c^2(\sqrt{6\xi B}-12\xi+3)+2(6\xi-1)(2\sqrt{6\xi B}-12\xi+3)]/B$	saddle, unstable, spiral, unstable	if $\xi < 0,\ \xi \neq 0$, if $0 < \xi < (-17+12c^2-\sqrt{1+24c^2})/[48(c^2-2)],\ \xi \neq 0$, if $(-17+12c^2-\sqrt{1+24c^2})/[48(c^2-2) < \xi],\ \xi \neq 0$
8	$12\xi+2\sqrt{6\xi B},\ [c^2(3-12\xi)+(6\xi-1)(-2\sqrt{6\xi B}-12\xi+3)]/B,$ $[2c^2(-\sqrt{6\xi B}-12\xi+2)+2(6\xi-1)(-2\sqrt{6\xi B}-12\xi+2)]/B,$ $[2c^2(-\sqrt{6\xi B}-12\xi+3)+2(6\xi-1)(-2\sqrt{6\xi B}-12\xi+3)]/B$	unstable, saddle, spiral, saddle	if $\xi < 0,\ \xi \neq 0$, if $0 < \xi < (-17+12c^2-\sqrt{1+24c^2})/[48(c^2-2)],\ \xi \neq 0$, if $(-17+12c^2+\sqrt{1+24c^2})/[48(c^2-2)] < \xi,\ \xi \neq 0$
9	$-3,\ -2,$ $\left[3+3(c^2-3)\xi-\sqrt{9(c^2+5)^2\xi^2-6(5c^2+17)\xi+9}\right]/(6\xi-2),$ $\left[3+3(c^2-3)\xi+\sqrt{9(c^2+5)^2\xi^2-6(5c^2+17)\xi+9}\right]/(6\xi-2)$	saddle, stable	if $\xi < 0$ and $1/3 < \xi,\ \xi \neq 0$, if $0 < \xi < 1/3,\ \xi \neq 0$

Table 5 **Effective equation of state of all fixed points for $n = 2$ and $B = -1 + c^2 + 6\xi$. This is found from the equation (6.25) with the values of dynamical variables at the fixed points.**

Fixed points	equation of state parameter, w_{eff}
1	Indeterminate
2	$-\frac{1}{3}$
3	$-\frac{1}{3}$
4	-1
5	$\frac{4\xi}{-3+12\xi}$
6	-1
7	$\left[c^2(3-24\xi+2\sqrt{6\xi B})+(-1+6\xi)(3-24\xi+4\sqrt{6\xi B})\right]/3B$
8	$\left[c^2(3-24\xi-2\sqrt{6\xi B})+(-1+6\xi)(3-24\xi-4\sqrt{6\xi B})\right]/3B$
9	-1

on the eigenvalue analysis, the stability of this point varies with ξ. Specifically, for $\xi < (8 - c^4 - 4c^2 + c^3\sqrt{8+c^2})/48$, the fixed point behaves as a saddle point. In contrast, when $\xi \geq (8 - c^4 - 4c^2 + c^3\sqrt{8+c^2})/48$, it becomes an unstable point.

6.2.2.4 Fixed point 4.

Fixed point 4 corresponds to an effective equation of state parameter $w_{\text{eff}} = -1$. Since one of its eigenvalues is positive, this fixed point behaves as a saddle for $0 \leq c < 1$. The requirement that the matter density parameter satisfies $0 \leq \Omega_{\text{m}} c \leq 1$ imposes a condition, $3/(20 + 4c^2) \leq \xi \leq 3/(16 + 4c^2)$ which implies positive value of ξ in the range. However, for the fixed point to be physically meaningful, the conditions $x_c > 0$ and $y_c > 0$ must also be satisfied. These conditions, however, require $\xi < 0$. The conditions are in conflict with each other, hence this point is non-physical.

6.2.2.5 Fixed point 5.

The eigenvalues of this fixed point depend on ξ only when $\xi \neq 0$. Since x_c must be positive, which corresponds to $\xi < 0$, the eigenvalues can be either positive or negative, indicating that this fixed point is a saddle point. At this fixed point, the effective equation of state parameter is given by

$$w_{\text{eff}} = \frac{4\xi}{-3 + 12\xi}, \tag{6.29}$$

which is independent of c. The condition for cosmic acceleration, $w_{\text{eff}} < -1/3$, permits a range of the NMC coupling, $1/8 < \xi < 1/4$. The dust-like equation of state, $w_{\text{eff}} = 0$, is approached as $\xi \to 0$, while a de Sitter-like equation of state, $w_{\text{eff}} = -1$, requires $\xi = 3/16$. However, the condition $x_c < 0$ requires $\xi \leq 0$, hence this fixed point does not result in acceleration nor dust-like expansion and nor (effectively) de-Sitter expansion. From Table 3, the constraint $0 \leq \Omega_{\text{mc}} \leq 1$, implies that ξ must satisfy

$$\frac{17 - 12c^2 + \sqrt{1 + 24c^2}}{96 - 48c^2} \leq \xi \leq \frac{5 - 12c^2 + \sqrt{25 + 24c^2}}{48 - 48c^2}, \tag{6.30}$$

and

$$\frac{-5 + 12c^2 + \sqrt{25 + 24c^2}}{-48 + 48c^2} \leq \xi \leq \frac{-17 + 12c^2 + \sqrt{1 + 24c^2}}{-96 + 48c^2}. \tag{6.31}$$

Both conditions depend on c. Since the requirement $x_c > 0$ enforces $\xi < 0$, only the second condition remains valid. (6.31). As indicated in Table 3, for dust matter to be completely dominating,

$$\Omega_{\text{mc}} = -c^2 + \frac{3 - 34\xi + 96\xi^2}{3(1 - 4\xi)^2} = 1, \tag{6.32}$$

it follows that as $\xi \to 0$ with $\Omega_{\text{mc}} \to 1$ directly gives $c \to 0$. Canonical scalar field in GR limit is approached when $\xi \to 0$ and $c \to 0$. However, this fixed point does not fully recover the GR limit with a canonical scalar field, as ξ must be negative. Approaching the limit, $\xi \to 0^-$ and $c \to 0^-$ results in $\Omega_{\text{mc}} \to 1^-$. Therefore, this

fixed point asymptotically approaches the matter-dominated limit as $\xi \to 0$ and it is a saddle point transition.

6.2.2.6 Fixed point 6.

The stability of this fixed point depends solely on ξ, which can be analyzed in three cases. First, for $0 < \xi < 1/4$, the fixed point behaves as a saddle. Second, for $\xi < 0$ or $1/4 < \xi$, it is stable. Third, for $\xi = 0$, the system becomes indeterminate due to zero denominators in equations (6.18), (6.19), (6.26). a redefinition of the dynamical variables is necessary, leading to a new autonomous system that avoids indeterminate terms. Here, this case is considered as approaching limit only. A fundamental requirement for validity is that the kinetic term must not be negative, enforcing the condition $x_c \geq 0$. As a result, this requires $\xi < 0$. This fixed point is characterized by an effective equation of state parameter $w_{\text{eff}} = -1$ for all ξ and $0 \leq c < 1$, corresponding a dark energy-dominated phase. NMC scalar field and the holographic vacuum energy contribute to the dark energy with density $\Omega_{\text{dec}} = \Omega_{\phi c} + \Omega_{\Lambda c} = x_c + y_c + s_c + \Omega_{\Lambda c} = 1$, implying dark energy domination. In the canonical scalar limit of GR, where $\xi \to 0, (\xi \neq 0)$ and $c \to 0$, the potential term dominates in the late-time universe, leading to $x_c \to 0, y_c \to 1$, meaning the potential alone drives dark energy. For $\xi \to 0$ and $c \neq 0$, the system evolves such that $x_c \to 0, y_c \to 1 - c^2$ and $\Omega_{\Lambda c} = c^2$. For $\xi \neq 0$ and $c = 0$, the results are consistent with those previously obtained by Sami *et al.* [95] for the non-holographic NMC theory.

6.2.2.7 Fixed point 7.

To avoid divergence in the eigenvalues, the coupling parameter must satisfy $\xi \neq (1 - c^2)/6$. For $\xi < 0$, and $0 \leq c < 1$, the fixed point behaves as a saddle. When $\xi \to 0^-$ and $0 \leq c < 1$, the system approaches the canonical scalar holographic case, where the NMC effect vanishes. In this limit, the effective equation of state parameter approaches $w_{\text{eff}} \to 1^-$, corresponding to a stiff fluid-dominated regime.

For $\xi > 0$, the stability of the fixed point depends on the value of ξ as follows: if $0 < \xi < (-17 + 12c^2 - \sqrt{1 + 24c^2})/[48(c^2 - 2)]$, the eigenvalues are unstable spiral; if $\xi > (-17 + 12c^2 - \sqrt{1 + 24c^2})/[48(c^2 - 2)]$, the point is unstable point. This is however, condition of the kinetic term, $x_c \geq 0$ with a condition $0 \leq c < 1$, implies that $\xi < 0$ (see Table 3) for the fixed point to be physically meaningful. In the canonical scalar GR limit, $\xi \to 0^-$ and $c \to 0^+$, the fixed point becomes a purely kinetic-dominated state with $x_c = 1$. The effective equation of state parameter in this limit is

$$\lim_{c \to 0^+, \xi \to 0^-} w_{\text{eff}} = 1\,, \tag{6.33}$$

which corresponds to a stiff fluid-dominated epoch.

6.2.2.8 Fixed point 8.

In the limit $\xi \to 0^-$ and $0 \leq c < 1$, this fixed point is similar to the fixed point 7, where the universe consists solely of a kinetic term and a constant vacuum energy. This results in stiff-fluid equation of state parameter $w_{\text{eff}} = 1$. A stiff fluid phase can also emerge in the canonical scalar GR limit, where $\xi \to 0^-$ and $c \to 0^+$, yielding

$$\lim_{c \to 0^+, \xi \to 0^-} w_{\text{eff}} = 1\,. \tag{6.34}$$

The stability of this fixed point can be categorized into three cases: For $\xi < 0$, the fixed point is a unstable point for $0 \leq c < 1$. For $\xi > 0$, stability depends on the range of ξ: if $0 < \xi < (-17 + 12c^2 - \sqrt{1 + 24c^2})/[48(c^2 - 2)]$, the point is saddle spiral; if $\xi > (-17 + 12c^2 - \sqrt{1 + 24c^2})/[48(c^2 - 2)]$, the stability is a saddle point. However, to ensure physical validity, the condition $x_c \geq 0$ must hold. Given $0 \leq c < 1$, this requirement forces $\xi < 0$, confirming that only negative values of ξ make this fixed point physically meaningful..

6.2.2.9 Fixed point 9.

Fixed point 9 represents a state where the universe is dominated by constant vacuum energy and potential, characterized by an effective equation of state

parameter $w_{\text{eff}} = -1$. The stability of this fixed point depends on the value of the NMC coupling parameter ξ: For $\xi < 0$ or $\xi > 1/3$ the fixed point behaves as a saddle. For $0 < \xi < 1/3$, the fixed point is stable. To ensure a well-defined system, the NMC coupling must not take the values $\xi = 0$ or $\xi = 1/3$, as these cases lead to singularities or undefined behavior. This point is potential and vacuum energy dominated as seen in Table 3. It corresponds to $w_{\text{eff}} = -1$.

6.2.3 Phase portrait

Observations of the current density parameter of spatial curvature, Ω_k, from DESI+CMB+Union3 data reveal a very small value about $\Omega_{k0} = -0.0004 \pm 0.0019$ [50]. Hence the present universe is very close to flatness, and we assume flat space here. According to Table 3, dynamical system analysis identifies three fixed points (point 1, 2, and 3) corresponding to non-flat case and six fixed points (points 4, 5, 6, 7, 8 and 9) corresponding to flat cases. Here, we discuss the flat cases which are of points 4 to 9

One can consider a universe where the radiation-dominated epoch is omitted, and its evolution is follows as: it initially begins with an almost stiff fluid-dominated phase, corresponding to fixed points 7 or 8 [9]. The physical constraint $x_c \geq 0$ requires $\xi < 0$, and for the theory to remain valid, ξ must be nonzero. This phase is then followed by a dust-dominated epoch, represented by fixed point 5. The condition $\xi \to 0^-$ is necessary for two reasons: first, to satisfy the dust-dominated condition approaching the saddle fixed point 5, and second, to ensure the kinetic-dominated (stiff-fluid) condition at fixed points 7 and 8. Finally, the universe transitions into a stable dark energy-dominated phase at fixed point 6. Fixed points 4 and 9 are excluded from this analysis since they do not correspond to stable solutions. Thus, the universe evolves through the sequence of fixed points:

[9]For the point 7 and 8, according to Table 5, as $\xi \to 0^-$, the effective equation of state approaches stiff-fluid condition, $w_{\text{eff}} \to 1^-$

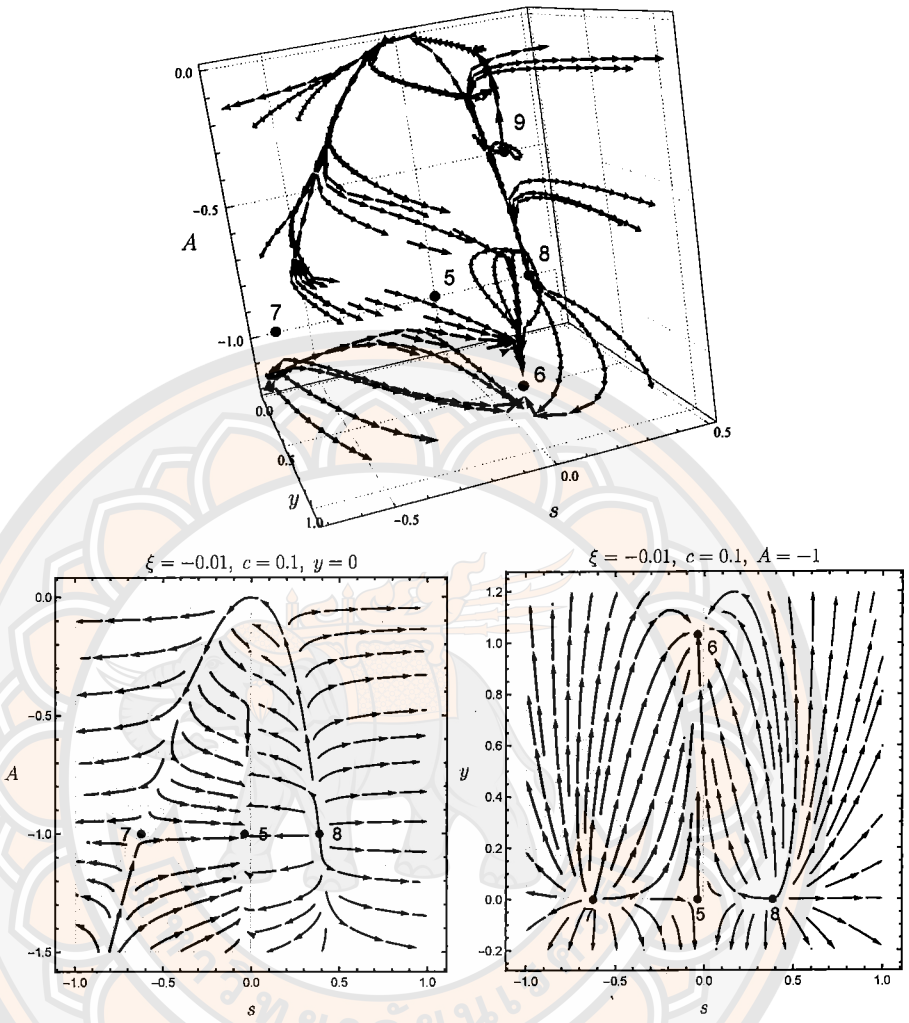

Figure 6 **Phase portrait of the autonomous system in flat universe, $\Omega_k = 0$, in the $x - y$ plane for $\xi = -10^{-4}$ and $c = 0.1$, with s fixed at $s = -1, -0.5, -0.001$, and 1**

7 or 8 $\rightarrow$ 5 $\rightarrow$ 6. For a complete dust-dominated phase and a smooth transition to the stable dark energy epoch, the coupling parameter should be negative and small for all $0 \leq c < 1$. We can conclude that this model require $\xi \rightarrow 0^-$ for physical viability. Under these conditions, the dynamical variable $s = 16\pi G_{\text{eff}} \xi \phi \dot{\phi}/H$ must be negative in an expanding universe ($H > 0$).

The evolution of the universe can be visualized through the phase portrait shown in Figure 6. In this plot, we assume a flat universe with $\Omega_k = 0$, a holographic parameter of $c = 0.1$, and a coupling parameter approaching $\xi \rightarrow -10^{-4}$. In

the flat universe case, the system consists of three dynamical variables:: x, y, s. According to Table 4, when $\xi \to 0^-$, fixed point 7 behaves as a saddle, while fixed point 8 is unstable. Additionally, for $\xi \to 0^-$, fixed point 8 is located in the $s > 0$ region, which is inconsistent with an expanding universe, as it would require $H < 0$ (assuming a positive field value). Moreover, under the condition $\xi \to 0^-$, the variables $y = 8\pi G_{\text{eff}} V_0 \phi^2 / 3H^2$ and $A = 8\pi G_{\text{eff}} \xi \phi^2$ must satisfy $y > 0$ and $A < 0$. Based on these constraints, we focus on fixed point 7, which is located in the allowed region ($s < 0, A < 0$ and $y > 0$), as the starting point of cosmic evolution. At this stage, the universe is dominated by the scalar kinetic term and holographic vacuum energy, leading to an almost stiff-fluid equation of state (saddle point 7). It then transitions into an approximately dust-dominated phase (saddle point 5).[10]. After leaving the saddle point 5, the universe evolves toward the stable fixed point 6, corresponding to a dark energy-dominated phase at late times. This evolutionary sequence follows the path: $7 \to 5 \to 6$. FIG 6 presents a three-dimensional phase portrait in the (s, y, A) space. Bottom panels of the figure display two planar slices: the left panel represents the $ys-$plane with $\xi = -0.01$, $c = 0.1$ and $A = -1$, while the right panel shows the $As-$plane with $\xi = -0.01$, $c = 0.1$ and $y = 0$. Fixed points are labeled in the figures, with shaded regions indicating the allowed parameter space. The trajectories illustrate the transition from fixed point $7 \to 5$, converging to the stable fixed point 6. This corresponds approximately to the values to $y_c \to 1.02$, $s_c \to -0.038$. Fixed point 6 represents a stable, cosmological constant-dominated epoch with $w_{\text{eff}} = -1$, which is consistent with current observations. Although fixed points 4 and 9 also correspond to dark energy domination, they are excluded from our analysis as they are not stable under the condition $\xi < 0$.

---

[10]For the fixed point 5, according to TABLE (5), there is no completely dust-dominated epoch ($w_{\text{eff}} = 0$) however as $\xi \to 0^-$, this approach dust-dominated condition.

Here the dark energy is effective contribution of both scalar field and holographic vacuum energy. From the Friedmann constraint, (6.14), the stable fixed point 6 satisfies $1 = x_c + y_c + s_c + \Omega_{mc} + \Omega_{kc} + \Omega_{\Lambda c}$, with $\Omega_{DEc} = x_c + y_c + s_c + \Omega_{\Lambda c} = \Omega_{\phi c} + \Omega_{\Lambda c} = 1$.

6.3 Numerical solution

The autonomous system (6.26) can be integrated numerically. Cosmological parameters are plotted as functions of e-folding number $N = \ln a$, including the effective equation of state parameter, $w_{\text{eff}}(N)$, the equation of state parameter for dark energy, $w_{\text{de}}(N)$, the density parameter for matter, $\Omega_{\text{m}}(N)$, the density parameter for dark energy, $\Omega_{\text{de}}(N)$, and spatial curvature density parameter, $\Omega_k(N)$. In this work, we consider the quadratic potential $V(\phi) = V_0\phi^2$. Figure 7 illustrates the effective and dark energy equations of state parameter by varying the holographic parameter $c = 0.1,\ 0.6,\ 0.8$ (left panel) and the coupling parameter $\xi = -10^{-2}, -10^{-3}, -10^{-4}, -10^{-5}$, and -10^{-6} (right panel). For this plot, the initial conditions are chosen as follows: $y_0 = 1 - s_0 - \Omega_{\text{m}0} - s_0^2/(24A_0\xi) - c^2(1 - \Omega_{k0}) - \Omega_{k0}$, $s_0 = -10^{-7}$, $A_0 = -0.7$. The initial value of y_0 is given by Friedmann constraint equation (6.19) with observational data $\Omega_{\text{m}0} = 0.3233, \Omega_{k0} = -0.0004$ from DESI+CMB+Union3 ($w_0w_a\text{CDM} + \Omega_k$ model) [50] where s_0 and A_0 are chosen by hand.

According to Table 5, no fixed points are completely dominated by dust or stiff fluids. For the cosmic evolution to approach dust or stiff fluid dominations, the coupling parameter must be small and negative ($\xi \to 0^-$), and the holographic parameter must also be small ($c \to 0$). Figure 7 shows that, for any values of ξ and c, the equation of state parameter w_{eff} approaches -1 at late times, corresponding to a cosmological constant-like behavior. For the parameter $\xi = -10^{-5}$, variations in the parameter c not significantly change the behavior of the effective equation

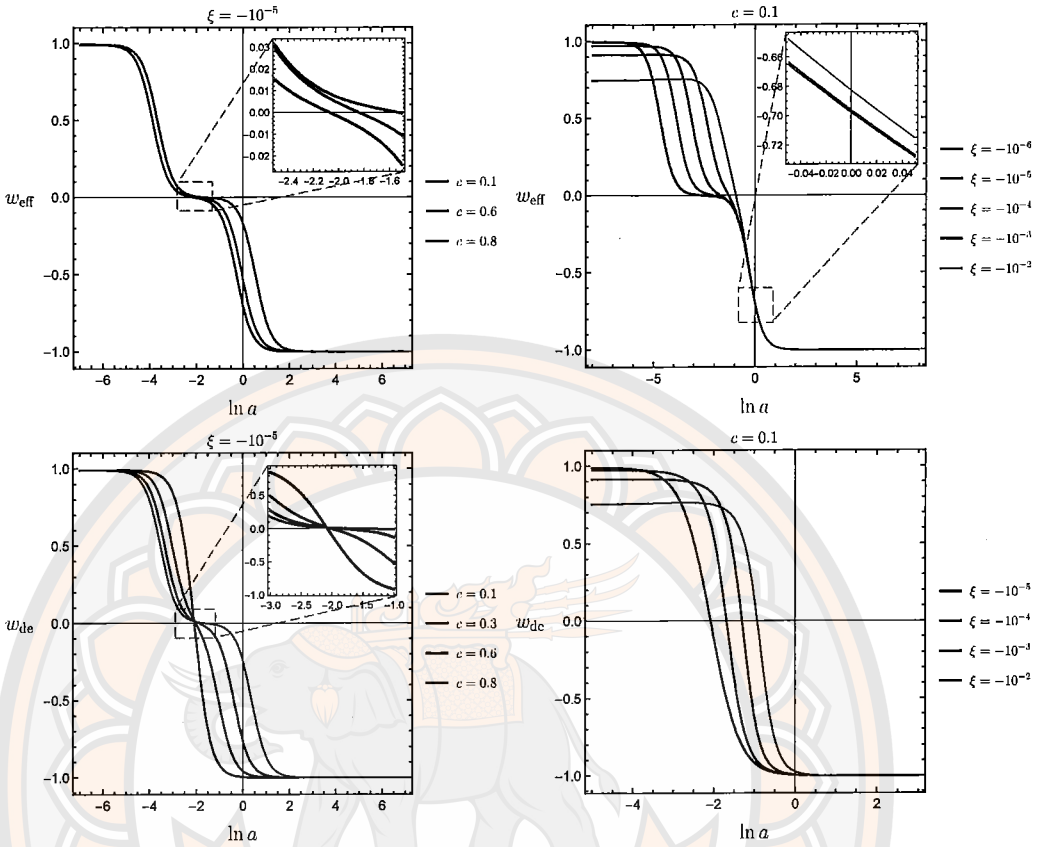

Figure 7 **The figure shows the effective equation of state parameter w_{eff} and dark energy equation of state parameter w_{de} plotting to $\ln a$.**

of state parameter. For small values of c, the universe is accelerated expansion, whereas larger values of c lead to ending of acceleration. When varying the coupling parameter ξ, smaller values of ξ result in a more completely matter-dominated epoach compared to larger values of ξ. The equation of state parameter of dark energy is also plotted. For a fixed $\xi = -10^{-5}$, small value of c make dark energy behave like a cosmological constant, while increasing c causes dark energy to scale with the effective equation of state parameter. Conversely, when $c = 0.1$ is fixed, varying ξ does not alter the late-time cosmological constant behavior of dark energy but significantly impacts its behavior during early times.

The density parameters for dust matter (Ω_{m}), dark energy (Ω_{de}), and spatial curvature (Ω_k) are shown in Figures 8, 9. At both early and late times, the universe

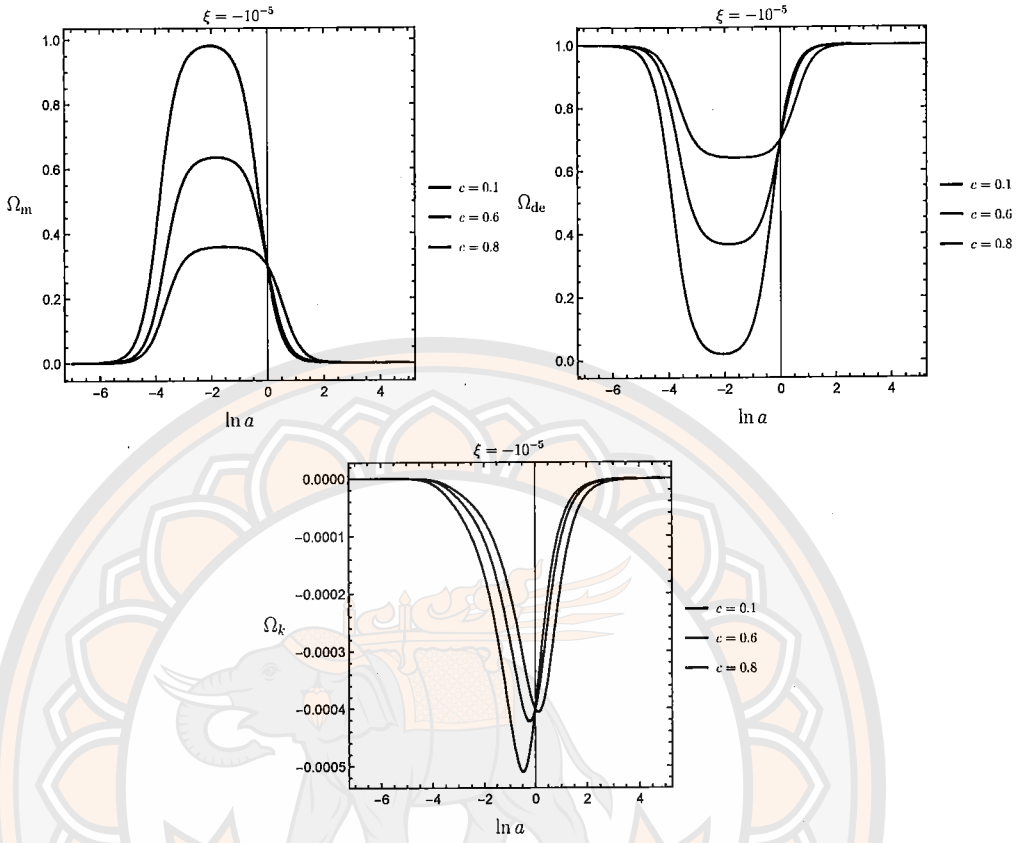

Figure 8 The figures show the density parameters for the dust matter field, $\Omega_{\rm m}$, dark energy, $\Omega_{\rm de}$, and spatial curvature Ω_k.

is dominated by the NMC scalar field togeter with holographic vacuum energy. At early times, the scalar field behaves like a stiff fluid, while at late times, the scalar field and the holographic vacuum energy behave like dark energy. Although c has negligible influence at early and late times, it significantly affects the matter-dominated epoch. As c, increases, the density of matter decreases, while the density of dark energy increase.

Figure 9 shows the density parameters plotted with respect to $\ln a$. At late times, the universe is dominated by dark energy $\Omega_{\rm de} = 1$, with the other components becoming negligible. However, during the matter-dominated epoch, when $\Omega_{\rm m} > \Omega_{\rm de}$, the coupling parameter ξ plays a crucial role. Smaller values of ξ increase both the density and the duration of the matter-dominated epoch, while the density of dark energy behaves oppositely. The density parameter for spatial

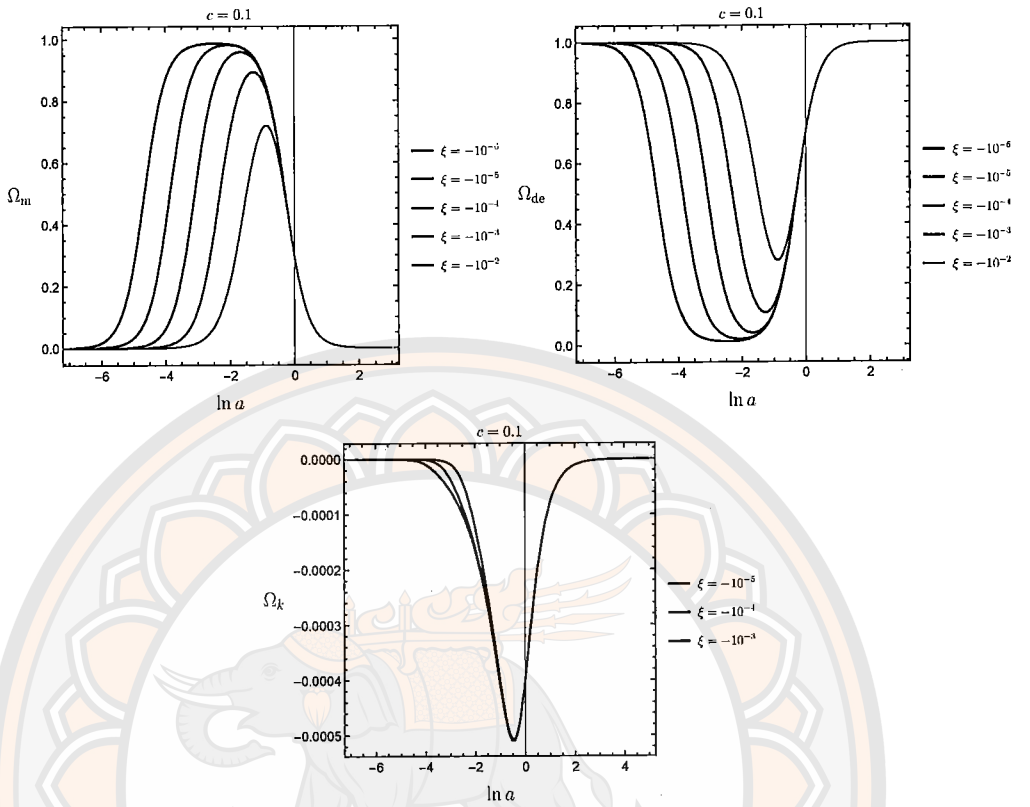

Figure 9 The figures show the density parameters for the dust matter field, Ω_{m}, dark energy, Ω_{de}, and spatial curvature Ω_k.

curvature remains very small throughout and can be neglected in this analysis.

Finally, based on the dynamical system analysis, the conditions for a realistic evolution of the universe require that the coupling parameter ξ be small and negative, while the holographic parameter c should also be small. For $\xi = -10^{-6}$ and $c = 0.1$, Figure 10 presents the density parameters of matter (red line), dark energy (blue line), and spatial curvature (green line). The plot shows that dark energy, which arises from the combined effects of the scalar field and holographic vacuum energy, behaves as a stiff fluid at early times and transitions to act as a cosmological constant at late times. Between these periods, the matter field dominates the evolution of the universe.

The figure 10 also includes the equation of state parameters: the effective equation of state (dashed line), the equation of state for dark energy (red line), and

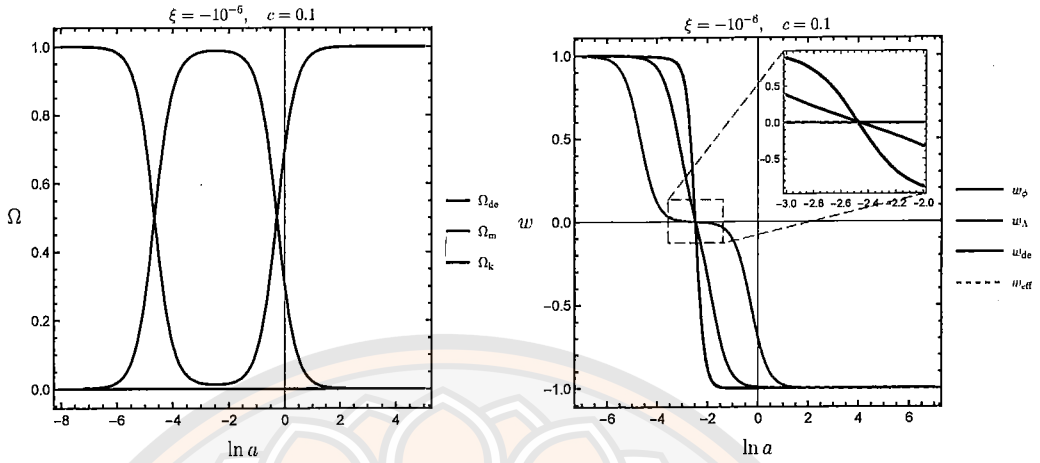

Figure 10 The figures show energy density parameters for dark energy Ω_{de}, dust Ω_m, and spatial curvature Ω_k in the left panel and the right panel shows equation of state parameters for scalar field w_ϕ, holographic vacuum energy w_Λ, dark energy w_{de}, and effective parameter w_{eff}.

its components, namely the NMC scalar field (blue line) and holographic vacuum energy (green line). The effective equation of state parameter indicates that the universe evolves from a stiff fluid $w_{eff} = 1$ to a matter-dominated state $w_{eff} = 0$, and finally to a cosmological constant-dominated state $w_{eff} = -1$. The scalar field transitions directly from a stiff fluid $w_\phi = 1$ to a cosmological constant $w_\phi = -1$, while the holographic vacuum energy evolves scaling with the background evolution.

CHAPTER VII

CONCLUSION AND DISCUSSION

We have examined a FLRW universe with arbitrary spatial curvature, considering cosmic contents that include dust matter, a NMDC field governed by a power-law potential, and holographic vacuum energy. The cosmological cutoff employed in this study is the apparent horizon, which reduces to the Hubble horizon in flat spacetime. For flat spacetime, an effective gravitational constant can be defined within the Friedmann equation. However, in the general case of non-flat geometry, such a constant cannot be defined in the same way.

A dynamical and stability analysis of the system reveals the existence of four distinct fixed points. One stable fixed point, denoted as point (b), corresponds to $w_{\text{eff}} = -1$. This point exists for any value of the NMDC coupling κ, although observational data favors negative values of κ. The cosmological implications of all fixed points are explored in this work. One branch of the stable fixed point (b) solution leads to de Sitter expansion.

We numerically integrated the dynamical system and compared the results with $H(z)$ data from [92]. For flat universes, the observational $H(z)$ data is qualitatively consistent with a large negative value of κ, approximately -200. Increasing the value of the parameter c raises the slope of the $H(z)$ plots. For positive or small negative values of κ, the numerical results align with $H(z)$ data only at lower redshift regimes. Increasing the magnitude of c steepens the slopes of both the effective equation of state, w_{eff}, and the Hubble parameter, $H(z)$.

A combination of large negative κ and larger c values could potentially lead to a phantom-like equation of state, $w_{\text{eff}} < -1$, in the near cosmological future, i.e., at small negative redshifts. The inclusion of spatial curvature introduces a coupling term between the NMDC field and curvature, influencing the sign of the scalar

field's kinetic energy based on the sign of κ. Negative values of κ are preferred, as they contribute to a larger scalar field kinetic energy term in the Friedmann equation.

The second part of this dissertation explores the non-minimally coupled (NMC) scalar field theory of gravity, incorporating holographic vacuum energy effects. Specifically, we investigate a subclass of the Horndeski theory that features non-minimal coupling. Previous studies indicate that an NMC theory with a quadratic potential remains viable for $\xi > -7.0 \times 10^{-3}$ [96]. We consider FRW universe containing NMC scalar field, dust matter and holographic vacuum energy. Our model considers an FRW universe containing an NMC scalar field, dust matter, and holographic vacuum energy. In this setup, the effective gravitational constant depends on the scalar field, denoted as $G_{\text{eff}}(\phi)$, and is naturally defined at the action level. Consequently, the universe is composed of a canonical scalar field, dust matter, and holographic vacuum energy, with the vacuum energy density taking the form $\rho_\Lambda = 3c^2/8\pi G_{\text{eff}} L^2$. The cutoff scale is chosen to be apparent horizon. We consider quadratic power-law scalar potential, $V(\phi) = V_0\phi^2$ here.

Our dynamical system analysis of the four independent dimensionless parameters reveals nine fixed points as shown in Table 3. The non-minimal coupling effects appear explicitly in all dynamical variables through G_{eff} except in Ω_k, while the holographic effect is present only in Ω_Λ. Both the holographic vacuum energy and the scalar field contribute to the total dark energy density that drives cosmic acceleration. Table 4, categorizes the fixed points stability. Points 1, 2, and 4 are non-physical, while fixed point 3 corresponds to a curvature-dominated regime that can be either a saddle or an unstable point. Fixed point 5 exists only for $\xi < 0$ and behaves as a saddle. As $\xi \to 0$ and $c \to 0$, this model approaches the canonical scalar field theory in the GR limit. Hence it is not a complete matter-domination but only a transient event in the evolution and this happens as $\xi \to 0^-$. Fixed point

6 represents a dark energy-dominated phase with $w_{\text{eff}} = -1$ for all ξ and $0 \leq c < 1$. The value range of ξ affects its stability directly. For $0 < \xi < 1/4$, it behaves as a saddle, whereas for $\xi < 0$ or $1/4 < \xi$, it is stable. The special case $\xi = 0$ is not allowed, as it renders the system indeterminate. We can not say that $\xi = 0$ is the canonical scalar holographic limit. This is because the dynamical variables must be re-defined from the beginning as such the system becomes completely different autonomous system and it is not our interest here. Generally, the condition $\xi < 0$ is favored and in the non-holographic limit, we recover the NMC results reported previously by Sami *et al.*. Fixed point 7 requires $\xi < 0$ and $0 \leq c < 1$,acting as a saddle. As $\xi \to 0^-$ with $0 \leq c < 1$, the effective equation of state approaches the stiff-fluid condition, $w_{\text{eff}} \to 1^-$, indicating that fixed point 7 corresponds to a stiff fluid-dominated phase. Similarly, fixed point 8 also represents stiff-fluid domination but specifically in the GR limit, where $\xi \to 0^-$ and $c \to 0^+$. Stability of the fixed point 8 comes in three cases. For $\xi < 0$, it is unstable otherwise they are either saddle spiral or saddle point. Nevertheless, it is only physically valid when $\xi < 0$. Fixed point 9 corresponds to a constant vacuum energy-dominated phase with $w_{\text{eff}} = -1$, where stability depends on the value of c. It behaves as a saddle for $\xi < 0$ or $1/3 < \xi$ and remains stable for $0 < \xi < 1/3$, with singularities occurring at $\xi = 0, 1/3$.

In our analysis, we focus only on the flat case. As shown in Table 4, points 1, 2, and 3 correspond to non-flat cases, while points 4, 5, 6, 7, 8, and 9 are relevant for flat space. A plausible cosmological scenario emerges in which the universe begins in a nearly stiff-fluid-dominated phase (fixed points 7 or 8). To achieve a near-dust-dominated state (fixed point 5) and maintain the kinetic term-dominated phase (fixed points 7 and 8), the condition $\xi \to 0^-$ must be met for physical consistency. Moreover, for an expanding universe, the dynamical variable s must be negative. Fixed point 8 resides in the $s > 0$ region, making it incompatible with cosmic expansion, whereas fixed point 7 is in the physically allowed region

$s < 0, A < 0, y > 0$, making it a viable starting point for cosmic evolution. The universe thus evolves through the sequence: $7 \to 5 \to 6$. The fixed points 4 and 9 are not interested as they are not stable for $\xi < 0$. The stable fixed point 6 corresponds to $\Omega_{\phi c} + \Omega_{\Lambda c} = 1$. as dark energy is contributed from both scalar field and holographic vacuum energy.

We numerically integrate the autonomous system equations (6.26) and plot the evolution of $w_{\text{eff}}(N)$, $\Omega_{\text{m}}(N)$, $\Omega_{\text{DE}}(N)$ and $\Omega_k(\ln a)$ as functions of the e-folding number $N = \ln a$. To approach dust or stiff fluid dominations, the NMC coupling must be small and negative, and the holographic parameter must also be small ($c \to 0^+$). For any allowed values of ξ and c, w_{eff} approaches -1 at late times. A more negative coupling suppresses the dust-dominated phase, raising w_{eff} at fixed point 5 while decreasing it at fixed point 7 (FIG. 7). Increasing of c does not change the qualitative shape of w_{eff}, but larger c increases w_{eff}. The NMC coupling ξ has little effect on Ω_Λ, whereas larger c increases Ω_Λ, which remains nearly constant due to the small value of Ω_k. For larger negative magnitude of the NMC coupling, Ω_ϕ is larger in the past. Larger c reduces the value of Ω_ϕ. For larger c, kinetic part x, NMC part s and potential part y are smaller. At latest stage of evolution, the potential term finally dominates. Very small negative magnitude of ξ and very small $0 < c \ll 1$ are favored in this model. Both the scalar field and holographic vacuum energy drive late-time acceleration. Future work will explore the effects of an exponential potential, along with kinematic and perturbation analyses against observational data.

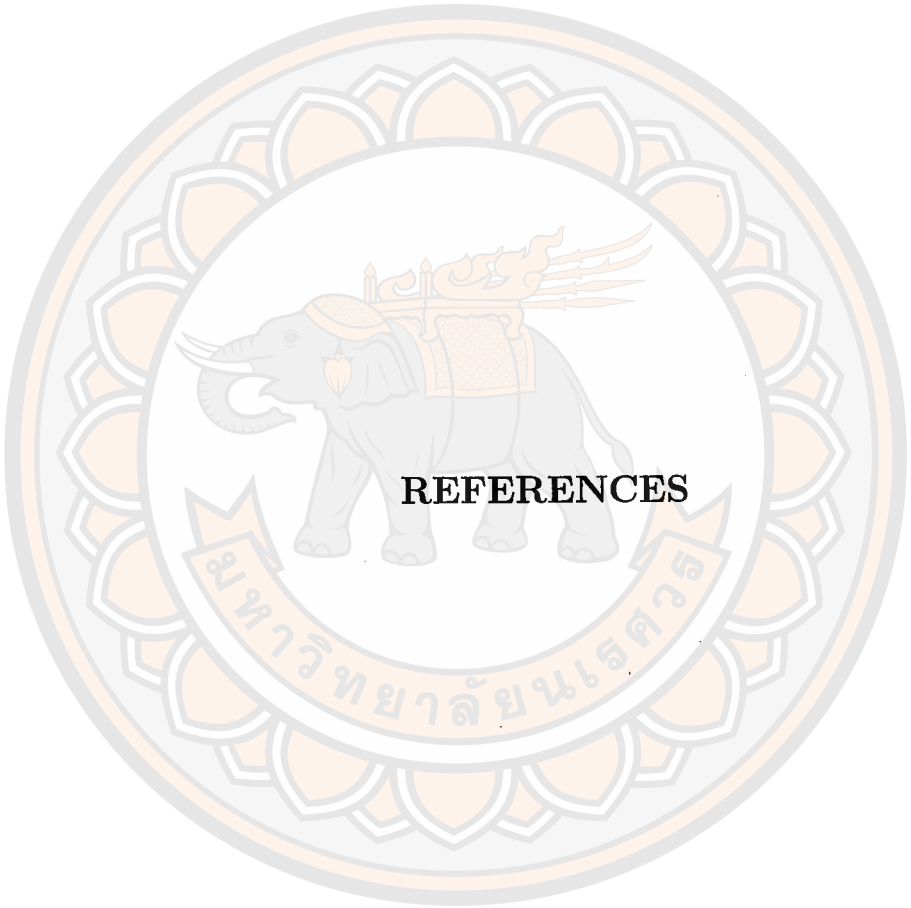

REFERENCES

REFERENCES

1. Faraoni V. Cosmology in Scalar-Tensor Gravity. Fundamental Theories of Physics. Springer Netherlands; 2004.

2. Capozziello S, De Laurentis M. Extended Theories of Gravity. Phys Rept. 2011;509:167-321.

3. Clifton T, Ferreira PG, Padilla A, Skordis C. Modified Gravity and Cosmology. Phys Rept. 2012;513:1-189.

4. Nojiri S, Odintsov SD. Introduction to modified gravity and gravitational alternative for dark energy. eConf. 2006;C0602061:06.

5. Amendola L, Tsujikawa S. Dark Energy: Theory and Observations. Dark Energy: Theory and Observations. Cambridge University Press; 2010.

6. Copeland EJ, Sami M, Tsujikawa S. Dynamics of dark energy. Int J Mod Phys D. 2006;15:1753-936.

7. Padmanabhan T. Dark energy: mystery of the millennium. AIP Conf Proc. 2006;861(1):179-96.

8. Amanullah R, Lidman C, Rubin D, Aldering G, Astier P, Barbary K, et al. Spectra and Hubble Space Telescope light curves of six type Ia supernovae at $0.511< z< 1.12$ and the Union2 compilation. The Astrophysical Journal. 2010;716(1):712.

9. Perlmutter S, et al. Measurements of Ω and Λ from 42 High Redshift Supernovae. Astrophys J. 1999;517:565-86.

10. Perlmutter S, et al. Discovery of a supernova explosion at half the age of the Universe and its cosmological implications. Nature. 1998;391:51-4.

11. Riess AG, et al. Observational evidence from supernovae for an accelerating universe and a cosmological constant. Astron J. 1998;116:1009-38.

12. De Felice A, Tsujikawa S. f(R) theories. Living Rev Rel. 2010;13:3.

13. Carroll SM, Duvvuri V, Trodden M, Turner MS. Is cosmic speed - up due to new gravitational physics? Phys Rev D. 2004;70:043528.

14. Brans C, Dicke RH. Mach's Principle and a Relativistic Theory of Gravitation. Phys Rev. 1961 Nov;124:925-35.

15. Fujii Y, Maeda K. The Scalar-Tensor Theory of Gravitation. Cambridge Monographs on Mathematical Physics. Cambridge University Press; 2003.

16. Amendola L. Cosmology with nonminimal derivative couplings. Physics Letters B. 1993;301(2–3):175–182.

17. Capozziello S, Lambiase G, Schmidt HJ. Nonminimal derivative couplings and inflation in generalized theories of gravity. Annalen der Physik. 2000;512(1):39-48.

18. Granda LN, Cardona W. General non-minimal kinetic coupling to gravity. Journal of Cosmology and Astroparticle Physics. 2010 Jul;2010(07):021–021.

19. Granda LN. Non-minimal Kinetic coupling to gravity and accelerated expansion. Journal of Cosmology and Astroparticle Physics. 2010;2010(07):006–006.

20. Sushkov SV. Exact cosmological solutions with nonminimal derivative coupling. Phys Rev D. 2009;80:103505.

21. Saridakis EN, Sushkov SV. Quintessence and phantom cosmology with non-minimal derivative coupling. Phys Rev D. 2010;81:083510.

22. Horndeski GW. Second-order scalar-tensor field equations in a four-dimensional space. Int J Theor Phys. 1974;10:363-84.

23. Deffayet C, Gao X, Steer DA, Zahariade G. From k-essence to generalised Galileons. Phys Rev D. 2011;84:064039.

24. Motohashi H, Suyama T. Third order equations of motion and the Ostrogradsky instability. Phys Rev D. 2015;91(8):085009.

25. Woodard RP. Ostrogradsky's theorem on Hamiltonian instability. Scholarpedia. 2015;10(8):32243.

26. Sushkov S. Realistic cosmological scenario with non-minimal kinetic coupling. Phys Rev D. 2012;85:123520.

27. Bruneton JP, Rinaldi M, Kanfon A, Hees A, Schlogel S, Fuzfa A. Fab Four: When John and George play gravitation and cosmology. Adv Astron. 2012;2012:430694.

28. Skugoreva MA, Sushkov SV, Toporensky AV. Cosmology with nonminimal kinetic coupling and a power-law potential. Phys Rev D. 2013;88:083539.

29. Dent JB, Dutta S, Saridakis EN, Xia JQ. Cosmology with non-minimal derivative couplings: perturbation analysis and observational constraints. Journal of Cosmology and Astroparticle Physics. 2013;2013(11):058.

30. Amendola L, Tsujikawa S. Dark energy: Theory and observations. Cambridge University Press; 2010.

31. Li M. A Model of holographic dark energy. Phys Lett B. 2004;603:1.

32. Hsu SD. Entropy bounds and dark energy. Physics Letters B. 2004;594(1-2):13-6.

33. Cui J, Zhang X. Cosmic age problem revisited in the holographic dark energy model. Phys Lett B. 2010;690:233-8.

34. Horava P, Minic D. Probable values of the cosmological constant in a holographic theory. Phys Rev Lett. 2000;85:1610-3.

35. Cai RG, Kim SP. First law of thermodynamics and Friedmann equations of Friedmann-Robertson-Walker universe. JHEP. 2005;02:050.

36. Tavayef M, Sheykhi A, Bamba K, Moradpour H. Tsallis Holographic Dark Energy. Phys Lett B. 2018;781:195-200.

37. Moradpour H, Moosavi S, Lobo I, Graça JM, Jawad A, Salako I. Thermodynamic approach to holographic dark energy and the Rényi entropy. The European Physical Journal C. 2018;78:1-6.

38. Nakarachinda R, Pongkitivanichkul C, Samart D, Tannukij L, Wongjun P. Rényi Holographic Dark Energy. Fortsch Phys. 2024;72(7-8):2400073.

39. Drepanou N, Lymperis A, Saridakis EN, Yesmakhanova K. Kaniadakis holographic dark energy and cosmology. Eur Phys J C. 2022;82(5):449.

40. Sayahian Jahromi A, Moosavi SA, Moradpour H, Morais Graça JP, Lobo IP, Salako IG, et al. Generalized entropy formalism and a new holographic dark energy model. Phys Lett B. 2018;780:21-4.

41. Baisri P, Gumjudpai B, Kritpetch C, Vanichchapongjaroen P. Cosmology in holographic non-minimal derivative coupling theory: Constraints from inflation and variation of gravitational constant. Physics of the Dark Universe. 2023;41:101251.

42. Avdeev NA, Toporensky AV. Ruling Out Inflation Driven by a Power Law Potential: Kinetic Coupling Does Not Help. Grav Cosmol. 2022;28(4):416-9.

43. Avdeev NA, Toporensky AV. Inflation in Scalar-Tensor Theory with Nonminimal Kinetic Coupling. Phys Part Nucl Lett. 2023;20(3):486-9.

44. Mather JC, et al. A Preliminary measurement of the Cosmic Microwave Background spectrum by the Cosmic Background Explorer (COBE) satellite. Astrophys J Lett. 1990;354:L37-40.

45. Hinshaw G, et al. Nine-year Wilkinson Microwave Anisotropy Probe (WMAP) observations: cosmological parameter results. The Astrophysical Journal Supplement Series. 2013;208(2):19.

46. Aghanim N, et al. Planck 2018 results. VI. Cosmological parameters. Astron Astrophys. 2020;641:A6.

47. Cole S, et al. The 2dF Galaxy Redshift Survey: Power-spectrum analysis of the final dataset and cosmological implications. Mon Not Roy Astron Soc. 2005;362:505-34.

48. Eisenstein DJ, et al. Detection of the Baryon Acoustic Peak in the Large-Scale Correlation Function of SDSS Luminous Red Galaxies. Astrophys J. 2005;633:560-74.

49. Riess AG, et al. A Comprehensive Measurement of the Local Value of the Hubble Constant with 1 km s^{-1} Mpc^{-1} Uncertainty from the Hubble Space Telescope and the SH0ES Team. Astrophys J Lett. 2022;934(1):L7.

50. Adame AG, et al. DESI 2024 VI: Cosmological Constraints from the Measurements of Baryon Acoustic Oscillations. 2024 4.

51. Liu H, Tseytlin AA. D = 4 superYang-Mills, D = 5 gauged supergravity, and D = 4 conformal supergravity. Nucl Phys B. 1998;533:88-108.

52. Nojiri S, Odintsov SD. Conformal anomaly for dilaton coupled theories from AdS / CFT correspondence. Phys Lett B. 1998;444:92-7.

53. Linde A. Particle physics and inflationary cosmology. arXiv preprint hep-th/0503203. 2005.

54. Magnano G, Ferraris M, Francaviglia M. Nonlinear gravitational Lagrangians. General Relativity and Gravitation. 1987;19:465-79.

55. Capozziello S, Lambiase G. Nonminimal Derivative Coupling and the Recovering of Cosmological Constant. General Relativity and Gravitation. 1999;31(7):1005–1014.

56. Daniel SF, Caldwell RR. Consequences of a cosmic scalar with kinetic coupling to curvature. Class Quant Grav. 2007;24:5573-80.

57. Granda LN. Non-minimal kinetic coupling and the phenomenology of dark energy. Classical and Quantum Gravity. 2010 Dec;28(2):025006.

58. Granda LN. Inflation driven by scalar field with non-minimal kinetic coupling with Higgs and quadratic potentials. Journal of Cosmology and Astroparticle Physics. 2011 Apr;2011(04):016–016.

59. Granda LN. Dark energy from scalar field with Gauss-Bonnet and non-minimal kinetic coupling. Modern Physics Letters A. 2012 Feb;27(04):1250018.

60. Granda LN, Loaiza E. Big Rip and Little Rip solutions in scalar model with kinetic and Gauss Bonnet couplings. Int J Mod Phys D. 2012;2:1250002.

61. Granda LN. Late time cosmological scenarios from scalar field with Gauss Bonnet and non-minimal kinetic couplings. Int J Theor Phys. 2012;51:2813-29.

62. Granda LN, Torrente-Luján E, Fernandez-Melgarejo JJ. Non-minimal kinetic coupling and Chaplygin gas cosmology. The European Physical Journal C. 2011 Jul;71(7).

63. Kobayashi T. Horndeski theory and beyond: a review. Rept Prog Phys. 2019;82(8):086901.

64. Gao C. When scalar field is kinetically coupled to the Einstein tensor. JCAP. 2010;06:023.

65. Feng K, Qiu T, Piao YS. Curvaton with nonminimal derivative coupling to gravity. Phys Lett B. 2014;729:99-107.

66. Gubitosi G, Linder EV. Purely Kinetic Coupled Gravity. Phys Lett B. 2011;703:113-8.

67. Koutsoumbas G, Ntrekis K, Papantonopoulos E. Gravitational Particle Production in Gravity Theories with Non-minimal Derivative Couplings. JCAP. 2013;08:027.

68. Gumjudpai B, Rangdee P. Non-minimal derivative coupling gravity in cosmology. Gen Rel Grav. 2015;47(11):140.

69. Darabi F, Parsiya A. Cosmology with non-minimal coupled gravity: inflation and perturbation analysis. Class Quant Grav. 2015;32(15):155005.

70. Bekenstein JD. Black Holes and Entropy. Phys Rev D. 1973 Apr;7:2333-46.

71. Hawking SW. Black hole explosions? Nature. 1974;248(5443):30-1.

72. Hawking SW. Particle Creation by Black Holes. Commun Math Phys. 1975;43:199-220. [Erratum: Commun.Math.Phys. 46, 206 (1976)].

73. Susskind L, Thorlacius L, Uglum J. The Stretched horizon and black hole complementarity. Phys Rev D. 1993;48:3743-61.

74. 't Hooft G. The black hole interpretation of string theory. Nucl Phys B. 1990;335:138-54.

75. 't Hooft G. Dimensional reduction in quantum gravity. Conf Proc C. 1993;930308:284-96.

76. Susskind L. The World as a hologram. J Math Phys. 1995;36:6377-96.

77. Bousso R. The Holographic principle. Rev Mod Phys. 2002;74:825-74.

78. Cohen AG, Kaplan DB, Nelson AE. Effective field theory, black holes, and the cosmological constant. Phys Rev Lett. 1999;82:4971-4.

79. Horvat R. Holography and a variable cosmological constant. Physical Review D. 2004;70(8):087301.

80. Hořava P, Minic D. Probable values of the cosmological constant in a holographic theory. Physical Review Letters. 2000;85(8):1610.

81. Fischler W, Susskind L. Holography and cosmology. arXiv preprint hep-th/9806039. 1998.

82. Cai RG. A dark energy model characterized by the age of the universe. Physics Letters B. 2007;657(4-5):228-31.

83. Neupane IP. A note on agegraphic dark energy. Physics Letters B. 2009;673(2):111-8.

84. Gao C, Wu F, Chen X, Shen YG. Holographic dark energy model from Ricci scalar curvature. Physical Review D. 2009;79(4):043511.

85. Granda L, Oliveros A. New infrared cut-off for the holographic scalar fields models of dark energy. Physics Letters B. 2009;671(2):199-202.

86. Zhang X. Holographic Ricci dark energy: Current observational constraints, quintom feature, and the reconstruction of scalar-field dark energy. Physical Review D. 2009;79(10):103509.

87. Cai RG, Kim SP. First law of thermodynamics and Friedmann equations of Friedmann-Robertson-Walker universe. Journal of High Energy Physics. 2005;2005(02):050.

88. Li M, Miao RX. A new model of holographic dark energy with action principle. arXiv preprint arXiv:12100966. 2012.

89. Li M, Li XD, Meng J, Zhang Z. Cosmological constraints on the new holographic dark energy model with action principle. Physical Review D—Particles, Fields, Gravitation, and Cosmology. 2013;88(2):023503.

90. Lin C. An effective field theory of holographic dark energy. Journal of Cosmology and Astroparticle Physics. 2021;2021(07):003.

91. Kritpetch C, Muhammad C, Gumjudpai B. Holographic dark energy with non-minimal derivative coupling to gravity effects. Physics of the Dark Universe. 2020;30:100712.

92. Farooq O, Madiyar FR, Crandall S, Ratra B. Hubble parameter measurement constraints on the redshift of the deceleration–acceleration transition, dynamical dark energy, and space curvature. The Astrophysical Journal. 2017;835(1):26.

93. Bahamonde S, Böhmer CG, Carloni S, Copeland EJ, Fang W, Tamanini N. Dynamical systems applied to cosmology: dark energy and modified gravity. Physics Reports. 2018;775:1-122.

94. Böhmer CG, Chan N. Dynamical systems in cosmology. In: Dynamical and Complex Systems. World Scientific; 2017. p. 121-56.

95. Sami M, Shahalam M, Skugoreva M, Toporensky A. Cosmological dynamics of a nonminimally coupled scalar field system and its late time cosmic relevance. Physical Review D—Particles, Fields, Gravitation, and Cosmology. 2012;86(10):103532.

96. Tsujikawa S, Gumjudpai B. Density perturbations in generalized Einstein scenarios and constraints on nonminimal couplings from the Cosmic Microwave Background. Phys Rev D. 2004;69:123523.

APPENDIX

APPENDIX A NMDC FIELD EQUATIONS

The action for a scalar field kinetically coupled to the Einstein tensor can be written as follows:

$$S = \mathrm{d}^4x \int \sqrt{-g}\left[\frac{R}{16\pi G} - \frac{1}{2}(\varepsilon g_{\mu\nu}\nabla^\mu\phi\nabla^\nu\phi + \kappa G_{\mu\nu}\nabla^\mu\phi\nabla^\nu\phi) - V(\phi)\right] + S_{\mathrm{m}}\,, \tag{A.1}$$

where S_{m} is the action of barotropic matter. The parameter $\varepsilon = 1, -1, 0$ corresponds to the canonical field, phantom field, and purely NMDC term, respectively. The parameter κ is the coupling constant between the kinetic term and the Einstein tensor. Now, let us consider the variation of the action in equation (A.1) with respect to the metric tensor $g^{\mu\nu}$. This yields

$$\begin{aligned}\delta_g S = & \int \mathrm{d}^4x\delta\sqrt{-g}\left[\frac{R}{16\pi G} - \frac{1}{2}(\varepsilon g_{\mu\nu} + \kappa G_{\mu\nu})\nabla^\mu\phi\nabla^\nu\phi - V(\phi) + \mathcal{L}_{\mathrm{m}}\right] \\ & + \int \mathrm{d}^4x\sqrt{-g}\Bigg[\underbrace{\frac{\delta R}{16\pi G}}_{\text{term 1}} - \frac{1}{2}\underbrace{\delta(\varepsilon g_{\mu\nu}\nabla^\mu\phi\nabla^\nu\phi)}_{\text{term 2}} - \frac{1}{2}\underbrace{\delta(\kappa G_{\mu\nu}\nabla^\mu\phi\nabla^\nu\phi)}_{\text{term 3}} \\ & - \delta V(\phi) + \frac{\delta\mathcal{L}_{\mathrm{m}}}{\delta g^{\mu\nu}}\delta g^{\mu\nu}\Bigg]\,.\end{aligned} \tag{A.2}$$

The matter action can be expressed as $S_{\mathrm{m}} = \int d^4x\sqrt{-g}\mathcal{L}_{\mathrm{m}}$, and the variation of the scalar potential is zero, i.e., $\delta V(\phi) = 0$.

The variation of the determinant, i.e., $\delta\sqrt{-g}$, can be expressed as $\delta\sqrt{-g} = -(1/2)g_{\mu\nu}\sqrt{-g}\delta g^{\mu\nu}$. Thus, the first part of equation (A.2) is given by

$$\begin{aligned}& \int \mathrm{d}^4x\delta\sqrt{-g}\left[\frac{R}{16\pi G} - \frac{1}{2}(\varepsilon g_{\mu\nu} + \kappa G_{\mu\nu})\nabla^\mu\phi\nabla^\nu\phi - V(\phi) + \mathcal{L}_{\mathrm{m}}\right] \\ & = -\int \mathrm{d}^4x\frac{1}{2}g_{\mu\nu}\sqrt{-g}\delta g^{\mu\nu}\left[\frac{R}{16\pi G} - \frac{1}{2}(\varepsilon g_{\alpha\beta} + \kappa G_{\alpha\beta})\nabla^\alpha\phi\nabla^\beta\phi - V(\phi) + \mathcal{L}_{\mathrm{m}}\right]\,.\end{aligned} \tag{A.3}$$

Now, let us consider the variation of term 1 of equation (A.2). This gives

$$\int \mathrm{d}^4x\sqrt{-g}\frac{1}{16\pi G}\delta R = \underbrace{\int \mathrm{d}^4x\sqrt{-g}\frac{1}{16\pi G}g^{\mu\nu}\delta R_{\mu\nu}}_{\text{boundary term=0}} + \int \mathrm{d}^4x\sqrt{-g}\frac{1}{16\pi G}R_{\mu\nu}\delta g^{\mu\nu}\,,$$

$$= \int \mathrm{d}^4x\sqrt{-g}\frac{1}{16\pi G}R_{\mu\nu}\delta g^{\mu\nu}\,. \tag{A.4}$$

Variation of the kinetic term, i.e., term 2 of the equation (A.2) read

$$\int \mathrm{d}^4x\sqrt{-g}\delta\left(-\frac{\varepsilon}{2}g_{\mu\nu}\nabla^\mu\phi\nabla^\nu\phi\right) = \int \mathrm{d}^4x\sqrt{-g}\left(-\frac{\varepsilon}{2}\nabla_\mu\phi\nabla_\nu\phi\delta g^{\mu\nu}\right)\,. \tag{A.5}$$

Finally, the variation of the coupling part, i.e., term 3 of equation (A.2), gives

$$\begin{aligned}
&\int \mathrm{d}^4x\sqrt{-g}\frac{\kappa}{2}\delta\left(-G_{\mu\nu}\nabla^\mu\phi\nabla^\nu\phi\right)\\
&= \int \mathrm{d}^4x\sqrt{-g}\frac{\kappa}{2}\delta\left[-(R_{\mu\nu}-\frac{1}{2}g_{\mu\nu}R)\nabla^\mu\phi\nabla^\nu\phi\right]\,,\\
&= \int \mathrm{d}^4x\sqrt{-g}\frac{1}{2}\kappa\left[-\underbrace{\delta\left(R_{\mu\nu}\nabla^\mu\phi\nabla^\nu\phi\right)}_{\text{term 3.1}}+\frac{1}{2}\underbrace{\delta\left(g_{\mu\nu}R\nabla^\mu\phi\nabla^\nu\phi\right)}_{\text{term 3.2}}\right]\,.
\end{aligned} \tag{A.6}$$

The variation of equation (A.6) gives two terms. Let us consider term 3.1. We have

$$\begin{aligned}
&\int \mathrm{d}^4x\sqrt{-g}\frac{\kappa}{2}\delta(-R_{\mu\nu}\nabla^\mu\phi\nabla^\nu\phi)\\
&= -\int \mathrm{d}^4x\sqrt{-g}\frac{\kappa}{2}\nabla_\rho\phi\nabla_\sigma\phi\delta\left(R_{\mu\nu}g^{\mu\rho}g^{\nu\sigma}\right)\,,\\
&= -\int \mathrm{d}^4x\sqrt{-g}\frac{\kappa}{2}\nabla_\rho\phi\nabla_\sigma\phi\left(\delta R_{\mu\nu}g^{\mu\rho}g^{\nu\sigma}+R_{\mu\nu}\delta g^{\mu\rho}g^{\nu\sigma}+R_{\mu\nu}g^{\mu\rho}\delta g^{\nu\sigma}\right)\,,\\
&= -\int \mathrm{d}^4x\sqrt{-g}\frac{\kappa}{2}\nabla_\rho\phi\nabla_\sigma\phi\left(\delta R_{\mu\nu}g^{\mu\rho}g^{\nu\sigma}+2R^\sigma_\mu\delta g^{\mu\rho}\right)\,,\\
&= \int \mathrm{d}^4x\sqrt{-g}\frac{\kappa}{2}\left(\underbrace{-\nabla_\rho\phi\nabla_\sigma\phi g^{\mu\rho}g^{\nu\sigma}\delta R_{\mu\nu}}_{\text{term 3.1.1}}-\underbrace{2\nabla_\sigma\phi\nabla_{(\nu}\phi R^\sigma_{\mu)}\delta g^{\mu\nu}}_{\text{term 3.1.2}}\right)\,.
\end{aligned} \tag{A.7}$$

The first term of equation (A.7) is expressed in terms of the variation of the Ricci tensor, which can be obtained as

$$\delta R_{\mu\nu} = \nabla_\rho\delta\Gamma^\rho_{\mu\nu}-\nabla_\mu\delta\Gamma^\rho_{\nu\rho}\,, \tag{A.8}$$

where the variation of the Christoffel symbols in equation (A.8) is

$$\delta\Gamma^\rho_{\mu\nu} = \frac{1}{2}g^{\rho\sigma}(\nabla_\mu\delta g_{\nu\sigma}+\nabla_\nu\delta g_{\mu\sigma}-\nabla_\sigma\delta g_{\mu\nu})\,, \tag{A.9}$$

$$\delta\Gamma^\rho_{\mu\rho} = \frac{1}{2}g^{\rho\sigma}\nabla_\mu\delta g_{\rho\sigma}. \tag{A.10}$$

Hence, term 3.1.1 in equation (A.7) can be expressed as

$$\int \mathrm{d}^4x\sqrt{-g}\frac{\kappa}{2}\left(-\nabla_\rho\phi\nabla_\sigma\phi g^{\mu\rho}g^{\nu\sigma}\delta R_{\mu\nu}\right)$$
$$= \int \mathrm{d}^4x\sqrt{-g}\frac{\kappa}{2}\left[-\nabla^\mu\phi\nabla^\nu\phi(\nabla_\rho\delta\Gamma^\rho_{\mu\nu}-\nabla_\mu\delta\Gamma^\rho_{\nu\rho})\right]. \tag{A.11}$$

Using integration by parts and applying boundary conditions, this gives

$$\begin{aligned}
&\int \mathrm{d}^4x\sqrt{-g}\frac{\kappa}{2}\left(-\nabla_\rho\phi\nabla_\sigma\phi g^{\mu\rho}g^{\nu\sigma}\delta R_{\mu\nu}\right)\\
&= \int \mathrm{d}^4x\sqrt{-g}\frac{\kappa}{2}\left[\nabla_\rho(\nabla^\mu\phi\nabla^\nu\phi)\delta\Gamma^\rho_{\mu\nu}-\nabla_\mu(\nabla^\mu\phi\nabla^\nu\phi)\delta\Gamma^\rho_{\nu\rho}\right],\\
&= \int \mathrm{d}^4x\sqrt{-g}\frac{\kappa}{4}\left[\nabla_\rho(\nabla^\mu\phi\nabla^\nu\phi)g^{\rho\sigma}(\nabla_\mu\delta g_{\nu\sigma}+\nabla_\nu\delta g_{\mu\sigma}-\nabla_\sigma\delta g_{\mu\nu})\right.\\
&\quad\left.-\nabla_\mu(\nabla^\mu\phi\nabla^\nu\phi)g^{\rho\sigma}\nabla_\nu\delta g_{\rho\sigma}\right],\\
&= \int \mathrm{d}^4x\sqrt{-g}\frac{\kappa}{4}\left[\nabla_\rho(\nabla^\mu\phi\nabla^\nu\phi)g^{\rho\sigma}\nabla_\mu\delta g_{\nu\sigma}+\nabla_\rho(\nabla^\mu\phi\nabla^\nu\phi)g^{\rho\sigma}\nabla_\nu\delta g_{\mu\sigma}\right.\\
&\quad\left.-\nabla_\rho(\nabla^\mu\phi\nabla^\nu\phi)g^{\rho\sigma}\nabla_\sigma\delta g_{\mu\nu}-\nabla_\mu(\nabla^\mu\phi\nabla^\nu\phi)g^{\rho\sigma}\nabla_\nu\delta g_{\rho\sigma}\right],\\
&= \int \mathrm{d}^4x\sqrt{-g}\frac{\kappa}{4}\left[-\nabla_\mu\nabla_\rho(\nabla^\mu\phi\nabla^\nu\phi)g^{\rho\sigma}\delta g_{\nu\sigma}-\nabla_\nu\nabla_\rho(\nabla^\mu\phi\nabla^\nu\phi)g^{\rho\sigma}\delta g_{\mu\sigma}\right.\\
&\quad\left.+\nabla_\sigma\nabla_\rho(\nabla^\mu\phi\nabla^\nu\phi)g^{\rho\sigma}\delta g_{\mu\nu}+\nabla_\nu\nabla_\mu(\nabla^\mu\phi\nabla^\nu\phi)g^{\rho\sigma}\delta g_{\rho\sigma}\right],\\
&= \int \mathrm{d}^4x\sqrt{-g}\frac{\kappa}{4}\left[-\nabla_\mu\nabla^\sigma(\nabla^\mu\phi\nabla^\nu\phi)\delta g_{\nu\sigma}-\nabla_\nu\nabla^\sigma(\nabla^\mu\phi\nabla^\nu\phi)\delta g_{\mu\sigma}\right.\\
&\quad\left.+\nabla_\sigma\nabla^\sigma(\nabla^\mu\phi\nabla^\nu\phi)\delta g_{\mu\nu}+\nabla_\nu\nabla_\mu(\nabla^\mu\phi\nabla^\nu\phi)g^{\rho\sigma}\delta g_{\rho\sigma}\right],\\
&= \int \mathrm{d}^4x\sqrt{-g}\frac{\kappa}{4}\left[\nabla_\mu\nabla^\sigma(\nabla^\mu\phi\nabla^\nu\phi)g_{\alpha\nu}g_{\beta\sigma}\delta g^{\alpha\beta}+\nabla_\nu\nabla^\sigma(\nabla^\mu\phi\nabla^\nu\phi)g_{\alpha\sigma}g_{\beta\mu}\delta g^{\alpha\beta}\right.\\
&\quad\left.-\nabla_\sigma\nabla^\sigma(\nabla^\mu\phi\nabla^\nu\phi)g_{\alpha\mu}g_{\beta\nu}\delta g^{\alpha\beta}-\nabla_\nu\nabla_\mu(\nabla^\mu\phi\nabla^\nu\phi)g^{\rho\sigma}g_{\alpha\rho}g_{\beta\sigma}\delta g^{\alpha\beta}\right],\\
&= \int \mathrm{d}^4x\sqrt{-g}\frac{\kappa}{4}\left[\nabla_\mu\nabla_\beta(\nabla^\mu\phi\nabla_\alpha\phi)+\nabla_\nu\nabla_\alpha(\nabla_\beta\phi\nabla^\nu\phi)\right.\\
&\quad\left.-\nabla_\sigma\nabla^\sigma(\nabla_\alpha\phi\nabla_\beta\phi)-\nabla_\nu\nabla_\mu(\nabla^\mu\phi\nabla^\nu\phi)g_{\alpha\beta}\right]\delta g^{\alpha\beta},\\
&= \int \mathrm{d}^4x\sqrt{-g}\frac{\kappa}{4}\left[\nabla_\rho\nabla_\nu(\nabla^\rho\phi\nabla_\mu\phi)+\nabla_\rho\nabla_\mu(\nabla^\rho\phi\nabla_\nu\phi)-\nabla_\sigma\nabla^\sigma(\nabla_\mu\phi\nabla_\nu\phi)\right.\\
&\quad\left.-\nabla_\sigma\nabla_\rho(\nabla^\rho\phi\nabla^\sigma\phi)g_{\mu\nu}\right]\delta g^{\mu\nu},
\end{aligned} \tag{A.12}$$

where $\delta g_{\mu\nu} = -g_{\alpha\mu}g_{\beta\nu}\delta g^{\alpha\beta}$. By combining equation (A.12) with term 3.1.2 of equation (A.7), term 3.1 of equation (A.6) is given by

$$\int \mathrm{d}^4x\sqrt{-g}\frac{\kappa}{2}\delta(-R_{\mu\nu}\nabla^\mu\phi\nabla^\nu\phi)$$
$$= \int \mathrm{d}^4x\sqrt{-g}\frac{\kappa}{4}[\nabla_\rho\nabla_\nu(\nabla^\rho\phi\nabla_\mu\phi)+\nabla_\rho\nabla_\mu(\nabla^\rho\phi\nabla_\nu\phi)-\nabla_\sigma\nabla^\sigma(\nabla_\mu\phi\nabla_\nu\phi)$$
$$-\nabla_\sigma\nabla_\rho(\nabla^\rho\phi\nabla^\sigma\phi)g_{\mu\nu}-4\nabla_\sigma\phi\nabla_{(\nu}\phi R^\sigma_{\mu)}]\delta g^{\mu\nu}\,. \tag{A.13}$$

There is another term in equation (A.6) i.e., term 3.2. Varying this term, we obtain

$$\int d^4x\sqrt{-g}\frac{\kappa}{2}\left[\frac{1}{2}\delta\left(g_{\mu\nu}R\nabla^\mu\phi\nabla^\nu\phi\right)\right]$$
$$= \int \mathrm{d}^4x\sqrt{-g}\frac{\kappa}{4}\nabla_\mu\phi\nabla_\nu\phi(g^{\alpha\beta}g^{\mu\nu}\delta R_{\alpha\beta}+R_{\alpha\beta}g^{\mu\nu}\delta g^{\alpha\beta}+R\delta g^{\mu\nu})\,,$$
$$= \int \mathrm{d}^4x\sqrt{-g}\frac{\kappa}{4}\left(\nabla_\alpha\phi\nabla_\beta\phi g^{\alpha\beta}g^{\mu\nu}\delta R_{\mu\nu}+\nabla_\alpha\phi\nabla^\alpha\phi R_{\mu\nu}\delta g^{\mu\nu}+\nabla_\mu\phi\nabla_\nu\phi R\delta g^{\mu\nu}\right)\,. \tag{A.14}$$

Considering the first term of equation (A.14). The variation of the Ricci tensor gives

$$\int \mathrm{d}^4x\sqrt{-g}\frac{\kappa}{4}\nabla_\alpha\phi\nabla^\alpha\phi g^{\mu\nu}\delta R_{\mu\nu}$$
$$= \int \mathrm{d}^4x\sqrt{-g}\frac{\kappa}{4}\left(\nabla_\alpha\phi\nabla^\alpha\phi g^{\mu\nu}\nabla_\rho\delta\Gamma^\rho_{\mu\nu}-\nabla_\alpha\phi\nabla^\alpha\phi g^{\mu\nu}\nabla_\mu\delta\Gamma^\rho_{\nu\rho}\right)\,,$$
$$= \int \mathrm{d}^4x\sqrt{-g}\frac{\kappa}{4}\left(-\nabla_\rho(\nabla_\alpha\phi\nabla^\alpha\phi)g^{\mu\nu}\delta\Gamma^\rho_{\mu\nu}+\nabla_\mu(\nabla_\alpha\phi\nabla^\alpha\phi)g^{\mu\nu}\delta\Gamma^\rho_{\nu\rho}\right)\,,$$
$$= \int \mathrm{d}^4x\sqrt{-g}\frac{\kappa}{8}\Big(-\nabla_\rho(\nabla_\alpha\phi\nabla^\alpha\phi)g^{\mu\nu}g^{\rho\sigma}(\nabla_\mu\delta g_{\nu\sigma}+\nabla_\nu\delta g_{\mu\sigma}-\nabla_\sigma\delta g_{\mu\nu})$$
$$+\nabla_\mu(\nabla_\alpha\phi\nabla^\alpha\phi)g^{\mu\nu}g^{\rho\sigma}\nabla_\nu\delta g_{\rho\sigma}\Big)\,,$$
$$= \int \mathrm{d}^4x\sqrt{-g}\frac{\kappa}{8}g^{\mu\nu}g^{\rho\sigma}\Big(-\nabla_\rho(\nabla_\alpha\phi\nabla^\alpha\phi)\nabla_\mu\delta g_{\nu\sigma}-\nabla_\rho(\nabla_\alpha\phi\nabla^\alpha\phi)\nabla_\nu\delta g_{\mu\sigma}$$
$$+\nabla_\rho(\nabla_\alpha\phi\nabla^\alpha\phi)\nabla_\sigma\delta g_{\mu\nu}+\nabla_\mu(\nabla_\alpha\phi\nabla^\alpha\phi)\nabla_\nu\delta g_{\rho\sigma}\Big)\,,$$
$$= \int \mathrm{d}^4x\sqrt{-g}\frac{\kappa}{8}g^{\mu\nu}g^{\rho\sigma}\Big(\nabla_\mu\nabla_\rho(\nabla_\alpha\phi\nabla^\alpha\phi)\delta g_{\nu\sigma}+\nabla_\nu\nabla_\rho(\nabla_\alpha\phi\nabla^\alpha\phi)\delta g_{\mu\sigma}$$
$$-\nabla_\sigma\nabla_\rho(\nabla_\alpha\phi\nabla^\alpha\phi)\delta g_{\mu\nu}-\nabla_\nu\nabla_\mu(\nabla_\alpha\phi\nabla^\alpha\phi)\delta g_{\rho\sigma}\Big)\,,$$
$$= \int \mathrm{d}^4x\sqrt{-g}\frac{\kappa}{4}\Big(-\frac{1}{2}\nabla_\mu\nabla_\nu(\nabla_\sigma\phi\nabla^\sigma\phi)-\frac{1}{2}\nabla_\nu\nabla_\mu(\nabla_\sigma\phi\nabla^\sigma\phi)$$
$$+g_{\mu\nu}\nabla_\rho\nabla^\rho(\nabla_\sigma\phi\nabla^\sigma\phi)\Big)\delta g^{\mu\nu}\,. \tag{A.15}$$

Combining with the last second term of the equation (A.14), the term 3.2 of the equation (A.6) can be expressed as

$$\begin{aligned}
&\int d^4x\sqrt{-g}\frac{\kappa}{2}\left[\frac{1}{2}\delta\left(g_{\mu\nu}R\nabla^\mu\phi\nabla^\nu\phi\right)\right] \\
&= \int \mathrm{d}^4x\sqrt{-g}\frac{\kappa}{4}\Big(-\frac{1}{2}\nabla_\mu\nabla_\nu(\nabla_\sigma\phi\nabla^\sigma\phi)-\frac{1}{2}\nabla_\nu\nabla_\mu(\nabla_\sigma\phi\nabla^\sigma\phi) \\
&\quad +g_{\mu\nu}\nabla_\rho\nabla^\rho(\nabla_\sigma\phi\nabla^\sigma\phi)+\nabla_\alpha\phi\nabla^\alpha\phi R_{\mu\nu}+\nabla_\mu\phi\nabla_\nu\phi R\Big)\delta g^{\mu\nu}\,. \qquad \text{(A.16)}
\end{aligned}$$

Hence, combining equation (A.13) and equation (A.16), the variation of the NMDC coupling term, i.e., term 3, of the action equation (A.2) can be expressed as

$$\begin{aligned}
&\int \mathrm{d}^4x\sqrt{-g}\frac{1}{2}\delta[-\kappa G_{\mu\nu}\nabla^\mu\phi\nabla^\nu\phi] \\
&= \int \mathrm{d}^4x\sqrt{-g}\frac{\kappa}{4}\Big[\nabla_\sigma\nabla_\nu(\nabla^\sigma\phi\nabla_\mu\phi)+\nabla_\sigma\nabla_\mu(\nabla^\sigma\phi\nabla_\nu\phi)-\nabla_\sigma\nabla^\sigma(\nabla_\mu\phi\nabla_\nu\phi) \\
&\quad -4\nabla_\sigma\phi\nabla_{(\nu}\phi R^\sigma_{\mu)}-\nabla_\sigma\nabla_\rho(\nabla^\rho\phi\nabla^\sigma\phi)g_{\mu\nu}-\frac{1}{2}\nabla_\mu\nabla_\nu(\nabla_\sigma\phi\nabla^\sigma\phi) \\
&\quad -\frac{1}{2}\nabla_\nu\nabla_\mu(\nabla_\sigma\phi\nabla^\sigma\phi)+g_{\mu\nu}\nabla_\rho\nabla^\rho(\nabla_\sigma\phi\nabla^\sigma\phi)+\nabla_\alpha\phi\nabla^\alpha\phi R_{\mu\nu}+\nabla_\mu\phi\nabla_\nu\phi R\Big]\delta g^{\mu\nu}\,. \qquad \text{(A.17)}
\end{aligned}$$

For simplicity, we use the notation $\phi_\rho \equiv \nabla_\rho\phi$, $\phi_{\rho\sigma} \equiv \nabla_\rho\nabla_\sigma\phi$, $\Box\phi \equiv \nabla_\rho\nabla^\rho\phi$, where $\phi_{\rho\sigma}$ is symmetric with respect to the indices ρ and σ as shown in the following proof

$$\begin{aligned}
\nabla_\rho\nabla_\sigma\phi &= \nabla_\rho(\partial_\sigma\phi)\,, \\
&= \partial_\rho\partial_\sigma\phi+\Gamma^\lambda_{\rho\sigma}\partial_\lambda\phi\,, \\
&= \partial_\sigma\partial_\rho\phi+\Gamma^\lambda_{\sigma\rho}\partial_\lambda\phi\,, \\
&= \nabla_\sigma(\partial_\rho\phi)\,, \\
&= \nabla_\sigma\nabla_\rho\phi\,, \\
&= \phi_{\sigma\rho}\,, \qquad \text{(A.18)}
\end{aligned}$$

where $\partial_\sigma\partial_\rho\phi = \partial_\rho\partial_\sigma\phi$ and $\Gamma^\lambda_{\rho\sigma} = \Gamma^\lambda_{\sigma\rho}$. The variation of the NMDC coupling term then gives

$$
\begin{aligned}
&\int \mathrm{d}^4x\sqrt{-g}\frac{1}{2}\delta[-\kappa G_{\mu\nu}\nabla^\mu\phi\nabla^\nu\phi] \\
&= \int \mathrm{d}^4x\sqrt{-g}\frac{\kappa}{4}\Big[\nabla_\sigma\nabla_\nu(\phi^\sigma\phi_\mu)+\nabla_\sigma\nabla_\mu(\phi^\sigma\phi_\nu)-\nabla_\sigma\nabla^\sigma(\phi_\mu\phi_\nu) \\
&\quad -4\phi_\sigma\phi_{(\nu}R^\sigma_{\mu)}-\nabla_\sigma\nabla_\rho(\phi^\rho\phi^\sigma)g_{\mu\nu}-\frac{1}{2}\nabla_\mu\nabla_\nu(\phi_\sigma\phi^\sigma) \\
&\quad -\frac{1}{2}\nabla_\nu\nabla_\mu(\phi_\sigma\phi^\sigma)+g_{\mu\nu}\nabla_\rho\nabla^\rho(\phi_\sigma\phi^\sigma)+\phi_\alpha\phi^\alpha R_{\mu\nu}+\phi_\mu\phi_\nu R\Big]\delta g^{\mu\nu}, \\
&= \int \mathrm{d}^4x\sqrt{-g}\frac{\kappa}{4}\Big[\nabla_\sigma(\phi_\mu\nabla_\nu\phi^\sigma+\phi^\sigma\nabla_\nu\phi_\mu)+\nabla_\sigma(\phi_\nu\nabla_\mu\phi^\sigma+\phi^\sigma\nabla_\mu\phi_\nu) \\
&\quad -\nabla_\sigma(\phi_\nu\nabla^\sigma\phi_\mu+\phi_\mu\nabla^\sigma\phi_\nu)-4\phi_\sigma\phi_{(\nu}R^\sigma_{\mu)}-\nabla_\sigma(\phi^\sigma\nabla_\rho\phi^\rho+\phi^\rho\nabla_\rho\phi^\sigma)g_{\mu\nu} \\
&\quad -\frac{1}{2}\nabla_\mu(\phi^\sigma\nabla_\nu\phi_\sigma+\phi_\sigma\nabla_\nu\phi^\sigma)-\frac{1}{2}\nabla_\nu(\phi^\sigma\nabla_\mu\phi_\sigma+\phi_\sigma\nabla_\mu\phi^\sigma) \\
&\quad +g_{\mu\nu}\nabla_\rho(\phi^\sigma\nabla^\rho\phi_\sigma+\phi_\sigma\nabla^\rho\phi^\sigma)+\phi_\alpha\phi^\alpha R_{\mu\nu}+\phi_\mu\phi_\nu R\Big]\delta g^{\mu\nu}, \\
&= \int \mathrm{d}^4x\sqrt{-g}\frac{\kappa}{4}\Big[(\nabla_\sigma\phi_\mu\nabla_\nu\phi^\sigma+\phi_\mu\nabla_\sigma\nabla_\nu\phi^\sigma+\nabla_\sigma\phi^\sigma\nabla_\nu\phi_\mu+\phi^\sigma\nabla_\sigma\nabla_\nu\phi_\mu) \\
&\quad +(\nabla_\sigma\phi_\nu\nabla_\mu\phi^\sigma+\phi_\nu\nabla_\sigma\nabla_\mu\phi^\sigma+\nabla_\sigma\phi^\sigma\nabla_\mu\phi_\nu+\phi^\sigma\nabla_\sigma\nabla_\mu\phi_\nu) \\
&\quad -(\nabla_\sigma\phi_\nu\nabla^\sigma\phi_\mu+\phi_\nu\nabla_\sigma\nabla^\sigma\phi_\mu+\nabla_\sigma\phi_\mu\nabla^\sigma\phi_\nu+\phi_\mu\nabla_\sigma\nabla^\sigma\phi_\nu)-4\phi_\sigma\phi_{(\nu}R^\sigma_{\mu)} \\
&\quad -(\nabla_\sigma\phi^\sigma\nabla_\rho\phi^\rho+\phi^\sigma\nabla_\sigma\nabla_\rho\phi^\rho+\nabla_\sigma\phi^\rho\nabla_\rho\phi^\sigma+\phi^\rho\nabla_\sigma\nabla_\rho\phi^\sigma)g_{\mu\nu} \\
&\quad -\frac{1}{2}(\nabla_\mu\phi^\sigma\nabla_\nu\phi_\sigma+\phi^\sigma\nabla_\mu\nabla_\nu\phi_\sigma+\nabla_\mu\phi_\sigma\nabla_\nu\phi^\sigma+\phi_\sigma\nabla_\mu\nabla_\nu\phi^\sigma) \\
&\quad -\frac{1}{2}(\nabla_\nu\phi^\sigma\nabla_\mu\phi_\sigma+\phi^\sigma\nabla_\nu\nabla_\mu\phi_\sigma+\nabla_\nu\phi_\sigma\nabla_\mu\phi^\sigma+\phi_\sigma\nabla_\nu\nabla_\mu\phi^\sigma) \\
&\quad +(\nabla_\rho\phi^\sigma\nabla^\rho\phi_\sigma+\phi^\sigma\nabla_\rho\nabla^\rho\phi_\sigma+\nabla_\rho\phi_\sigma\nabla^\rho\phi^\sigma+\phi_\sigma\nabla_\rho\nabla^\rho\phi^\sigma)g_{\mu\nu} \\
&\quad +\phi_\alpha\phi^\alpha R_{\mu\nu}+\phi_\mu\phi_\nu R\Big]\delta g^{\mu\nu}, \\
&= \int \mathrm{d}^4x\sqrt{-g}\frac{\kappa}{4}\Big[\phi_{\sigma\mu}\phi^\sigma_\nu+\phi_\mu\nabla_\sigma\nabla_\nu\phi^\sigma+\Box\phi\phi_{\nu\mu}+\phi^\sigma\nabla_\sigma\nabla_\nu\phi_\mu+\phi_{\sigma\nu}\phi^\sigma_\mu \\
&\quad +\phi_\nu\nabla_\sigma\nabla_\mu\phi^\sigma+\Box\phi\phi_{\mu\nu}+\phi^\sigma\nabla_\sigma\nabla_\mu\phi_\nu-\phi_{\sigma\nu}\phi^\sigma_\mu-\phi_\nu\Box\phi_\mu-\phi_{\sigma\mu}\phi^\sigma_\nu \\
&\quad -\phi_\mu\Box\phi_\nu-4\phi_\sigma\phi_{(\nu}R^\sigma_{\mu)}-((\Box\phi)^2+\phi^\sigma\nabla_\sigma\nabla_\rho\phi^\rho+\phi_{\sigma\rho}\phi^{\sigma\rho}+\phi^\rho\nabla_\sigma\nabla_\rho\phi^\sigma)g_{\mu\nu} \\
&\quad -\frac{1}{2}\phi^\sigma_\mu\phi_{\nu\sigma}-\frac{1}{2}\phi^\sigma\nabla_\mu\nabla_\nu\phi_\sigma-\frac{1}{2}\phi_{\mu\sigma}\phi^\sigma_\nu-\frac{1}{2}\phi_\sigma\nabla_\mu\nabla_\nu\phi^\sigma-\frac{1}{2}\phi^\sigma_\nu\phi_{\mu\sigma}-\frac{1}{2}\phi^\sigma\nabla_\nu\nabla_\mu\phi_\sigma \\
&\quad -\frac{1}{2}\phi_{\nu\sigma}\phi^\sigma_\mu-\frac{1}{2}\phi_\sigma\nabla_\nu\nabla_\mu\phi^\sigma+(\phi^{\rho\sigma}\phi_{\rho\sigma}+\phi^\sigma\nabla_\rho\nabla^\rho\phi_\sigma+\phi_{\rho\sigma}\phi^{\rho\sigma}+\phi_\sigma\nabla_\rho\nabla^\rho\phi^\sigma)g_{\mu\nu} \\
&\quad +\phi_\alpha\phi^\alpha R_{\mu\nu}+\phi_\mu\phi_\nu R\Big]\delta g^{\mu\nu},
\end{aligned}
$$

$$
\begin{aligned}
&= \int \mathrm{d}^4x\sqrt{-g}\frac{\kappa}{4}\Big[\phi_\mu\nabla_\sigma\nabla_\nu\phi^\sigma + 2\Box\phi\phi_{\mu\nu} + \phi^\sigma\nabla_\sigma\nabla_\nu\phi_\mu + \phi_\nu\nabla_\sigma\nabla_\mu\phi^\sigma \\
&\quad +\phi^\sigma\nabla_\sigma\nabla_\mu\phi_\nu - \phi_\nu\Box\phi_\mu - \phi_\mu\Box\phi_\nu - 4\phi_\sigma\phi_{(\nu}R^\sigma_{\mu)} - (\Box\phi)^2 g_{\mu\nu} \\
&\quad -\phi^\sigma\nabla_\sigma\nabla_\rho\phi^\rho g_{\mu\nu} - \phi^\rho\nabla_\sigma\nabla_\rho\phi^\sigma g_{\mu\nu} - \phi_{\nu\sigma}\phi^\sigma_\mu - \phi^\sigma\nabla_\mu\nabla_\nu\phi_\sigma - \phi_{\mu\sigma}\phi^\sigma_\nu \\
&\quad -\phi^\sigma\nabla_\nu\nabla_\mu\phi_\sigma + 2\phi^\sigma\nabla_\rho\nabla^\rho\phi_\sigma g_{\mu\nu} + \phi_{\rho\sigma}\phi^{\rho\sigma}g_{\mu\nu} + \phi_\alpha\phi^\alpha R_{\mu\nu} + \phi_\mu\phi_\nu R\Big]\delta g^{\mu\nu}, \\
&= \int \mathrm{d}^4x\sqrt{-g}\frac{\kappa}{4}\Big[2\Box\phi\phi_{\mu\nu} + \phi^\sigma\nabla_\sigma\nabla_\nu\phi_\mu + \phi_\nu\nabla_\sigma\nabla_\mu\phi^\sigma + \phi_\mu\nabla_\sigma\nabla_\nu\phi^\sigma \\
&\quad +\phi^\sigma\nabla_\sigma\nabla_\mu\phi_\nu - \phi_\nu\Box\phi_\mu - \phi_\mu\Box\phi_\nu - 4\phi_\sigma\phi_{(\nu}R^\sigma_{\mu)} - (\Box\phi)^2 g_{\mu\nu} \\
&\quad -\phi^\rho(R^\sigma{}_{\lambda\rho\sigma}\phi^\lambda + \nabla_\sigma\nabla_\rho\phi^\sigma)g_{\mu\nu} - \phi^\rho\nabla_\sigma\nabla_\rho\phi^\sigma g_{\mu\nu} - \phi_{\nu\sigma}\phi^\sigma_\mu - \phi_{\mu\sigma}\phi^\sigma_\nu + 2\phi^\sigma\Box\phi_\sigma g_{\mu\nu} \\
&\quad -\phi_\sigma(R^\sigma{}_{\lambda\nu\mu}\phi^\lambda + \nabla_\mu\nabla_\nu\phi^\sigma) - \phi_\sigma\nabla_\mu\nabla_\nu\phi^\sigma + \phi_{\rho\sigma}\phi^{\rho\sigma}g_{\mu\nu} + \phi_\alpha\phi^\alpha R_{\mu\nu} + \phi_\mu\phi_\nu R\Big]\delta g^{\mu\nu}, \\
&= \int \mathrm{d}^4x\sqrt{-g}\frac{\kappa}{4}\Big[2\Box\phi\phi_{\mu\nu} + \phi^\sigma\nabla_\sigma\nabla_\nu\phi_\mu + \phi_\nu\nabla_\sigma\nabla_\mu\phi^\sigma + \phi_\mu\nabla_\sigma\nabla_\nu\phi^\sigma \\
&\quad +\phi^\sigma\nabla_\sigma\nabla_\mu\phi_\nu - \phi_\nu\Box\phi_\mu - \phi_\mu\Box\phi_\nu - 4\phi_\sigma\phi_{(\nu}R^\sigma_{\mu)} - (\Box\phi)^2 g_{\mu\nu} \\
&\quad -\phi^\rho\phi^\lambda R^\sigma{}_{\lambda\rho\sigma}g_{\mu\nu} - 2\phi^\rho\nabla_\sigma\nabla_\rho\phi^\sigma g_{\mu\nu} - \phi_{\nu\sigma}\phi^\sigma_\mu - \phi_{\mu\sigma}\phi^\sigma_\nu + 2\phi^\sigma\Box\phi_\sigma g_{\mu\nu} \\
&\quad -\phi^\sigma\phi^\lambda R_{\sigma\lambda\nu\mu} - 2\phi_\sigma\nabla_\mu\nabla_\nu\phi^\sigma + \phi_{\rho\sigma}\phi^{\rho\sigma}g_{\mu\nu} + \phi_\alpha\phi^\alpha R_{\mu\nu} + \phi_\mu\phi_\nu R\Big]\delta g^{\mu\nu}, \\
&= \int \mathrm{d}^4x\sqrt{-g}\frac{\kappa}{4}\Big[2\Box\phi\phi_{\mu\nu} + \phi^\sigma\nabla_\sigma\nabla_\nu\phi_\mu + \phi_\nu\nabla_\sigma\nabla_\mu\phi^\sigma + \phi_\mu\nabla_\sigma\nabla_\nu\phi^\sigma \\
&\quad +\phi^\sigma\nabla_\sigma\nabla_\mu\phi_\nu - \phi_\nu\Box\phi_\mu - \phi_\mu\Box\phi_\nu - 4\phi_\sigma\phi_{(\nu}R^\sigma_{\mu)} - (\Box\phi)^2 g_{\mu\nu} \\
&\quad -\phi^\rho\phi^\lambda R^\sigma{}_{\lambda\rho\sigma}g_{\mu\nu} - 2\phi^\rho\nabla_\sigma\nabla^\sigma\phi_\rho g_{\mu\nu} - \phi_{\nu\sigma}\phi^\sigma_\mu - \phi_{\mu\sigma}\phi^\sigma_\nu + 2\phi^\sigma\Box\phi_\sigma g_{\mu\nu} \\
&\quad -\phi^\sigma\phi^\lambda R_{\sigma\lambda\nu\mu} - 2\phi_\sigma\nabla_\mu\nabla_\nu\phi^\sigma + \phi_{\rho\sigma}\phi^{\rho\sigma}g_{\mu\nu} + \phi_\alpha\phi^\alpha R_{\mu\nu} + \phi_\mu\phi_\nu R\Big]\delta g^{\mu\nu}.
\end{aligned}
\tag{A.19}
$$

Using the fact that $\delta g^{\mu\nu}$ is a symmetric tensor under interchange of μ and ν, and that the Riemann tensor is antisymmetric under the interchange of its last two indices, i.e., $R^\rho_{\lambda\nu\mu} = -R^\rho_{\lambda\mu\nu}$, we have $R^\sigma_{\lambda\nu\mu}\delta g^{\mu\nu} = 0$. Moreover, since the covariant derivatives commute, we have $\nabla_\mu\nabla_\nu\phi = \nabla_\nu\nabla_\mu\phi$, which gives

$$
\begin{aligned}
&\int \mathrm{d}^4x\sqrt{-g}\frac{1}{2}\delta[-\kappa G_{\mu\nu}\nabla^\mu\phi\nabla^\nu\phi] \\
&\quad = \int \mathrm{d}^4x\sqrt{-g}\frac{\kappa}{4}\Big[2\Box\phi\phi_{\mu\nu} + \phi^\sigma\nabla_\sigma\nabla_\mu\phi_\nu + \phi_\nu\nabla^\sigma\nabla_\sigma\phi_\mu + \phi_\mu\nabla^\sigma\nabla_\sigma\phi_\nu \\
&\qquad +\phi^\sigma\nabla_\sigma\nabla_\mu\phi_\nu - \phi_\nu\Box\phi_\mu - \phi_\mu\Box\phi_\nu - 4\phi_\sigma\phi_{(\nu}R^\sigma_{\mu)} - (\Box\phi)^2 g_{\mu\nu}
\end{aligned}
$$

$$
\begin{aligned}
&-\phi^\rho\phi^\lambda R^\sigma{}_{\lambda\rho\sigma}g_{\mu\nu} - 2\phi^\rho\nabla_\sigma\nabla^\sigma\phi_\rho g_{\mu\nu} - \phi_{\nu\sigma}\phi^\sigma_\mu - \phi_{\mu\sigma}\phi^\sigma_\nu + 2\phi^\sigma\Box\phi_\sigma g_{\mu\nu} \\
&-2\phi^\sigma\nabla_\mu\nabla_\sigma\phi_\nu + \phi_{\rho\sigma}\phi^{\rho\sigma}g_{\mu\nu} + \phi_\alpha\phi^\alpha R_{\mu\nu} + \phi_\mu\phi_\nu R\Big]\delta g^{\mu\nu}\,, \\
= &\int \mathrm{d}^4x\sqrt{-g}\frac{\kappa}{4}\Big[2\Box\phi\phi_{\mu\nu} + 2\phi^\sigma\nabla_\sigma\nabla_\mu\phi_\nu + \phi_\nu\Box\phi_\mu + \phi_\mu\Box\phi_\nu - \phi_\nu\Box\phi_\mu - \phi_\mu\Box\phi_\nu \\
&-4\phi_\sigma\phi_{(\nu}R^\sigma_{\mu)} - (\Box\phi)^2 g_{\mu\nu} + \phi^\rho\phi^\lambda R_{\lambda\rho}g_{\mu\nu} - \phi_{\nu\sigma}\phi^\sigma_\mu - \phi_{\mu\sigma}\phi^\sigma_\nu \\
&-2\phi^\sigma\nabla_\mu\nabla_\sigma\phi_\nu + \phi_{\rho\sigma}\phi^{\rho\sigma}g_{\mu\nu} + \phi_\alpha\phi^\alpha R_{\mu\nu} + \phi_\mu\phi_\nu R\Big]\delta g^{\mu\nu}\,, \\
= &\int \mathrm{d}^4x\sqrt{-g}\frac{\kappa}{4}\Big[2\Box\phi\phi_{\mu\nu} + 2\phi^\sigma\nabla_\sigma\nabla_\mu\phi_\nu - 4\phi_\sigma\phi_{(\nu}R^\sigma_{\mu)} - (\Box\phi)^2 g_{\mu\nu} + \phi^\rho\phi^\lambda R_{\lambda\rho}g_{\mu\nu} \\
&-2\phi^\sigma(g_{\xi\nu}R^\xi{}_{\lambda\mu\sigma}\phi^\lambda + \nabla_\sigma\nabla_\mu\phi_\nu) - \phi_{\nu\sigma}\phi^\sigma_\mu - \phi_{\mu\sigma}\phi^\sigma_\nu + \phi_{\rho\sigma}\phi^{\rho\sigma}g_{\mu\nu} \\
&+\phi_\alpha\phi^\alpha R_{\mu\nu} + \phi_\mu\phi_\nu R\Big]\delta g^{\mu\nu}\,, \\
= &\int \mathrm{d}^4x\sqrt{-g}\frac{\kappa}{4}\Big[2\Box\phi\phi_{\mu\nu} - 4\phi_\sigma\phi_{(\nu}R^\sigma_{\mu)} - (\Box\phi)^2 g_{\mu\nu} + \phi^\rho\phi^\lambda R_{\lambda\rho}g_{\mu\nu} - 2\phi^\sigma\phi^\lambda R_{\nu\lambda\mu\sigma} \\
&-\phi_{\nu\sigma}\phi^\sigma_\mu - \phi_{\mu\sigma}\phi^\sigma_\nu + \phi_{\rho\sigma}\phi^{\rho\sigma}g_{\mu\nu} + \phi_\alpha\phi^\alpha R_{\mu\nu} + \phi_\mu\phi_\nu R\Big]\delta g^{\mu\nu}\,, \\
= &\int \mathrm{d}^4x\sqrt{-g}\frac{\kappa}{4}\Big[2(\nabla_\mu\nabla_\nu\phi)\Box\phi - 4(\nabla_\sigma\phi)\nabla_{(\nu}\phi R^\sigma_{\mu)} - (\Box\phi)^2 g_{\mu\nu} + (\nabla^\rho\phi)(\nabla^\lambda\phi)R_{\lambda\rho}g_{\mu\nu} \\
&-2(\nabla^\sigma\phi)(\nabla^\lambda\phi)R_{\nu\lambda\mu\sigma} - (\nabla_\nu\nabla_\sigma\phi)(\nabla_\mu\nabla^\sigma\phi) - (\nabla_\mu\nabla_\sigma\phi)(\nabla_\nu\nabla^\sigma\phi) \\
&+(\nabla_\rho\nabla_\sigma\phi)(\nabla^\rho\nabla^\sigma\phi)g_{\mu\nu} + (\nabla_\alpha\phi)(\nabla^\alpha\phi)R_{\mu\nu} + (\nabla_\mu\phi)(\nabla_\nu\phi)R\Big]\delta g^{\mu\nu}\,.
\end{aligned}
\tag{A.20}
$$

Combining the equations (A.3), (A.4), (A.5), and (A.20), the variation of the action with respect to the metric tensor can be obtained as

$$
\begin{aligned}
\delta_g S = &\int \mathrm{d}^4x\sqrt{-g}\frac{1}{2}\Big\{-\frac{Rg_{\mu\nu}}{16\pi G} + \frac{1}{2}g_{\mu\nu}(\varepsilon g_{\alpha\beta} + \kappa G_{\alpha\beta})\nabla^\alpha\phi\nabla^\beta\phi + V(\phi)g_{\mu\nu} - g_{\mu\nu}\mathcal{L}_\mathrm{m} \\
&+\frac{R_{\mu\nu}}{8\pi G} - \varepsilon\nabla_\mu\phi\nabla_\nu\phi + \frac{\kappa}{2}\Big[2(\nabla_\mu\nabla_\nu\phi)\Box\phi - 4(\nabla_\sigma\phi)\nabla_{(\nu}\phi R^\sigma_{\mu)} - (\Box\phi)^2 g_{\mu\nu} \\
&+(\nabla^\rho\phi)(\nabla^\lambda\phi)R_{\lambda\rho}g_{\mu\nu} - 2(\nabla^\sigma\phi)(\nabla^\lambda\phi)R_{\nu\lambda\mu\sigma} - (\nabla_\nu\nabla_\sigma\phi)(\nabla_\mu\nabla^\sigma\phi) \\
&-(\nabla_\mu\nabla_\sigma\phi)(\nabla_\nu\nabla^\sigma\phi) + (\nabla_\rho\nabla_\sigma\phi)(\nabla^\rho\nabla^\sigma\phi)g_{\mu\nu} + (\nabla_\alpha\phi)(\nabla^\alpha\phi)R_{\mu\nu} \\
&+(\nabla_\mu\phi)(\nabla_\nu\phi)R\Big] + \frac{\delta\mathcal{L}_\mathrm{m}}{\delta g^{\mu\nu}}\Big\}\delta g^{\mu\nu}\,.
\end{aligned}
\tag{A.21}
$$

According to the principle of least action, $\delta S = 0$, the equation (A.21) can be

expressed as

$$\frac{1}{8\pi G}\left(R_{\mu\nu}-\frac{1}{2}g_{\mu\nu}R\right)-\varepsilon\nabla_\mu\phi\nabla_\nu\phi+\frac{1}{2}\varepsilon g_{\mu\nu}\nabla_\beta\phi\nabla^\beta\phi+V(\phi)g_{\mu\nu}-g_{\mu\nu}\mathcal{L}_{\rm m}+\frac{\delta\mathcal{L}_{\rm m}}{\delta g^{\mu\nu}}$$
$$+\frac{\kappa}{2}\Big[g_{\mu\nu}G_{\alpha\beta}\nabla^\alpha\phi\nabla^\beta\phi+2(\nabla_\mu\nabla_\nu\phi)\Box\phi-4(\nabla_\sigma\phi)\nabla_{(\nu}\phi R^\sigma_{\mu)}-(\Box\phi)^2g_{\mu\nu}$$
$$+(\nabla^\rho\phi)(\nabla^\lambda\phi)R_{\lambda\rho}g_{\mu\nu}-2(\nabla^\sigma\phi)(\nabla^\lambda\phi)R_{\nu\lambda\mu\sigma}-(\nabla_\nu\nabla_\sigma\phi)(\nabla_\mu\nabla^\sigma\phi)$$
$$-(\nabla_\mu\nabla_\sigma\phi)(\nabla_\nu\nabla^\sigma\phi)+(\nabla_\rho\nabla_\sigma\phi)(\nabla^\rho\nabla^\sigma\phi)g_{\mu\nu}+(\nabla_\alpha\phi)(\nabla^\alpha\phi)R_{\mu\nu}$$
$$+(\nabla_\mu\phi)(\nabla_\nu\phi)R\Big]=0\,. \tag{A.22}$$

This gives

$$\begin{aligned}G_{\mu\nu} &= 8\pi G\Big\{\varepsilon\nabla_\mu\phi\nabla_\nu\phi-\frac{1}{2}\varepsilon g_{\mu\nu}\nabla_\beta\phi\nabla^\beta\phi-V(\phi)g_{\mu\nu}+g_{\mu\nu}\mathcal{L}_{\rm m}-\frac{\delta\mathcal{L}_{\rm m}}{\delta g^{\mu\nu}}\\ &\quad+\kappa\Big[-\frac{1}{2}(\nabla_\mu\phi)(\nabla_\nu\phi)R+2(\nabla_\sigma\phi)\nabla_{(\nu}\phi R^\sigma_{\mu)}+(\nabla^\sigma\phi)(\nabla^\lambda\phi)R_{\nu\lambda\mu\sigma}\\ &\quad+\frac{1}{2}(\nabla_\nu\nabla_\sigma\phi)(\nabla_\mu\nabla^\sigma\phi)+\frac{1}{2}(\nabla_\mu\nabla_\sigma\phi)(\nabla_\nu\nabla^\sigma\phi)-(\nabla_\mu\nabla_\nu\phi)\Box\phi\\ &\quad-\frac{1}{2}(\nabla_\alpha\phi)(\nabla^\alpha\phi)R_{\mu\nu}-\frac{1}{2}g_{\mu\nu}R_{\alpha\beta}\nabla^\alpha\phi\nabla^\beta\phi+\frac{1}{2}(\nabla_\alpha)(\phi\nabla^\alpha\phi)(\frac{1}{2}g_{\mu\nu}R)\\ &\quad+g_{\mu\nu}\left(+\frac{1}{2}(\Box\phi)^2-\frac{1}{2}(\nabla^\rho\phi)(\nabla^\lambda\phi)R_{\lambda\rho}-\frac{1}{2}(\nabla_\rho\nabla_\sigma\phi)(\nabla^\rho\nabla^\sigma\phi)\right)\Big]\Big\}\,,\end{aligned} \tag{A.23}$$

$$\begin{aligned}G_{\mu\nu} &= 8\pi G\Big\{\varepsilon\nabla_\mu\phi\nabla_\nu\phi-\frac{1}{2}\varepsilon g_{\mu\nu}\nabla_\beta\phi\nabla^\beta\phi-V(\phi)g_{\mu\nu}+g_{\mu\nu}\mathcal{L}_{\rm m}-\frac{\delta\mathcal{L}_{\rm m}}{\delta g^{\mu\nu}}\\ &\quad+\kappa\Big[-\frac{1}{2}(\nabla_\mu\phi)(\nabla_\nu\phi)R+2(\nabla_\sigma\phi)\nabla_{(\nu}\phi R^\sigma_{\mu)}+(\nabla^\sigma\phi)(\nabla^\lambda\phi)R_{\nu\lambda\mu\sigma}\\ &\quad+(\nabla_\mu\nabla_\sigma\phi)(\nabla_\nu\nabla^\sigma\phi)-(\nabla_\mu\nabla_\nu\phi)\Box\phi-\frac{1}{2}(\nabla_\alpha\phi)(\nabla^\alpha\phi)G_{\mu\nu}\\ &\quad+g_{\mu\nu}\left(\frac{1}{2}(\Box\phi)^2-(\nabla^\alpha\phi)(\nabla^\beta\phi)R_{\alpha\beta}-\frac{1}{2}(\nabla_\rho\nabla_\sigma\phi)(\nabla^\rho\nabla^\sigma\phi)\right)\Big]\Big\}\,.\end{aligned} \tag{A.24}$$

According to the Einstein field equations (A.24), the stress-energy tensors of dust matter, the scalar field, and the NMDC coupling term can be expressed as

$$G_{\mu\nu} = 8\pi G\left(T^{(\rm m)}_{\mu\nu}+T^{(\phi)}_{\mu\nu}+\kappa\Theta_{\mu\nu}\right)\,, \tag{A.25}$$

where

$$
\begin{aligned}
T^{(\mathrm{m})}_{\mu\nu} &= g_{\mu\nu}\mathcal{L}_{\mathrm{m}} - \frac{\delta\mathcal{L}_{\mathrm{m}}}{\delta g^{\mu\nu}}\,, \\
T^{(\phi)}_{\mu\nu} &= \varepsilon\nabla_\mu\phi\nabla_\nu\phi - \frac{1}{2}\varepsilon g_{\mu\nu}\nabla_\beta\phi\nabla^\beta\phi - V(\phi)g_{\mu\nu}\,, \\
\Theta_{\mu\nu} &= -\frac{1}{2}(\nabla_\mu\phi)(\nabla_\nu\phi)R + 2(\nabla_\sigma\phi)\nabla_{(\nu}\phi R^\sigma_{\mu)} + (\nabla^\sigma\phi)(\nabla^\lambda\phi)R_{\nu\lambda\mu\sigma} \\
&\quad +(\nabla_\mu\nabla_\sigma\phi)(\nabla_\nu\nabla^\sigma\phi) - (\nabla_\mu\nabla_\nu\phi)\Box\phi - \frac{1}{2}(\nabla_\alpha\phi)(\nabla^\alpha\phi)G_{\mu\nu} \\
&\quad +g_{\mu\nu}\left(\frac{1}{2}(\Box\phi)^2 - (\nabla^\alpha\phi)(\nabla^\beta\phi)R_{\alpha\beta} - \frac{1}{2}(\nabla_\rho\nabla_\sigma\phi)(\nabla^\rho\nabla^\sigma\phi)\right)\,.
\end{aligned}
\tag{A.26}
$$

According to the action (A.1), the variation of the action with respect to the scalar field, ϕ, yields the Klein-Gordon equation for NMDC interaction

$$
\delta_\phi S = \mathrm{d}^4x\int\sqrt{-g}\left(\frac{\delta R}{16\pi G} - \frac{1}{2}(\varepsilon g_{\mu\nu} + \kappa G_{\mu\nu})\delta(\nabla^\mu\phi\nabla^\nu\phi) - \delta V_\phi\right)\,. \tag{A.27}
$$

There is no scalar field present inside the Ricci scalar, R. Therefore, the variation of the Ricci scalar with respect to the scalar field is zero. We have

$$
\begin{aligned}
\delta_\phi S &= \mathrm{d}^4x\int\sqrt{-g}\left(-\frac{1}{2}(\varepsilon g_{\mu\nu} + \kappa G_{\mu\nu})(\nabla^\mu\phi\delta\nabla^\nu\phi + \nabla^\nu\phi\delta\nabla^\mu\phi) - V_{,\phi}\delta\phi\right)\,, \\
&= \mathrm{d}^4x\int\sqrt{-g}\Big[-\frac{1}{2}\varepsilon g_{\mu\nu}(\nabla^\mu\phi\delta\nabla^\nu\phi + \nabla^\nu\phi\delta\nabla^\mu\phi) \\
&\quad -\frac{1}{2}\kappa G_{\mu\nu}(\nabla^\mu\phi\delta\nabla^\nu\phi + \nabla^\nu\phi\delta\nabla^\mu\phi) - V_{,\phi}\delta\phi\Big]\,, \\
&= \mathrm{d}^4x\int\sqrt{-g}\,(-\varepsilon g_{\mu\nu}\nabla^\mu\phi\delta\nabla^\nu\phi - \kappa G_{\mu\nu}\nabla^\mu\phi\delta\nabla^\nu\phi - V_{,\phi}\delta\phi)\,.
\end{aligned}
\tag{A.28}
$$

where $V_{,\phi} = \partial V/\partial\phi$ is the derivative of the potential with respect to the scalar field. Using integration by parts, boundary conditions, and the zero divergence of the Einstein tensor, i.e., $\nabla^\mu G_{\mu\nu} = 0$, we obtain

$$
\delta_\phi S = \int\mathrm{d}^4x\sqrt{-g}\,(\varepsilon\nabla_\mu\nabla^\mu\phi + \kappa G_{\mu\nu}\nabla^\mu\nabla^\nu\phi - V_{,\phi})\,\delta\phi\,. \tag{A.29}
$$

The principle of least action, $\delta_\phi S = 0$ gives modified Klein-Gordon equation

$$
\varepsilon\nabla_\mu\nabla^\mu\phi + \kappa G_{\mu\nu}\nabla^\mu\nabla^\nu\phi - V_{,\phi} = 0\,. \tag{A.30}
$$

APPENDIX B NMDC COSMOLOGICAL EQUATIONS

Now, let us consider the FLRW background. The line element corresponding to the FLRW universe is given by

$$\mathrm{d}s^2 = -\mathrm{d}t^2 + a^2(t)\left(\frac{\mathrm{d}r^2}{1-kr^2} + r^2\mathrm{d}\theta^2 + r^2\sin^2\theta\mathrm{d}\phi^2\right). \tag{B.1}$$

The scalar field that satisfies the FLRW universe depends only on time, i.e., $\phi = \phi(t)$. According to the line element, the metric tensor can be expressed as

$$g_{\mu\nu} = \begin{pmatrix} -1 & 0 & 0 & 0 \\ 0 & \dfrac{a^2(t)}{1-kr^2} & 0 & 0 \\ 0 & 0 & a^2(t)r^2 & 0 \\ 0 & 0 & 0 & a^2(t)r^2\sin^2\theta \end{pmatrix}. \tag{B.2}$$

By following the procedures of General Relativity, the Christoffel symbols, Ricci tensor, Ricci scalar, and Einstein tensor can be derived from the metric tensor. The non-zero components are

$$\begin{aligned} &R_{00} = -3(\dot{H}+H^2),\ \ R_{ij} = g_{ij}\left(\dot{H}+3H^2+\frac{2k}{a^2}\right),\ \ R = 6\left(\dot{H}+2H^2+\frac{k}{a^2}\right), \\ &\Gamma^i_{0j} = \delta^i_j H,\ \ \Gamma^0_{ij} = g_{ij}H,\ \ G_{00} = 3\left(H^2+\frac{k}{a^2}\right),\ \ G_{ij} = -g_{ij}\left(2\dot{H}+3H^2+\frac{k}{a^2}\right), \end{aligned} \tag{B.3}$$

where $H = \dot{a}/a$ is the Hubble parameter and $\dot{H}$ is the derivative with respect to time.

Notice that the equation (B.3) separates the components into $(0,0)$ and (i,j) components. The $(0,0)$ component of the energy-momentum tensor equation (A.26) is given by

$$\begin{aligned} T^{(\phi)}_{\mu\nu} &= \varepsilon\nabla_\mu\phi\nabla_\nu\phi - \frac{\varepsilon}{2}g_{\mu\nu}\nabla_\beta\phi\nabla^\beta\phi - V(\phi)g_{\mu\nu}, \\ T^{(\phi)}_{00} &= \varepsilon\dot{\phi}^2 - \frac{\varepsilon}{2}\dot{\phi}^2 + V(\phi) = \frac{\varepsilon}{2}\dot{\phi}^2 + V(\phi). \end{aligned} \tag{B.4}$$

And the $(0,0)$ component of $\Theta_{\mu\nu}$ is given by

$$
\begin{aligned}
\Theta_{00} &= -\frac{1}{2}(\nabla_0\phi)(\nabla_0\phi)R + 2(\nabla_\sigma\phi)\nabla_{(0}\phi R^{\sigma}_{0)} + (\nabla^\sigma\phi)(\nabla^\lambda\phi)R_{0\lambda0\sigma} \\
&\quad +(\nabla_0\nabla_\sigma\phi)(\nabla_0\nabla^\sigma\phi) - (\nabla_0\nabla_0\phi)\Box\phi - \frac{1}{2}(\nabla_\alpha\phi)(\nabla^\alpha\phi)G_{00} \\
&\quad +g_{00}\left(\frac{1}{2}(\Box\phi)^2 - (\nabla^\alpha\phi)(\nabla^\beta\phi)R_{\alpha\beta} - \frac{1}{2}(\nabla_\rho\nabla_\sigma\phi)(\nabla^\rho\nabla^\sigma\phi)\right), \\
&= -\frac{1}{2}\dot\phi^2 R + 2g^{\sigma\lambda}(\nabla_\sigma\phi)(\nabla_0\phi)R_{0\lambda} + g^{\sigma\alpha}g^{\lambda\beta}(\nabla_\alpha\phi)(\nabla_\beta\phi)R_{0\lambda0\sigma} \\
&\quad +(\nabla_0\nabla_\sigma\phi)(\nabla_0\nabla^\sigma\phi) - (\nabla_0\nabla_0\phi)\Box\phi - g^{\alpha\lambda}\frac{1}{2}(\nabla_\alpha\phi)(\nabla_\lambda\phi)G_{00} \\
&\quad +g_{00}\left(\frac{1}{2}(\Box\phi)^2 - g^{\alpha\sigma}g^{\beta\rho}(\nabla_\sigma\phi)(\nabla_\rho\phi)R_{\alpha\beta} - \frac{1}{2}g^{\rho\gamma}g^{\sigma\lambda}(\nabla_\rho\nabla_\sigma\phi)(\nabla_\gamma\nabla_\lambda\phi)\right), \\
&= -\frac{1}{2}\dot\phi^2 R + 2g^{00}(\nabla_0\phi)(\nabla_0\phi)R_{00} + g^{00}g^{00}(\nabla_0\phi)(\nabla_0\phi)R_{0000} \\
&\quad +(\nabla_0\nabla_\sigma\phi)(\nabla_0\nabla^\sigma\phi) - (\nabla_0\nabla_0\phi)g^{\sigma\rho}\nabla_\sigma\nabla_\rho\phi - g^{00}\frac{1}{2}(\nabla_0\phi)(\nabla_0\phi)G_{00} \\
&\quad +g_{00}\left(\frac{1}{2}(g^{\sigma\rho}\nabla_\sigma\nabla_\rho\phi)^2 - g^{00}g^{00}(\nabla_0\phi)(\nabla_0\phi)R_{00} - \frac{1}{2}g^{\rho\gamma}g^{\sigma\lambda}(\nabla_\rho\nabla_\sigma\phi)(\nabla_\gamma\nabla_\lambda\phi)\right), \\
&= -\frac{1}{2}\dot\phi^2 R - 2\dot\phi^2 R_{00} + \dot\phi^2 R_{0000} + (\partial_0\partial_\sigma\phi - \Gamma^\lambda_{0\sigma}\partial_\lambda\phi)(\partial_0\phi\partial^\sigma\phi + \Gamma^\sigma_{0\lambda}\partial^\lambda\phi) \\
&\quad -(\partial_0\partial_0\phi - \Gamma^\lambda_{00}\partial_\lambda\phi)g^{\sigma\rho}(\partial_\sigma\partial_\rho\phi - \Gamma^\lambda_{\sigma\rho}\partial_\lambda\phi) + \frac{1}{2}\dot\phi^2 G_{00} \\
&\quad -\left(\frac{1}{2}(g^{\sigma\rho}\partial_\sigma\partial_\rho\phi - g^{\sigma\rho}\Gamma^\lambda_{\sigma\rho}\partial_\lambda\phi)^2 - \dot\phi^2 R_{00}\right. \\
&\quad \left.-\frac{1}{2}(\partial_\rho\partial_\sigma\phi - \Gamma^\xi_{\rho\sigma}\partial_\xi\phi)g^{\rho\gamma}g^{\sigma\lambda}(\partial_\gamma\partial_\lambda\phi - \Gamma^\xi_{\gamma\lambda}\partial_\xi\phi)\right), \\
&= -\frac{1}{2}\dot\phi^2 R - 2\dot\phi^2 R_{00} + \dot\phi^2 R_{0000} + (\partial_0\partial_0\phi - \Gamma^0_{00}\partial_0\phi)(\partial_0\phi\partial^0\phi + \Gamma^0_{00}\partial^0\phi) \\
&\quad -(\partial_0\partial_0\phi - \Gamma^0_{00}\partial_0\phi)\left[g^{00}(\partial_0\partial_0\phi - \Gamma^0_{00}\partial_0\phi) + g^{ij}(\partial_i\partial_j\phi - \Gamma^0_{ij}\partial_0\phi)\right] + \frac{1}{2}\dot\phi^2 G_{00} \\
&\quad -\left(\frac{1}{2}(g^{00}\partial_0\partial_0\phi - g^{00}\Gamma^0_{00}\partial_0\phi + g^{ij}\partial_i\partial_j\phi - g^{ij}\Gamma^0_{ij}\partial_0\phi)^2 - \dot\phi^2 R_{00}\right. \\
&\quad -\frac{1}{2}g^{00}g^{00}(\partial_0\partial_0\phi - \Gamma^0_{00}\partial_0\phi)(\partial_0\partial_0\phi - \Gamma^0_{00}\partial_0\phi) \\
&\quad \left.-\frac{1}{2}g^{ij}g^{kl}(\partial_i\partial_k\phi - \Gamma^0_{ik}\partial_0\phi)(\partial_j\partial_l\phi - \Gamma^0_{jl}\partial_0\phi)\right), \\
&= -\frac{1}{2}\dot\phi^2 R - 2\dot\phi^2 R_{00} - \ddot\phi^2 + \ddot\phi^2 + \ddot\phi g^{ij}\Gamma^0_{ij}\dot\phi + \frac{1}{2}\dot\phi^2 G_{00} \\
&\quad -\left(\frac{1}{2}(-\ddot\phi - g^{ij}\Gamma^0_{ij}\dot\phi)^2 - \dot\phi^2 R_{00} - \frac{1}{2}\ddot\phi^2 - \frac{1}{2}g^{ij}g^{kl}(\Gamma^0_{ik}\dot\phi)(\Gamma^0_{jl}\dot\phi)\right), \\
&= -\frac{1}{2}\dot\phi^2 R - 2\dot\phi^2 R_{00} + \ddot\phi g^{ij}\Gamma^0_{ij}\dot\phi + \frac{1}{2}\dot\phi^2 G_{00} - \frac{1}{2}(-\ddot\phi - g^{ij}\Gamma^0_{ij}\dot\phi)^2 + \dot\phi^2 R_{00}
\end{aligned}
$$

$$+\frac{1}{2}\ddot{\phi}^2+\frac{1}{2}g^{ij}g^{kl}\Gamma^0_{ik}\Gamma^0_{jl}\dot{\phi}^2\,. \tag{B.5}$$

Using the set of equations (B.3), Θ_{00} can be expressed as

$$\begin{aligned}
\Theta_{00} &= -3\dot{\phi}^2\left(\dot{H}+2H^2+\frac{k}{a^2}\right)+6\dot{\phi}^2\left(\dot{H}+H^2\right)+\ddot{\phi}\delta^i_i H\dot{\phi}+\frac{3}{2}\dot{\phi}^2\left(H^2+\frac{k}{a^2}\right)\\
&\quad -\frac{1}{2}(-\ddot{\phi}-\delta^i_i H\dot{\phi})^2-3\dot{\phi}^2\left(\dot{H}+H^2\right)+\frac{1}{2}\ddot{\phi}^2+\frac{1}{2}\delta^j_k\delta^k_j H^2\dot{\phi}^2\,,\\
&= -3\dot{\phi}^2\dot{H}-6\dot{\phi}^2H^2-3\dot{\phi}^2\frac{k}{a^2}+6\dot{\phi}^2\dot{H}+6\dot{\phi}^2H^2+3H\ddot{\phi}\dot{\phi}+\frac{3}{2}\dot{\phi}^2H^2+\frac{3}{2}\dot{\phi}^2\frac{k}{a^2}\\
&\quad -\frac{1}{2}\ddot{\phi}^2-3H\dot{\phi}\ddot{\phi}-\frac{9}{2}H^2\dot{\phi}^2-3\dot{\phi}^2\dot{H}-3\dot{\phi}^2H^2+\frac{1}{2}\ddot{\phi}^2+\frac{3}{2}H^2\dot{\phi}^2\,,\\
&= -\frac{9}{2}\dot{\phi}^2H^2-\frac{3}{2}\dot{\phi}^2\frac{k}{a^2}\,.
\end{aligned} \tag{B.6}$$

The $(0,0)$-component of the dust matter, which we define as a perfect fluid, $T^{(\mathrm{m})}_{00}$, represents the energy density of baryons and radiation,

$$T^{(\mathrm{m})}_{00} = \rho_{\mathrm{m}}+\rho_{\mathrm{r}}\,. \tag{B.7}$$

Therefore, the $(0,0)$-component of the Einstein field equation (A.25) is given by

$$\begin{aligned}
G_{00} &= 8\pi G\left(T^{(\phi)}_{00}+\kappa\Theta_{00}+T^{(\mathrm{m})}_{00}\right),\\
3(H^2+\frac{k}{a^2}) &= 8\pi G\left[\frac{\varepsilon}{2}\dot{\phi}^2+V(\phi)-\frac{9}{2}\kappa\dot{\phi}^2H^2-\frac{3}{2}\kappa\dot{\phi}^2\frac{k}{a^2}+\rho_{\mathrm{m}}+\rho_{\mathrm{r}}\right],\\
H^2+\frac{k}{a^2} &= \frac{8\pi G}{3}\left\{\frac{\dot{\phi}^2}{2}\left[\varepsilon-9\kappa H^2-\frac{3\kappa k}{a^2}\right]+V(\phi)+\rho_{\mathrm{m}}++\rho_{\mathrm{r}}\right\}.
\end{aligned} \tag{B.8}$$

The equation (B.8) is referred to as the Friedmann equation. Furthermore, equation (B.8) can be rewritten to incorporate a modification of the gravitational constant, G_{eff}, as follows

$$H^2 = \frac{8\pi G_{\mathrm{eff}}}{3}\left[\frac{1}{2}\dot{\phi}^2\left(\varepsilon-\frac{3\kappa k}{a^2}\right)+V(\phi)+\rho_{\mathrm{m}}+\rho_{\mathrm{r}}\right]-\frac{3k}{(1+12\pi G\kappa\dot{\phi}^2)a^2}\,, \tag{B.9}$$

where the effective gravitational constant, G_{eff}, can be identified as

$$G_{\mathrm{eff}}(\dot{\phi}) = \frac{G}{1+12\pi G\kappa\dot{\phi}^2}\,. \tag{B.10}$$

Next, we will consider the (i,j)-component of the energy-momentum tensor for the scalar field, given by equation (A.26)

$$\begin{aligned} T_{ij}^{(\phi)} &= \varepsilon\nabla_i\phi\nabla_j\phi - \frac{1}{2}\varepsilon g_{ij}\nabla^\rho\phi\nabla_\rho\phi - g_{ij}V(\phi)\,, \\ &= \left(\frac{\varepsilon}{2}\dot{\phi}^2 - V(\phi)\right)g_{ij}\,. \end{aligned} \tag{B.11}$$

The (i,j)-component of Θ_{ij}, as given by equation (A.26), can be expressed by

$$\begin{aligned} \Theta_{ij} &= -\frac{1}{2}(\nabla_i\phi)(\nabla_j\phi)R + 2(\nabla_\sigma\phi)\nabla_{(j}\phi R^\sigma_{i)} + (\nabla^\sigma\phi)(\nabla^\lambda\phi)R_{j\lambda i\sigma} \\ &\quad +(\nabla_i\nabla_\sigma\phi)(\nabla_j\nabla^\sigma\phi) - (\nabla_i\nabla_j\phi)\Box\phi - \frac{1}{2}(\nabla_\alpha\phi)(\nabla^\alpha\phi)G_{ij} \\ &\quad +g_{ij}\left(\frac{1}{2}(\Box\phi)^2 - (\nabla^\alpha\phi)(\nabla^\beta\phi)R_{\alpha\beta} - \frac{1}{2}(\nabla_\rho\nabla_\sigma\phi)(\nabla^\rho\nabla^\sigma\phi)\right), \\ &= (\nabla^0\phi)(\nabla^0\phi)R_{j0i0} + (\nabla_i\nabla_\sigma\phi)(\nabla_j\nabla^\sigma\phi) - (\nabla_i\nabla_j\phi)\Box\phi - \frac{1}{2}(\nabla_0\phi)(\nabla^0\phi)G_{ij} \\ &\quad +g_{ij}\left(\frac{1}{2}(\Box\phi)^2 - (\nabla^0\phi)(\nabla^0\phi)R_{00} - \frac{1}{2}(\nabla_\rho\nabla_\sigma\phi)(\nabla^\rho\nabla^\sigma\phi)\right), \\ &= \dot{\phi}^2R_{j0i0} + (\partial_i\partial_\sigma\phi - \Gamma^\lambda_{i\sigma}\partial_\lambda\phi)(\partial_j\partial^\sigma\phi + \Gamma^\sigma_{j\lambda}\partial^\lambda\phi) \\ &\quad -(\partial_i\partial_j\phi - \Gamma^\lambda_{ij}\partial_\lambda\phi)(\partial_\sigma\partial^\sigma\phi + \Gamma^\sigma_{\sigma\lambda}\partial^\lambda\phi) \\ &\quad +\frac{1}{2}\dot{\phi}^2G_{ij} + g_{ij}\left(\frac{1}{2}(\partial_\sigma\partial^\sigma\phi + \Gamma^\sigma_{\sigma\lambda}\partial^\lambda\phi)^2 - \dot{\phi}^2R_{00}\right. \\ &\quad \left.-\frac{1}{2}(\partial_\rho\partial_\sigma\phi - \Gamma^\lambda_{\rho\sigma}\partial_\lambda\phi)g^{\rho\alpha}(\partial_\alpha\partial^\sigma\phi + \Gamma^\sigma_{\alpha\beta}\partial^\beta\phi)\right), \\ &= \dot{\phi}^2R_{j0i0} + (\partial_i\partial_\sigma\phi - \Gamma^0_{i\sigma}\dot{\phi})(\partial_j\partial^\sigma\phi - \Gamma^\sigma_{j0}\dot{\phi}) - (\partial_i\partial_j\phi - \Gamma^0_{ij}\dot{\phi})(\partial_\sigma\partial^\sigma\phi - \Gamma^\sigma_{\sigma0}\dot{\phi}) \\ &\quad +\frac{1}{2}\dot{\phi}^2G_{ij} + g_{ij}\left(\frac{1}{2}(\partial_\sigma\partial^\sigma\phi - \Gamma^\sigma_{\sigma0}\dot{\phi})^2 - \dot{\phi}^2R_{00}\right. \\ &\quad \left.-\frac{1}{2}(\partial_\rho\partial_\sigma\phi - \Gamma^0_{\rho\sigma}\dot{\phi})g^{\rho\alpha}(\partial_\alpha\partial^\sigma\phi - \Gamma^\sigma_{\alpha0}\dot{\phi})\right), \\ &= \dot{\phi}^2R_{j0i0} + (\partial_i\partial_0\phi - \Gamma^0_{i0}\dot{\phi})(\partial_j\partial^0\phi - \Gamma^0_{j0}\dot{\phi}) + (\partial_i\partial_k\phi - \Gamma^0_{ik}\dot{\phi})(\partial_j\partial^k\phi - \Gamma^k_{j0}\dot{\phi}) \\ &\quad -(\partial_i\partial_j\phi - \Gamma^0_{ij}\dot{\phi})(\partial_0\partial^0\phi - \Gamma^0_{00}\dot{\phi}) - (\partial_i\partial_j\phi - \Gamma^0_{ij}\dot{\phi})(\partial_k\partial^k\phi - \Gamma^k_{k0}\dot{\phi}) \\ &\quad +\frac{1}{2}\dot{\phi}^2G_{ij} + g_{ij}\left(\frac{1}{2}(\partial_0\partial^0\phi - \Gamma^0_{00}\dot{\phi} + \partial_k\partial^k\phi - \Gamma^k_{k0}\dot{\phi})^2 - \dot{\phi}^2R_{00}\right. \\ &\quad \left.-\frac{1}{2}(\partial_0\partial_0\phi - \Gamma^0_{00}\dot{\phi})g^{00}(\partial_0\partial^0\phi - \Gamma^0_{00}\dot{\phi}) - \frac{1}{2}(\partial_k\partial_l\phi - \Gamma^0_{kl}\dot{\phi})g^{km}(\partial_m\partial^l\phi - \Gamma^l_{m0}\dot{\phi})\right), \\ &= \dot{\phi}^2R_{j0i0} + \Gamma^0_{ik}\Gamma^k_{j0}\dot{\phi}^2 + \Gamma^0_{ij}\dot{\phi}(-\ddot{\phi}) - \Gamma^0_{ij}\Gamma^k_{k0}\dot{\phi}^2 + \frac{1}{2}\dot{\phi}^2G_{ij} \\ &\quad +g_{ij}\left(\frac{1}{2}(-\ddot{\phi} - \Gamma^k_{k0}\dot{\phi})^2 - \dot{\phi}^2R_{00} - \frac{1}{2}\ddot{\phi}^2 - \frac{1}{2}(-\Gamma^0_{kl}\dot{\phi})g^{km}(-\Gamma^l_{m0}\dot{\phi})\right). \end{aligned} \tag{B.12}$$

Using the expression from equation (B.3), we obtain

$$\begin{aligned}
\Theta_{ij} &= \dot{\phi}^2 R_{j0i0} + (g_{ik}H)(\delta^k_j H)\dot{\phi}^2 - g_{ij}H\dot{\phi}\ddot{\phi} - g_{ij}H^2\delta^k_k\dot{\phi}^2 - \frac{1}{2}\dot{\phi}^2 g_{ij}\left(2\dot{H} + 3H^2 + \frac{k}{a^2}\right) \\
&\quad + g_{ij}\left(\frac{1}{2}(-\ddot{\phi} - \delta^k_k H\dot{\phi})^2 + 3\dot{\phi}^2(\dot{H} + H^2) - \frac{1}{2}\ddot{\phi}^2 - \frac{1}{2}g^{km}(g_{kl}H)(\delta^l_m H)\dot{\phi}^2\right), \\
&= \dot{\phi}^2 R_{j0i0} + g_{ij}H^2\dot{\phi}^2 - g_{ij}H\dot{\phi}\ddot{\phi} - 3g_{ij}H^2\dot{\phi}^2 - \frac{1}{2}\dot{\phi}^2 g_{ij}\left(2\dot{H} + 3H^2 + \frac{k}{a^2}\right) \\
&\quad + g_{ij}\left(\frac{1}{2}\ddot{\phi}^2 + \frac{9}{2}H^2\dot{\phi}^2 + 3H\dot{\phi}\ddot{\phi} + 3\dot{\phi}^2\dot{H} + 3\dot{\phi}^2H^2 - \frac{1}{2}\ddot{\phi}^2 - \frac{3}{2}H^2\dot{\phi}^2\right), \\
&= \dot{\phi}^2 R_{j0i0} + \frac{5}{2}g_{ij}H^2\dot{\phi}^2 - \frac{1}{2}g_{ij}\frac{k\dot{\phi}^2}{a^2} + 2g_{ij}H\dot{\phi}\ddot{\phi} + 2g_{ij}\dot{\phi}^2\dot{H}\,. \qquad \text{(B.13)}
\end{aligned}$$

The Riemann tensor, $R_{i0j0} = g_{ki}R^k{}_{0j0}$, can be expressed as

$$\begin{aligned}
R^k{}_{0j0} &= \partial_j\Gamma^k_{00} - \partial_0\Gamma^k_{j0} + \Gamma^k_{j\lambda}\Gamma^\lambda_{00} - \Gamma^k_{0\lambda}\Gamma^\lambda{}_{j0}\,, \\
&= \partial_j\Gamma^k_{00} - \partial_0\Gamma^k_{j0} + \Gamma^k_{j0}\Gamma^0_{00} + \Gamma^k_{jl}\Gamma^l_{00} - \Gamma^k_{00}\Gamma^0{}_{j0} - \Gamma^k_{0l}\Gamma^l{}_{j0}\,, \\
&= -\partial_0\Gamma^k_{j0} - \Gamma^k_{0l}\Gamma^l{}_{j0}\,, \\
&= -\partial_0(\delta^k_j H) - H^2\delta^k_l\delta^l_j\,, \\
&= -\dot{H}\delta^k_j - H^2\delta^k_j\,, \\
R_{i0j0} &= -g_{ij}\dot{H} - g_{ij}H^2\,. \qquad \text{(B.14)}
\end{aligned}$$

By using the expression for the Riemann tensor, equation (B.13) reads

$$\begin{aligned}
\Theta_{ij} &= -g_{ij}\dot{H}\dot{\phi}^2 - g_{ij}H^2\dot{\phi}^2 + \frac{5}{2}g_{ij}H^2\dot{\phi}^2 - \frac{1}{2}g_{ij}\frac{k\dot{\phi}^2}{a^2} + 2g_{ij}H\dot{\phi}\ddot{\phi} + 2g_{ij}\dot{\phi}^2\dot{H}\,, \\
&= \frac{3}{2}g_{ij}H^2\dot{\phi}^2 - \frac{1}{2}g_{ij}\frac{k\dot{\phi}^2}{a^2} + 2g_{ij}H\dot{\phi}\ddot{\phi} + g_{ij}\dot{\phi}^2\dot{H}\,, \\
&= \frac{\dot{\phi}^2}{2}\left(3H^2 + 2\dot{H} + 4H\ddot{\phi}\dot{\phi}^{-1} - \frac{k}{a^2}\right)g_{ij}\,. \qquad \text{(B.15)}
\end{aligned}$$

The (i,j)-component of the dust matter, defined as a perfect fluid, $T^{(\mathrm{m})}_{ij}$, represents the pressure

$$T^{(\mathrm{m})}_{ij} = (P_{\mathrm{m}} + P_{\mathrm{r}})g_{ij}\,. \qquad \text{(B.16)}$$

Therefore, by combining equations (B.11), (B.15), and (B.16), the (i,j)-component of the Einstein field equation (A.25) reads

$$G_{ij} = 8\pi G\left(T^{(\phi)}_{ij} + \kappa\Theta_{ij} + T^{(\mathrm{m})}_{ij}\right), \qquad \text{(B.17)}$$

$$-\left(2\dot{H}+3H^2+\frac{k}{a^2}\right)g_{ij} = 8\pi G\left[\frac{\varepsilon}{2}\dot{\phi}^2-V(\phi)+\kappa\frac{\dot{\phi}^2}{2}\left(3H^2+2\dot{H}+4H\ddot{\phi}\dot{\phi}^{-1}-\frac{k}{a^2}\right)+P_{\rm m}+P_{\rm r}\right]g_{ij}\,. \tag{B.18}$$

This equation is referred to as the second Friedmann equation, which gives

$$2\dot{H}+3H^2+\frac{k}{a^2} = -8\pi G\left\{\frac{\dot{\phi}^2}{2}\left[\varepsilon+\kappa\left(3H^2+2\dot{H}+4H\ddot{\phi}\dot{\phi}^{-1}-\frac{k}{a^2}\right)\right]-V(\phi)+P_{\rm m}+P_{\rm r}\right\}. \tag{B.19}$$

The Klein-Gordon equation in a FLRW universe can be expressed as

$$\begin{aligned}
\varepsilon\nabla_\mu\nabla^\mu\phi+\kappa G_{\mu\nu}\nabla^\mu\nabla^\nu\phi-V_{,\phi} &= 0\,,\\
\varepsilon(\partial_\mu\partial^\mu\phi+\Gamma^\mu_{\sigma\mu}\partial^\sigma\phi)+\kappa G^{\mu\nu}(\partial_\mu\partial_\nu\phi-\Gamma^\sigma_{\mu\nu}\partial_\sigma\phi)-V_{,\phi} &= 0\,,\\
\varepsilon(-\ddot{\phi}-\Gamma^i_{0i}\dot{\phi})+\kappa G^{00}\ddot{\phi}-\kappa G^{ij}\Gamma^0_{ij}\dot{\phi}-V_{,\phi} &= 0\,,\\
\varepsilon(-\ddot{\phi}-3H\dot{\phi})+3\kappa\left(H^2+\frac{k}{a^2}\right)\ddot{\phi}+\kappa g^{ij}g_{ij}(2\dot{H}+3H^2+\frac{k}{a^2})H\dot{\phi}-V_{,\phi} &= 0\,,\\
\varepsilon(-\ddot{\phi}-3H\dot{\phi})+\kappa\left[3H^2(\ddot{\phi}+3H\dot{\phi})+\frac{3k}{a^2}(\ddot{\phi}+H\dot{\phi})+6H\dot{H}\dot{\phi}\right]-V_{,\phi} &= 0\,,\\
-\varepsilon(\ddot{\phi}+3H\dot{\phi})+\kappa\left(3H^2+\frac{3k}{a^2}\right)(\ddot{\phi}+3H\dot{\phi})+\kappa\left(-6H\frac{k\dot{\phi}}{a^2}+6H\dot{H}\dot{\phi}\right)-V_{,\phi} &= 0\,.
\end{aligned} \tag{B.20}$$

Hence, the Klein-Gordon equation of NMDC interaction theory can be expressed as

$$\left[\varepsilon-\left(3\kappa H^2+\frac{3\kappa k}{a^2}\right)\right](\ddot{\phi}+3H\dot{\phi})+V_{,\phi}-6\kappa H\dot{H}\dot{\phi}+6\kappa H\frac{k\dot{\phi}}{a^2} = 0\,. \tag{B.21}$$

We can express the equation from two perspectives as follows. Firstly, we can write it in terms of effective potential

$$\ddot{\phi}+3H\dot{\phi}+V_{\rm eff} = 0\,, \tag{B.22}$$

where $V_{\rm eff}$ is

$$V_{\rm eff} = \frac{V_{,\phi}-6\kappa H\dot{H}\dot{\phi}+\dfrac{6\kappa Hk\dot{\phi}}{a^2}}{\varepsilon-3\kappa\left(H^2+\dfrac{k}{a^2}\right)}\,. \tag{B.23}$$

Secondly, we can express the Klein-Gordon equation, in which the damped term and potential are modified by the NMDC field, as follows

$$\ddot{\phi}+3H\dot{\phi}\left[1-\frac{2\kappa\left(\dot{H}-\frac{k}{a^2}\right)}{\varepsilon-3\kappa\left(H^2+\frac{k}{a^2}\right)}\right]+\frac{V_{,\phi}}{\varepsilon-3\kappa\left(H^2+\frac{k}{a^2}\right)} = 0. \quad \text{(B.24)}$$

APPENDIX C NMC FIELD EQUATIONS

The action for the non-minimal coupling between the scalar field, ϕ, and the Ricci scalar, R, can be expressed as

$$S = \int \mathrm{d}^4x\sqrt{-g}\left(\frac{R}{16\pi G} - \frac{1}{2}g^{\mu\nu}\nabla_\mu\phi\nabla_\nu\phi - V(\phi) - \frac{1}{2}\xi\phi^2 R + \mathcal{L}_\mathrm{m}\right) . \quad \text{(C.1)}$$

Varying the action with respect to the metric tensor $g^{\mu\nu}$ yields the modified Einstein field equations, which are given by

$$\begin{aligned}\delta_g S = & \int \mathrm{d}^4x\delta\sqrt{-g}\left[\left(\frac{1}{16\pi G} - \frac{1}{2}\xi\phi^2\right)R - \frac{1}{2}g^{\mu\nu}\nabla_\mu\phi\nabla_\nu\phi + V(\phi) + \mathcal{L}_\mathrm{m}\right] \\ & + \int \mathrm{d}^4x\sqrt{-g}\left[\left(\frac{1}{16\pi G} - \frac{1}{2}\xi\phi^2\right)\delta R - \frac{1}{2}\delta g^{\mu\nu}\nabla_\mu\phi\nabla_\nu\phi + \delta\mathcal{L}_\mathrm{m}\right] . \quad \text{(C.2)}\end{aligned}$$

Varying the Ricci scalar with respect to the metric tensor is given by $\delta R = g^{\mu\nu}\delta R_{\mu\nu} + R_{\mu\nu}\delta g^{\mu\nu}$. This leads to

$$\begin{aligned}\delta_g S = & \int \mathrm{d}^4x\delta\sqrt{-g}\left[\left(\frac{1}{16\pi G} - \frac{1}{2}\xi\phi^2\right)R - \frac{1}{2}g^{\mu\nu}\nabla_\mu\phi\nabla_\nu\phi + V(\phi) + \mathcal{L}_\mathrm{m}\right] \\ & + \int \mathrm{d}^4x\sqrt{-g}\left[\left(\frac{1}{16\pi G} - \frac{1}{2}\xi\phi^2\right)g^{\mu\nu}\delta R_{\mu\nu} + \left(\frac{1}{16\pi G} - \frac{1}{2}\xi\phi^2\right)R_{\mu\nu}\delta g^{\mu\nu}\right. \\ & \left. - \frac{1}{2}\delta g^{\mu\nu}\nabla_\mu\phi\nabla_\nu\phi + \delta\mathcal{L}_\mathrm{m}\right] . \quad \text{(C.3)}\end{aligned}$$

Varying the determinant of the metric tensor can be expressed as

$$\delta\sqrt{-g} = -\frac{1}{2}\sqrt{-g}g_{\mu\nu}\delta g^{\mu\nu} . \quad \text{(C.4)}$$

Let us consider the variation of the Ricci tensor term in equation (C.3)

$$\delta R_{\mu\nu} = \nabla_\rho\delta\Gamma^\rho_{\mu\nu} - \nabla_\mu\delta\Gamma^\rho_{\nu\rho} , \quad \text{(C.5)}$$

where $\delta\Gamma^\rho_{\mu\nu}$ is the variation of the Christoffel symbols. We obtain

$$\int \mathrm{d}^4x\sqrt{-g}\left(\frac{1}{16\pi G}-\frac{1}{2}\xi\phi^2\right)\delta R_{\mu\nu}g^{\mu\nu}$$
$$= \int \mathrm{d}^4x\sqrt{-g}\left(\frac{1}{16\pi G}-\frac{1}{2}\xi\phi^2\right)g^{\mu\nu}\left(\nabla_\rho\delta\Gamma^\rho_{\mu\nu}-\nabla_\mu\delta\Gamma^\rho_{\nu\rho}\right). \qquad \text{(C.6)}$$

Upon applying integration by parts and imposing the boundary condition that the variation of the boundary term vanishes, we obtain

$$\begin{aligned}
&\int \mathrm{d}^4x\sqrt{-g}\left(\frac{1}{16\pi G}-\frac{1}{2}\xi\phi^2\right)\delta R_{\mu\nu}g^{\mu\nu}\\
&= \int \mathrm{d}^4x\sqrt{-g}\Bigg\{-\delta\Gamma^\rho_{\mu\nu}\nabla_\rho\left[\left(\frac{1}{16\pi G}-\frac{1}{2}\xi\phi^2\right)g^{\mu\nu}\right]\\
&\quad+\delta\Gamma^\rho_{\nu\rho}\nabla_\mu\left[\left(\frac{1}{16\pi G}-\frac{1}{2}\xi\phi^2\right)g^{\mu\nu}\right]\Bigg\},\\
&= \int \mathrm{d}^4x\sqrt{-g}\Bigg\{-\delta\Gamma^\rho_{\mu\nu}\left[\nabla_\rho\left(\frac{g^{\mu\nu}}{16\pi G}\right)-\nabla_\rho\left(\frac{1}{2}g^{\mu\nu}\xi\phi^2\right)\right]\\
&\quad+\delta\Gamma^\rho_{\nu\rho}\left[\nabla_\mu\left(\frac{g^{\mu\nu}}{16\pi G}\right)-\nabla_\mu\left(\frac{1}{2}g^{\mu\nu}\xi\phi^2\right)\right]\Bigg\},\\
&= \int \mathrm{d}^4x\sqrt{-g}\frac{1}{2}\xi g^{\mu\nu}\left[\delta\Gamma^\rho_{\mu\nu}(\nabla_\rho\phi^2)-\delta\Gamma^\rho_{\nu\rho}(\nabla_\mu\phi^2)\right]. \qquad \text{(C.7)}
\end{aligned}$$

In the final equation, we apply the principle of metric compatibility, which states that the covariant derivative of the metric tensor vanishes, $\nabla_\mu g^{\mu\nu}$. By expanding the Christoffel symbols in terms of the metric tensor, we obtain

$$\delta\Gamma^\rho_{\mu\nu} = \frac{1}{2}g^{\rho\sigma}\left(\nabla_\mu\delta g_{\nu\sigma}+\nabla_\nu\delta g_{\mu\sigma}-\nabla_\sigma\delta g_{\mu\nu}\right), \qquad \text{(C.8)}$$

$$\begin{aligned}
\delta\Gamma^\rho_{\nu\rho} &= \frac{1}{2}\left(g^{\rho\sigma}\nabla_\nu\delta g_{\rho\sigma}+\nabla^\sigma\delta g_{\nu\sigma}-\nabla^\rho\delta g_{\nu\rho}\right),\\
&= \frac{1}{2}g^{\rho\sigma}\nabla_\nu\delta g_{\rho\sigma}. \qquad \text{(C.9)}
\end{aligned}$$

Hence, we obtain

$$\int \mathrm{d}^4x\sqrt{-g}\left(\frac{1}{16\pi G}-\frac{1}{2}\xi\phi^2\right)\delta R_{\mu\nu}g^{\mu\nu}$$
$$= \int \mathrm{d}^4x\sqrt{-g}\frac{1}{2}g^{\mu\nu}\xi[\nabla_\rho\phi^2 g^{\rho\sigma}\left(\nabla_\mu\delta g_{\nu\sigma}+\nabla_\nu\delta g_{\mu\sigma}-\nabla_\sigma\delta g_{\mu\nu}\right)-\nabla_\mu\phi^2 g^{\rho\sigma}\nabla_\nu\delta g_{\rho\sigma}],$$

$$
\begin{aligned}
&= \int \mathrm{d}^4x\sqrt{-g}\frac{1}{4}\xi[\nabla_\rho\phi^2 g^{\mu\nu}g^{\rho\sigma}\left(\nabla_\mu\delta g_{\nu\sigma}+\nabla_\nu\delta g_{\mu\sigma}-\nabla_\sigma\delta g_{\mu\nu}\right)\\
&\quad -\nabla_\mu\phi^2 g^{\mu\nu}g^{\rho\sigma}\nabla_\nu\delta g_{\rho\sigma}],\\
&= \int \mathrm{d}^4x\sqrt{-g}\frac{1}{4}\xi\nabla_\rho\phi^2[g^{\mu\nu}g^{\rho\sigma}\left(\nabla_\mu\delta g_{\nu\sigma}+\nabla_\nu\delta g_{\mu\sigma}-\nabla_\sigma\delta g_{\mu\nu}\right)\\
&\quad -g^{\rho\nu}g^{\mu\sigma}\nabla_\nu\delta g_{\mu\sigma}],\\
&= \int \mathrm{d}^4x\sqrt{-g}\frac{\xi}{4}\nabla_\rho\phi^2[g^{\mu\nu}g^{\rho\sigma}\nabla_\mu\delta g_{\nu\sigma}+g^{\mu\nu}g^{\rho\sigma}\nabla_\nu\delta g_{\mu\sigma}-g^{\mu\nu}g^{\rho\sigma}\nabla_\sigma\delta g_{\mu\nu}\\
&\quad -g^{\rho\nu}g^{\mu\sigma}\nabla_\nu\delta g_{\mu\sigma}],\\
&= \int \mathrm{d}^4x\sqrt{-g}\frac{\xi}{2}\nabla_\rho\phi^2\left[g^{\mu\nu}g^{\rho\sigma}\nabla_\nu\delta g_{\mu\sigma}-g^{\rho\nu}g^{\mu\sigma}\nabla_\nu\delta g_{\mu\sigma}\right],\\
&= \int \mathrm{d}^4x\sqrt{-g}\frac{\xi}{2}\left[-g^{\mu\nu}g^{\rho\sigma}\delta g_{\mu\sigma}\nabla_\nu\nabla_\rho\phi^2+g^{\rho\nu}g^{\mu\sigma}\delta g_{\mu\sigma}\nabla_\nu\nabla_\rho\phi^2\right],\\
&= \int \mathrm{d}^4x\sqrt{-g}\frac{\xi}{2}\left[\delta g^{\nu\rho}\nabla_\nu\nabla_\rho\phi^2+g^{\rho\nu}g^{\mu\sigma}\left(-g_{\mu\alpha}g_{\sigma\beta}\delta g^{\alpha\beta}\right)\nabla_\nu\nabla_\rho\phi^2\right],\\
&= \int \mathrm{d}^4x\sqrt{-g}\frac{\xi}{2}\left[\delta g^{\nu\rho}\nabla_\nu\nabla_\rho\phi^2-g_{\mu\nu}\delta g^{\mu\nu}\nabla_\rho\nabla^\rho\phi^2\right],\\
&= \int \mathrm{d}^4x\sqrt{-g}\frac{\xi}{2}\left[\nabla_\mu\nabla_\nu\phi^2-g_{\mu\nu}\nabla_\rho\nabla^\rho\phi^2\right]\delta g^{\mu\nu}. \qquad \text{(C.10)}
\end{aligned}
$$

Substituting equations (C.4) and (C.10) into the action equation (C.3), we obtain

$$
\begin{aligned}
\delta_g S &= \int \mathrm{d}^4x\left(-\frac{1}{2}\sqrt{-g}g_{\mu\nu}\delta g^{\mu\nu}\right)\left(\frac{1}{16\pi G}R-\frac{1}{2}\xi\phi^2R-\frac{1}{2}g^{\sigma\rho}\nabla_\sigma\phi\nabla_\rho\phi-V(\phi)+\mathcal{L}_\mathrm{m}\right)\\
&\quad +\int \mathrm{d}^4x\sqrt{-g}\left[\left(\frac{1}{16\pi G}-\frac{1}{2}\xi\phi^2\right)\delta g^{\mu\nu}R_{\mu\nu}+\frac{1}{2}\xi\left(\nabla_\mu\nabla_\nu\phi^2-g_{\mu\nu}\nabla_\rho\nabla^\rho\phi^2\right)\delta g^{\mu\nu}\right.\\
&\quad \left.-\frac{1}{2}\nabla_\mu\phi\nabla_\nu\phi\delta g^{\mu\nu}+\delta\mathcal{L}_\mathrm{m}\right],\\
&= \int \mathrm{d}^4x\sqrt{-g}\delta g^{\mu\nu}\left[-\frac{1}{2}g_{\mu\nu}R\left(\frac{1}{16\pi G}-\frac{1}{2}\xi\phi^2\right)+\frac{1}{4}g_{\mu\nu}\nabla^\rho\phi\nabla_\rho\phi+\frac{1}{2}g_{\mu\nu}V(\phi)\right.\\
&\quad -\frac{1}{2}g_{\mu\nu}\mathcal{L}_\mathrm{m}+\left(\frac{1}{16\pi G}-\frac{1}{2}\xi\phi^2\right)R_{\mu\nu}+\frac{1}{2}\xi\left(\nabla_\mu\nabla_\nu\phi^2-g_{\mu\nu}\nabla_\rho\nabla^\rho\phi^2\right)\\
&\quad \left.-\frac{1}{2}\nabla_\mu\phi\nabla_\nu\phi+\frac{\delta\mathcal{L}_\mathrm{m}}{\delta g^{\mu\nu}}\right],\\
&= \int \mathrm{d}^4x\sqrt{-g}\delta g^{\mu\nu}\left[\left(\frac{1}{16\pi G}-\frac{1}{2}\xi\phi^2\right)G_{\mu\nu}+\frac{1}{4}g_{\mu\nu}\nabla^\rho\phi\nabla_\rho\phi+\frac{1}{2}g_{\mu\nu}V(\phi)\right.\\
&\quad \left.-\frac{1}{2}g_{\mu\nu}\mathcal{L}_\mathrm{m}+\frac{1}{2}\xi\left(\nabla_\mu\nabla_\nu\phi^2-g_{\mu\nu}\nabla_\rho\nabla^\rho\phi^2\right)-\frac{1}{2}\nabla_\mu\phi\nabla_\nu\phi+\frac{\delta\mathcal{L}_\mathrm{m}}{\delta g^{\mu\nu}}\right]. \qquad \text{(C.11)}
\end{aligned}
$$

According to least action principle, $\delta_g S = 0$, the equation (C.11) yields modified

Einstein field equation

$$\left(\frac{1}{16\pi G}-\frac{1}{2}\xi\phi^2\right)G_{\mu\nu}+\frac{1}{4}g_{\mu\nu}\nabla^\rho\phi\nabla_\rho\phi+\frac{1}{2}g_{\mu\nu}V(\phi)-\frac{1}{2}g_{\mu\nu}\mathcal{L}_{\rm m}$$
$$+\frac{1}{2}\xi\left(\nabla_\mu\nabla_\nu\phi^2-g_{\mu\nu}\nabla_\rho\nabla^\rho\phi^2\right)-\frac{1}{2}\nabla_\mu\phi\nabla_\nu\phi+\frac{\delta\mathcal{L}_{\rm m}}{\delta g^{\mu\nu}} = 0\,. \qquad \text{(C.12)}$$

By factorizing the equation into the form of the original Einstein equation, we obtain

$$G_{\mu\nu} = \frac{8\pi G}{1-8\pi G\xi\phi^2}\Bigg[\nabla_\mu\phi\nabla_\nu\phi-\frac{1}{2}g_{\mu\nu}\nabla^\rho\phi\nabla_\rho\phi-V(\phi)g_{\mu\nu}$$
$$-\xi\left(\nabla_\mu\nabla_\nu\phi^2-g_{\mu\nu}\nabla_\rho\nabla^\rho\phi^2\right)+g_{\mu\nu}\mathcal{L}_{\rm m}-2\frac{\delta\mathcal{L}_{\rm m}}{\delta g^{\mu\nu}}\Bigg]\,. \qquad \text{(C.13)}$$

The Einstein field equation is given by

$$G_{\mu\nu} = 8\pi G_{\rm eff}\left(T^{(\phi)}_{\mu\nu}+T^{(\rm m)}_{\mu\nu}\right)\,, \qquad \text{(C.14)}$$

where the effective gravitational constant is defined as $G_{\rm eff}=G/\left(1-8\pi G\xi\phi^2\right)$. The energy-momentum tensors for the NMC field, $T^{(\phi)}_{\mu\nu}$, and the non-relativistic matter field, $T^{(\rm m)}_{\mu\nu}$, are given by

$$T^{(\phi)}_{\mu\nu} = \nabla_\mu\phi\nabla_\nu\phi-\frac{1}{2}g_{\mu\nu}\nabla^\rho\phi\nabla_\rho\phi-V(\phi)g_{\mu\nu}-\xi\left(\nabla_\mu\nabla_\nu\phi^2-g_{\mu\nu}\nabla_\rho\nabla^\rho\phi^2\right)\,,$$
$$T^{(\rm m)}_{\mu\nu} = g_{\mu\nu}\mathcal{L}_{\rm m}-2\frac{\delta\mathcal{L}_{\rm m}}{\delta g^{\mu\nu}}\,. \qquad \text{(C.15)}$$

Varying the action in equation (C.1) with respect to the scalar field, ϕ, yields the following equation of motion for the scalar field

$$\delta_\phi S = \int {\rm d}^4x\sqrt{-g}\left\{-\frac{1}{2}g^{\mu\nu}\left[(\nabla_\mu\delta\phi)\nabla_\nu\phi+\nabla_\mu\phi(\nabla_\nu\delta\phi)\right]-V_{,\phi}\delta\phi-\xi R\phi\delta\phi\right\}\,. \qquad \text{(C.16)}$$

By applying integration by parts and imposing the boundary condition, we obtain

$$\delta_\phi S = \int {\rm d}^4x\sqrt{-g}\left\{\frac{1}{2}g^{\mu\nu}\left[(\nabla_\mu\nabla_\nu\phi)\delta\phi+(\nabla_\nu\nabla_\mu\phi)\delta\phi\right]-V_{,\phi}\delta\phi-\xi R\phi\delta\phi\right\}\,,$$
$$= \int {\rm d}^4x\sqrt{-g}\left[g^{\mu\nu}(\nabla_\mu\nabla_\nu\phi)-V_{,\phi}-\xi R\phi\right]\delta\phi\,,$$

$$= \int \mathrm{d}^4x\sqrt{-g}\left[(\nabla_\mu\nabla^\mu\phi) - V_{,\phi} - \xi R\phi\right]\delta\phi\,, \tag{C.17}$$

where $V_{,\phi}$ represents the derivative of the potential with respect to the scalar field. According to the principle of least action, $\delta_\phi S = 0$, the variation in equation (C.17) yield a modified Klein-Gordon equation given by

$$\nabla_\mu\nabla^\mu\phi - V_{,\phi} - \xi R\phi \;=\; 0\,. \tag{C.18}$$

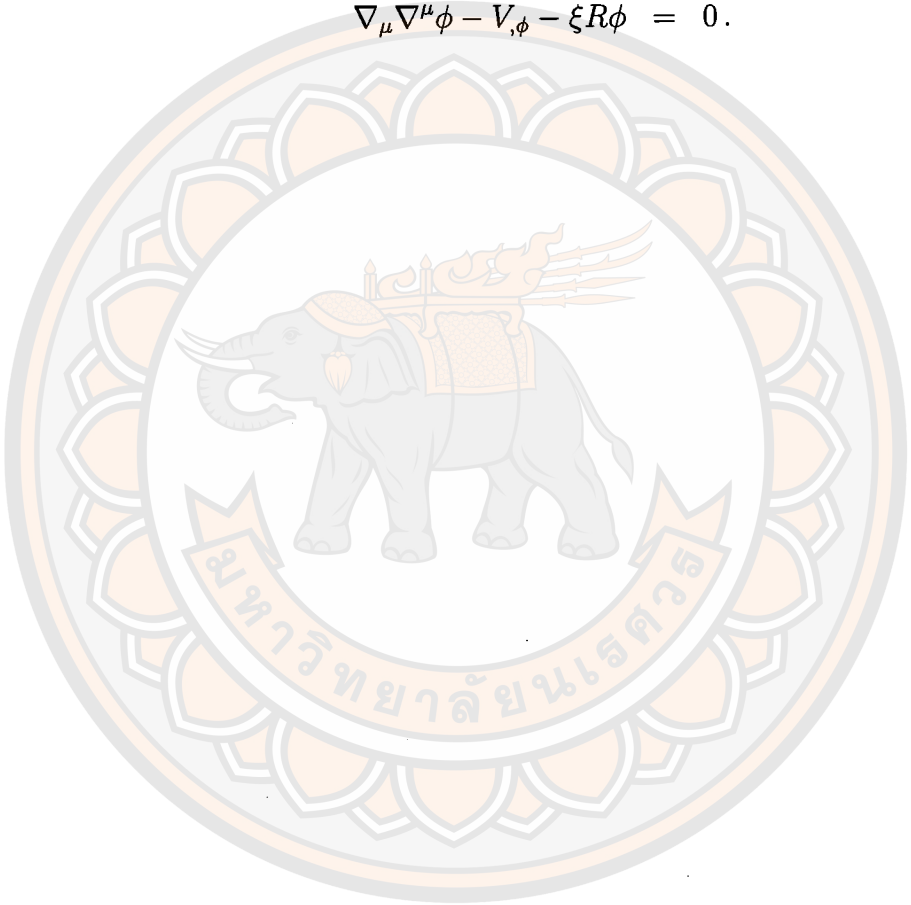

APPENDIX D NMC COSMOLOGICAL EQUATIONS

NMC theory in the FLRW background described by equation (B.1) is considered. The energy-momentum tensor from the NMC field is given by equation (C.15)

$$T_{\nu}^{\mu(\phi)} = \nabla^{\mu}\phi\nabla_{\nu}\phi - \frac{1}{2}\delta_{\nu}^{\mu}\nabla^{\rho}\phi\nabla_{\rho}\phi - V(\phi)\delta_{\nu}^{\mu} - \xi\left(\nabla^{\mu}\nabla_{\nu}\phi^2 - \delta_{\nu}^{\mu}\nabla_{\rho}\nabla^{\rho}\phi^2\right). \tag{D.1}$$

Expanding the last two terms of the covariant derivative, we obtain

$$\begin{aligned}
\nabla^{\mu}\nabla_{\nu}\phi^2 &= g^{\lambda\mu}\nabla_{\lambda}\nabla_{\nu}\phi^2, \\
&= g^{\lambda\mu}\nabla_{\lambda}(\partial_{\nu}\phi^2), \\
&= g^{\lambda\mu}\left(\partial_{\lambda}\partial_{\nu}\phi^2 - \Gamma_{\lambda\nu}^{\rho}\partial_{\rho}\phi^2\right), \\
&= g^{\lambda\mu}\left(\partial_{\lambda}\partial_{\nu}\phi^2 - \Gamma_{\lambda\nu}^{\rho}\partial_{\rho}\phi^2\right), \\
&= \partial^{\mu}\partial_{\nu}\phi^2 - g^{\lambda\mu}\Gamma_{\lambda\nu}^{\rho}\partial_{\rho}\phi^2,
\end{aligned} \tag{D.2}$$

$$\nabla_{\rho}\nabla^{\rho}\phi^2 = \partial_{\rho}\partial^{\rho}\phi^2 + \Gamma_{\lambda\rho}^{\rho}\partial^{\lambda}\phi^2. \tag{D.3}$$

Let us consider the (0,0)-component of the energy-momentum tensor. This gives

$$\begin{aligned}
T_0^{0(\phi)} &= g^{00}\partial_0\phi\partial_0\phi - \frac{1}{2}g^{00}\partial_0\phi\partial_0\phi - V(\phi) \\
&\quad -\xi\left(\partial^0\partial_0\phi^2 - g^{00}\Gamma_{00}^0\partial_0\phi^2 - \partial_0\partial^0\phi^2 - g^{00}\Gamma_{\rho 0}^{\rho}\partial_0\phi^2\right), \\
&= -\dot{\phi}^2 + \frac{1}{2}\dot{\phi}^2 - V(\phi) - \xi\left(\Gamma_{00}^0\partial_0\phi^2 + \Gamma_{\rho 0}^{\rho}\partial_0\phi^2\right).
\end{aligned} \tag{D.4}$$

In the FLRW universe, the non-zero components of the Christoffel symbols are given by

$$\Gamma_{ij}^0 = Hg_{ij}, \quad \Gamma_{0j}^i = H\delta_j^i, \quad \Gamma_{00}^0 = 0, \quad \Gamma_{00}^i = 0, \tag{D.5}$$

where $H = \dot{a}/a$ is the Hubble parameter, g_{ij} represents the spatial part of the metric, and δ_j^i is the Kronecker delta. This gives the $(0,0)$-component of the energy

momentum tensor as

$$\begin{aligned} T_0^{0(\phi)} &= -\dot{\phi}^2 + \frac{1}{2}\dot{\phi}^2 - V(\phi) - \xi\Gamma^i_{0i}2\phi\dot{\phi}\,, \\ &= -\dot{\phi}^2 + \frac{1}{2}\dot{\phi}^2 - V(\phi) - \xi H\delta^i_i 2\phi\dot{\phi}\,, \\ &= -\frac{\dot{\phi}^2}{2} - V(\phi) - 6\xi H\phi\dot{\phi}\,. \end{aligned} \tag{D.6}$$

In the FLRW universe, the energy-momentum tensor for a perfect fluid is characterized by its energy density ρ and pressure P. This gives

$$T_0^{0(\phi)} = -\left(\frac{\dot{\phi}^2}{2} + V(\phi) + 6\xi H\phi\dot{\phi}\right) = -\rho_\phi\,. \tag{D.7}$$

Hence, the energy density of the scalar field, modified by the NMC, is given by

$$\rho_\phi = \frac{\dot{\phi}^2}{2} + V(\phi) + 6\xi H\phi\dot{\phi}\,, \tag{D.8}$$

According to the (0,0) component of the Einstein tensor in the spatially curved FLRW background, we have

$$G_0^0 = -3(H^2 + \frac{k}{a^2})\,. \tag{D.9}$$

Thus, the Einstein field equation yields the Friedmann equation

$$\begin{aligned} G_0^0 &= 8\pi G_{\text{eff}}\left(T_0^{0(\phi)} + T_0^{0(\text{m})}\right), \\ H^2 + \frac{k}{a^2} &= \frac{8\pi G_{\text{eff}}}{3}\left(\frac{\dot{\phi}^2}{2} + V(\phi) + 6\xi H\phi\dot{\phi} + \rho_{\text{m}} + \rho_{\text{r}}\right). \end{aligned} \tag{D.10}$$

where ρ_{m} and ρ_{r} are energy density of dust and radiation, respectively.

The (i,j) component of the scalar field energy-momentum tensor is given by

$$\begin{aligned} T_j^{i(\phi)} &= \partial^i\phi\partial_j\phi - \frac{1}{2}\delta^i_j\partial^\rho\phi\partial_\rho\phi - V(\phi)\delta^i_j - \xi\Big(\partial^i\partial_j\phi^2 - g^{ik}\Gamma^\rho_{kj}\partial_\rho\phi^2 \\ &\quad -\delta^i_j\partial_\rho\partial^\rho\phi^2 - \delta^i_j\Gamma^\rho_{\lambda\rho}\partial^\lambda\phi^2\Big)\,, \\ &= -\frac{1}{2}g^{00}\partial_0\phi\partial_0\phi\delta^i_j - V(\phi)\delta^i_j - \xi\left(-g^{ik}\Gamma^0_{kj}\partial_0\phi^2 - g^{00}\partial_0\partial_0\phi^2\delta^i_j - g^{00}\Gamma^k_{0k}\partial_0\phi^2\delta^i_j\right)\,, \end{aligned}$$

$$
\begin{aligned}
&= \frac{\dot{\phi}^2}{2}\delta^i_j - V(\phi)\delta^i_j - \xi\left[-\underbrace{g^{ik}g_{kj}}_{\delta^i_j} H 2\phi\dot{\phi} + 2(\ddot{\phi}\phi + \dot{\phi}^2)\delta^i_j + 6H\phi\dot{\phi}\delta^i_j\right], \\
&= \left[\frac{\dot{\phi}^2}{2} - V(\phi) + 2\xi H\phi\dot{\phi} - 2\xi(\ddot{\phi}\phi + \dot{\phi}^2) - 6\xi H\phi\dot{\phi}\right]\delta^i_j, \\
&= \left[\frac{\dot{\phi}^2}{2} - V(\phi) - \xi\left(4H\phi\dot{\phi} + 2\ddot{\phi}\phi + 2\dot{\phi}^2\right)\right]\delta^i_j . \qquad \text{(D.11)}
\end{aligned}
$$

The (i,j) component of the energy-momentum tensor represents the pressure of a perfect fluid

$$T^{i(\phi)}_j = P_\phi \delta^i_j . \qquad \text{(D.12)}$$

Hence, the pressure of the NMC scalar field can be expressed as

$$P_\phi = \frac{\dot{\phi}^2}{2} - V(\phi) - \xi\left(4H\phi\dot{\phi} + 2\ddot{\phi}\phi + 2\dot{\phi}^2\right). \qquad \text{(D.13)}$$

The (i,j)-component of the Einstein tensor in the spatially curved FLRW background is

$$G^i_j = -\left(2\dot{H} + 3H^2 + \frac{k}{a^2}\right)\delta^i_j . \qquad \text{(D.14)}$$

Therefore, the (i,j) component of Einstein field equation yields

$$
\begin{aligned}
G^i_j &= 8\pi G_{\text{eff}}\left(T^{i(\phi)}_j + T^{i(\text{m})}_j\right), \\
-\left(2\dot{H} + 3H^2 + \frac{k}{a^2}\right)\delta^i_j &= 8\pi G_{\text{eff}}\left[\frac{\dot{\phi}^2}{2} - V(\phi) - \xi\left(4H\phi\dot{\phi} + 2\ddot{\phi}\phi + 2\dot{\phi}^2\right)\right. \\
&\quad \left. -P_{\text{m}} - P_{\text{r}}\right]\delta^i_j , \\
2\dot{H} + 3H^2 + \frac{k}{a^2} &= -8\pi G_{\text{eff}}\left[\frac{\dot{\phi}^2}{2} - V(\phi) - \xi\left(4H\phi\dot{\phi} + 2\ddot{\phi}\phi + 2\dot{\phi}^2\right)\right. \\
&\quad \left. -P_{\text{m}} - P_{\text{r}}\right]. \qquad \text{(D.15)}
\end{aligned}
$$

Here, P_{m} and P_{r} represent the pressures of dust and radiation, respectively. Since the dust field exhibits pressureless behavior, we can set $P_{\text{m}} = 0$. However, to maintain the general form, we include P_{m} in the second Friedmann equation.

The cosmological Klein-Gordon equation is given by

$$\begin{aligned}
\nabla_\mu \nabla^\mu \phi - V_{,\phi} - \xi R\phi &= 0\,, \\
\partial_\mu \partial^\mu \phi + \Gamma^\mu_{\sigma\mu} \partial^\sigma \phi - V_\phi - \xi R\phi &= 0\,, \\
-\ddot{\phi} - 3H\dot{\phi} - V_\phi - 6\xi\phi\left(\dot{H} + 2H^2 + \frac{k}{a^2}\right) &= 0\,, \\
\ddot{\phi} + 3H\dot{\phi} + V_\phi + 6\xi\phi\left(\dot{H} + 2H^2 + \frac{k}{a^2}\right) &= 0\,. \qquad \text{(D.16)}
\end{aligned}$$

Hence, the equation of motion for the scalar field influenced by NMC can be expressed as

$$\ddot{\phi} + 3H\dot{\phi} = -V_\phi - 6\xi\phi\left(\dot{H} + 2H^2 + \frac{k}{a^2}\right). \qquad \text{(D.17)}$$

APPENDIX E NMDC MODEL: AUTONOMOUS SYSTEM

E.1 Dimensionless dynamical variables

The Friedmann equation, with the kinetic term modified by NMDC, is given by

$$3H^2+\frac{3k}{a^2} = 8\pi G\left\{\frac{\dot{\phi}^2}{2}\left[1-\kappa\left(9H^2+\frac{3k}{a^2}\right)\right]+V(\phi)+\rho_{\rm m}+\rho_\Lambda\right\}, \quad \text{(E.1)}$$

The matter contents include a dust field and holographic vacuum energy. The Universe has the standard Newton's gravitational constant G. From this perspective, the holographic energy density at the cosmological scale is

$$\rho_\Lambda = \frac{3c^2}{8\pi G}\left(H^2+\frac{k}{a^2}\right), \quad \text{(E.2)}$$

Substituting the holographic vacuum energy density into the Friedmann equation (E.1), we obtain

$$\begin{aligned}
3H^2+\frac{3k}{a^2} &= 8\pi G\left[\frac{\dot{\phi}^2}{2}-\frac{9}{2}\kappa\dot{\phi}^2H^2-\frac{3}{2}\frac{\kappa k\dot{\phi}^2}{a^2}+V(\phi)+\rho_m+\frac{3c^2}{8\pi G}\left(H^2+\frac{k}{a^2}\right)\right],\\
3H^2+\frac{3k}{a^2} &= 8\pi G\frac{\dot{\phi}^2}{2}-8\pi G\frac{9}{2}\kappa\dot{\phi}^2H^2-8\pi G\frac{3}{2}\frac{\kappa k\dot{\phi}^2}{a^2}+8\pi GV(\phi)+8\pi G\rho_m\\
&\quad +3c^2\left(H^2+\frac{k}{a^2}\right),\\
1+\frac{k}{a^2H^2} &= \frac{8\pi G\dot{\phi}^2}{6H^2}-12\pi G\kappa\dot{\phi}^2-\frac{4\pi G\kappa k\dot{\phi}^2}{a^2H^2}+\frac{8\pi GV(\phi)}{3H^2}+\frac{8\pi G\rho_m}{3H^2}\\
&\quad +c^2\left(1+\frac{k}{a^2H^2}\right),\\
1 &= x+y+r+s+\Omega_m+\Omega_\Lambda+\Omega_k, \quad \text{(E.3)}
\end{aligned}$$

where the dimensionless dynamical variables are defined as

$$\begin{aligned}
&x=\frac{8\pi G\dot{\phi}^2}{6H^2}, \quad y=\frac{8\pi GV(\phi)}{3H^2}, \quad r=-12\pi G\kappa\dot{\phi}^2, \quad s=-\frac{4\pi G\kappa k\dot{\phi}^2}{a^2H^2},\\
&\Omega_m=\frac{8\pi G\rho_m}{3H^2}, \quad \Omega_\Lambda=c^2\left(1+\frac{k}{a^2H^2}\right), \quad \Omega_k=-\frac{k}{a^2H^2}. \quad \text{(E.4)}
\end{aligned}$$

E.2 Autonomous system

To construct the autonomous system, let us consider the derivative of x with respect to $N = \ln a$. We use the relation between the derivative with respect to N and t, i.e., $\mathrm{d}x/\mathrm{d}N = (1/H)\mathrm{d}x/\mathrm{d}t$. This approach simplifies the study of the evolution of the system by transforming time derivatives into derivatives with respect to the scale factor, making the equations easier to handle in the context of cosmological evolution. This gives

$$\begin{aligned} x' &= \frac{1}{H}\frac{8\pi G}{6}\left(\frac{H^2 2\dot{\phi}\ddot{\phi} - \dot{\phi}^2 2H\dot{H}}{H^4}\right), \\ &= \frac{8\pi G\dot{\phi}^2}{6H^2}\left(2\frac{\ddot{\phi}}{\dot{\phi}H} - 2\frac{\dot{H}}{H^2}\right), \\ &= 2x\left((-\delta) - (-\epsilon)\right), \\ &= 2x\left(\epsilon - \delta\right), \end{aligned} \tag{E.5}$$

where we denote $\epsilon = -\dot{H}/H^2$ and $\delta = -\ddot{\phi}/(\dot{\phi}H)$. Taking the derivative of y with respect to $N = \ln a$, we obtain

$$\begin{aligned} y' &= \frac{8\pi G}{3H}\left(\frac{H^2 V_{,\phi}\dot{\phi} - V 2H\dot{H}}{H^4}\right), \\ &= \frac{8\pi G V}{3H^2}\left(\frac{V_{,\phi}\dot{\phi}}{VH} - \frac{2\dot{H}}{H^2}\right), \\ &= y\left(\frac{V_{,\phi}\dot{\phi}}{VH} - 2\frac{\dot{H}}{H^2}\right). \end{aligned} \tag{E.6}$$

Power-law potential is considered

$$V(\phi) = V_0\phi^n, \quad V_{,\phi} = nV_0\frac{\phi^n}{\phi} = \frac{nV}{\phi}. \tag{E.7}$$

This gives

$$\begin{aligned} y' &= y\left(\frac{2n}{2}\frac{\dot{\phi}}{\phi H} - 2\frac{\dot{H}}{H^2}\right), \\ &= 2y\left(\frac{1}{2}nu + \epsilon\right), \end{aligned} \tag{E.8}$$

Taking the derivative of r with respect to $N = \ln a$, we obtain

$$\begin{aligned} r' &= \frac{1}{H}(-12\pi G\kappa 2\dot{\phi}\ddot{\phi})\,, \\ &= 2(-12\pi G\kappa\dot{\phi}^2)\frac{\ddot{\phi}}{H\dot{\phi}}\,, \\ &= -2r\delta\,. \end{aligned} \tag{E.9}$$

Taking the derivative of s with respect to $N = \ln a$, we obtain

$$\begin{aligned} s' &= \frac{-4\pi G\kappa k}{H}\left(\frac{a^2H^2 2\dot{\phi}\ddot{\phi} - \dot{\phi}^2(a^2 2H\dot{H} + 2a\dot{a}H^2)}{a^4H^4}\right), \\ &= \frac{-4\pi G\kappa k}{H}\left(\frac{a^2H^2 2\dot{\phi}\ddot{\phi}}{a^4H^4} - \frac{\dot{\phi}^2(a^2 2H\dot{H} + 2a\dot{a}H^2)}{a^4H^4}\right), \\ &= \frac{-4\pi G\kappa k}{H}\left(\frac{2\dot{\phi}\ddot{\phi}}{a^2H^2} - \frac{2\dot{H}\dot{\phi}^2}{a^2H^3} - \frac{2H^2\dot{\phi}^2}{a^2H^3}\right), \\ &= 2\left(\frac{-4\pi G\kappa k\dot{\phi}^2}{a^2H^2}\right)\left(\frac{\ddot{\phi}}{H\dot{\phi}} - \frac{\dot{H}}{H^2} - 1\right), \\ &= 2s\left(-\delta - (-\epsilon) - 1\right), \\ &= 2s\left(\epsilon - \delta - 1\right). \end{aligned} \tag{E.10}$$

According to the new dimensionless dynamical variable $u = \dot{\phi}/(\phi H)$, differentiating u with respect to N gives

$$\begin{aligned} u' &= \frac{\phi H\ddot{\phi} - \dot{\phi}(\phi\dot{H} + \dot{\phi}H)}{H(\phi H)^2}, \\ &= \frac{\dot{\phi}\ddot{\phi}}{\dot{\phi}\phi H^2} - \frac{\dot{\phi}}{\phi H}\left(\frac{\phi\dot{H} + \dot{\phi}H}{\phi H^2}\right), \\ &= \frac{\dot{\phi}}{\phi H}\frac{\ddot{\phi}}{H\dot{\phi}} - \frac{\dot{\phi}}{\phi H}\left(\frac{\dot{H}}{H^2} + \frac{\dot{\phi}}{\phi H}\right), \\ &= u(-\delta) - u(-\epsilon + u), \\ &= -u\delta + u\epsilon - u^2, \\ &= u(\epsilon - \delta - u). \end{aligned} \tag{E.11}$$

Taking the derivative of Ω_k with respect to $N = \ln a$, we obtain

$$\begin{aligned}
\Omega_k' &= \frac{1}{H}(-k)(-2)a^{-3}H^{-3}(\dot{a}H + \dot{H}a)\,, \\
&= \frac{2k}{H}\left(\frac{\dot{a}H}{a^3H^3} + \frac{\dot{H}a}{a^3H^3}\right)\,, \\
&= \frac{2k}{H}\left(\frac{H}{a^2H^2} + \frac{\dot{H}}{H^3a^2}\right)\,, \\
&= \frac{2k}{a^2H^2} + \frac{\dot{H}}{H^2}\left(\frac{2k}{a^2H^2}\right)\,, \\
&= 2\left(\frac{-k}{a^2H^2}\right)\left(-1 - \frac{\dot{H}}{H^2}\right)\,, \\
&= 2\Omega_k\left(-1 - \frac{\dot{H}}{H^2}\right)\,, \\
&= 2\Omega_k(\epsilon - 1)\,.
\end{aligned} \tag{E.12}$$

In order to obtain a closed autonomous system, we need to express ϵ and δ in terms of the dimensionless dynamical variables. Let us consider the (i,j)-component of the Einstein equation, which gives

$$\begin{aligned}
2\dot{H} + 3H^2 + \frac{k}{a^2} &= -8\pi G\left[\frac{\dot{\phi}^2}{2} + \frac{\kappa\dot{\phi}^2}{2}\left(2\dot{H} + 3H^2 + 4H\ddot{\phi}\dot{\phi}^{-1} - \frac{k}{a^2}\right)\right. \\
&\qquad \left. -V(\phi) + p_m + p_\Lambda\right]\,, \\
\frac{2\dot{H}}{3\dot{H}^2} + 1 + \frac{k}{3a^2H^2} &= -\frac{8\pi G\dot{\phi}^2}{6H^2} - \frac{2}{9}(12\pi G\kappa\dot{\phi}^2)\frac{\dot{H}}{H^2} - \frac{1}{3}(12\pi G\kappa\dot{\phi}^2) \\
&\qquad -\frac{4}{9}(12\pi G\kappa\dot{\phi}^2)\frac{\ddot{\phi}}{H\dot{\phi}} + \frac{1}{3}\left(\frac{4\pi G\kappa k\dot{\phi}^2}{a^2H^2}\right) + \frac{8\pi GV(\phi)}{3H^2} \\
&\qquad -w_m\frac{8\pi G\rho_m}{3H^2} - w_\Lambda\frac{8\pi G\rho_\Lambda}{3H^2}\,, \\
\frac{2}{3}(-\epsilon) + 1 + \frac{1}{3}(-\Omega_k) &= -x - \frac{2}{9}(-r)(-\epsilon) - \frac{1}{3}(-r) - \frac{4}{9}(-r)(-\delta) \\
&\qquad +\frac{1}{3}(-s) + y - w_m\omega_m - w_\Lambda\Omega_\Lambda\,, \\
-2\epsilon + 3 - \Omega_k &= -3x - \frac{2}{3}r\epsilon + r - \frac{4}{3}r\delta - s + 3y - 3w_m\omega_m - 3w_\Lambda\Omega_\Lambda\,.
\end{aligned} \tag{E.13}$$

The holographic dark energy satisfies the conservation law as follows

$$\dot{\rho}_\Lambda + 3H\rho_\Lambda(1+w_\Lambda) = 0. \tag{E.14}$$

This expresses the standard continuity equation for holographic dark energy, ensuring the conservation of energy in the cosmological model. According to the holographic dark energy density, the time derivative ρ_Λ with respect to cosmic time t is given by

$$\begin{aligned}
\dot{\rho}_\Lambda &= \left(\frac{3c^2}{8\pi G}\right)\left(2H\dot{H} - 2\frac{k}{a^3}\dot{a}\right), \\
&= \left(\frac{3c^2}{8\pi G}\right)\left(H^2+\frac{k}{a^2}\right)\frac{\left(2H\dot{H} - 2\frac{k}{a^3}\dot{a}\right)}{H^2+\frac{k}{a^2}}, \\
&= 2H\rho_\Lambda\frac{\left(\frac{\dot{H}}{H^2} - \frac{k}{a^2H^2}\right)}{1+\frac{k}{a^2H^2}}, \\
&= 2H\rho_\Lambda\left(\frac{-\epsilon+\Omega_k}{1-\Omega_k}\right).
\end{aligned} \tag{E.15}$$

Substituting into conservation equation,

$$\begin{aligned}
2H\rho_\Lambda\left(\frac{-\epsilon+\Omega_k}{1-\Omega_k}\right) + 3H\rho_\Lambda(1+w_\Lambda) &= 0, \\
2\left(\frac{-\epsilon+\Omega_k}{1-\Omega_k}\right) + 3(1+w_\Lambda) &= 0, \\
w_\Lambda &= -1+\frac{2}{3}\left(\frac{\epsilon-\Omega_k}{1-\Omega_k}\right),
\end{aligned} \tag{E.16}$$

this gives

$$\begin{aligned}
-2\epsilon+3-\Omega_k &= -3x-\frac{2}{3}r\epsilon+r-\frac{4}{3}r\delta-s+3y \\
&\quad -3\left[-1+\frac{2}{3}\left(\frac{\epsilon-\Omega_k}{1-\Omega_k}\right)\right]c^2(1-\Omega_k),
\end{aligned} \tag{E.17}$$

Now let us consider Klein-Gordon equation

$$\ddot{\phi}+3H\dot{\phi} = \frac{-V_{,\phi}+6\kappa H\dot{H}\dot{\phi}-6\kappa H\dot{\phi}\frac{k}{a^2}}{1-3\kappa(H^2+\frac{k}{a^2})}. \tag{E.18}$$

This gives

$$\left[1-3\kappa(H^2+\frac{k}{a^2})\right]\left(\ddot{\phi}+3H\dot{\phi}\right) = -V_{,\phi}+6\kappa H\dot{H}\dot{\phi}-6\kappa H\dot{\phi}\frac{k}{a^2}. \tag{E.19}$$

Then, multiplying the equation by $\frac{8\pi G\dot{\phi}}{6H^3}$, we have

$$\begin{aligned}
&\frac{8\pi G\dot{\phi}^2\ddot{\phi}}{6H^3\dot{\phi}}+3\frac{8\pi G\dot{\phi}^2}{6H^2},-\frac{3\kappa\ddot{\phi}\left(H^2+\frac{k}{a^2}\right)8\pi G\dot{\phi}}{6H^3}-\frac{9\kappa H\dot{\phi}^2\left(H^2+\frac{k}{a^2}\right)8\pi G}{6H^3}\\
&= -\frac{V_{,\phi}8\pi G\dot{\phi}}{6H^3}+\frac{6\kappa H\dot{H}\dot{\phi}(8\pi G\dot{\phi})}{6H^3}-\frac{6\kappa kH\dot{\phi}^2 8\pi G}{6a^2H^3},\\
&x\frac{\ddot{\phi}}{H\dot{\phi}}+3x-3\frac{8\pi G\kappa\dot{\phi}^2\ddot{\phi}}{6H\dot{\phi}}-3\frac{8\pi G\kappa\frac{k}{a^2}\dot{\phi}^2\ddot{\phi}}{6H^3\dot{\phi}}-9\frac{8\pi G\kappa\dot{\phi}^2}{6}-9\frac{8\pi G\kappa\frac{k}{a^2}\dot{\phi}^2}{6H^2}\\
&= -\frac{8\pi GV_{,\phi}\dot{\phi}}{6H^3}+\frac{8\pi G\kappa\dot{\phi}^2\dot{H}}{H^2}-\frac{8\pi G\kappa k\dot{\phi}^2}{a^2H^2},\\
&x\frac{\ddot{\phi}}{H\dot{\phi}}+3x-4\pi G\kappa\dot{\phi}^2\frac{\ddot{\phi}}{H\dot{\phi}}-\frac{4\pi G\kappa k\dot{\phi}^2}{a^2H^2}\frac{\ddot{\phi}}{H\dot{\phi}}-12\pi G\kappa\dot{\phi}^2-\frac{12\pi G\kappa k\dot{\phi}^2}{a^2H^2}\\
&= -\frac{8\pi GV_{,\phi}\dot{\phi}}{6H^3}+\frac{8\pi G\kappa\dot{\phi}^2\dot{H}}{H^2}-\frac{8\pi G\kappa k\dot{\phi}^2}{a^2H^2},\\
&x(-\delta)+3x+\frac{r}{3}(-\delta)+s(-\delta)+r+3s = -\frac{1}{2}ynu-\frac{2r}{3}(-\epsilon)+2s. \qquad \text{(E.20)}
\end{aligned}$$

This gives

$$-x\delta+3x-\frac{r\delta}{3}-s\delta+r+s = -\frac{1}{2}ynu+\frac{2r\epsilon}{3} \qquad \text{(E.21)}$$

Solving equation (E.17) and (E.21), We can express ϵ and δ in terms of dimensionless dynamical as follows

$$\begin{aligned}
\epsilon = &\Big\{-3r\left[c^2(\Omega_k^2-4\Omega_k+3)-2nuy+4x(\Omega_k-3)-3y\Omega_k+3y-\Omega_k^2+4\Omega_k-3\right]\\
&+9x\left[c^2(\Omega_k-3)+3x-3y-\Omega_k+3\right]+r^2(\Omega_k^2-2\Omega_k+9)\Big\}\Big/\\
&\Big\{-18x(c^2-1)+2r^2(3+\Omega_k)+6r\left[c^2(\Omega_k-1)-x-\Omega_k+1\right]\Big\},
\end{aligned} \qquad \text{(E.22)}$$

and

$$\delta = \frac{-18x(3c^2+2r-3)+18ry+4r^2\Omega_k-3nuy(3c^2+r-3)}{-18x(c^2-1)+2r^2(3+\Omega_k)+6r\left[c^2(\Omega_k-1)-x-\Omega_k+1\right]}. \qquad \text{(E.23)}$$

Effective equation of state parameter can be written as

$$w_{\text{eff}}=\frac{p_{\text{tot}}}{\rho_{\text{tot}}}=-1-\frac{2\dot{H}}{3H^2}=-1+\frac{2\epsilon}{3}. \qquad \text{(E.24)}$$

APPENDIX F NMC MODEL: AUTONOMOUS SYSTEM

F.1 Dimensionless dynamical variables

The dimensionless dynamical variables are derived based on the Friedmann equation

$$
\begin{aligned}
H^2+\frac{k}{a^2} &= \frac{8\pi G_{\text{eff}}}{3}\left(\frac{\dot{\phi}^2}{2}+V_0\phi^n+6\xi H\phi\dot{\phi}+\rho_{\text{m}}+\rho_\Lambda\right), \\
1+\frac{k}{a^2H^2} &= \frac{8\pi G_{\text{eff}}}{3H^2}\left(\frac{\dot{\phi}^2}{2}+V_0\phi^n+6\xi H\phi\dot{\phi}+\rho_{\text{m}}+\rho_\Lambda\right), \\
1+\frac{k}{a^2H^2} &= \frac{8\pi G_{\text{eff}}\dot{\phi}^2}{6H^2}+\frac{8\pi G_{\text{eff}}V_0\phi^n}{3H^2}+\frac{8\pi G_{\text{eff}}2\xi\phi\dot{\phi}}{H}+\frac{8\pi G_{\text{eff}}\rho_{\text{m}}}{3H^2} \\
&\quad +\frac{8\pi G_{\text{eff}}\rho_\Lambda}{3H^2}, \\
1 &= \frac{8\pi G_{\text{eff}}\dot{\phi}^2}{6H^2}+\frac{8\pi G_{\text{eff}}V_0\phi^n}{3H^2}+\frac{16\pi G_{\text{eff}}\xi\phi\dot{\phi}}{H}+\frac{8\pi G_{\text{eff}}\rho_{\text{m}}}{3H^2} \\
&\quad +\frac{8\pi G_{\text{eff}}\rho_\Lambda}{3H^2}-\frac{k}{a^2H^2}, \\
1 &= x+y+s+\Omega_{\text{m}}+\Omega_\Lambda+\Omega_k,
\end{aligned}
\tag{F.1}
$$

where

$$
\begin{aligned}
x &= \frac{8\pi G_{\text{eff}}\dot{\phi}^2}{6H^2}, \quad y = \frac{8\pi G_{\text{eff}}V_0\phi^n}{3H^2}, \quad s = \frac{16\pi G_{\text{eff}}\xi\phi\dot{\phi}}{H}, \\
\Omega_{\text{m}} &= \frac{8\pi G_{\text{eff}}\rho_{\text{m}}}{3H^2}, \quad \Omega_\Lambda = \frac{8\pi G_{\text{eff}}\rho_\Lambda}{3H^2}, \quad \Omega_k = -\frac{k}{a^2H^2}.
\end{aligned}
\tag{F.2}
$$

The constraint between the HDE density parameter Ω_Λ and the spatial curvature density parameter Ω_k is derived from the expression for the HDE densitty,

$$
\rho_\Lambda = \frac{3c^2}{8\pi G_{\text{eff}}}\left(H^2+\frac{k}{a^2}\right), \tag{F.3}
$$

leading to the relation

$$
\begin{aligned}
\Omega_\Lambda &= \frac{8\pi G_{\text{eff}}}{3H^2}\left[\frac{3c^2}{8\pi G_{\text{eff}}}\left(H^2+\frac{k}{a^2}\right)\right], \\
&= c^2\left(1+\frac{k}{a^2H^2}\right),
\end{aligned}
$$

which simplifies as

$$\Omega_\Lambda \;=\; c^2\,(1-\Omega_k)\;. \tag{F.4}$$

This show that the dependence of Ω_Λ on the curvature parameter Ω_k. The Friedmann equation (F.1) provides an additional constraint,

$$\Omega_{\rm m} \;=\; 1-x-y-s-\Omega_{\rm m}-c^2\,(1-\Omega_k)-\Omega_k\;, \tag{F.5}$$

which links the matter density parameter $\Omega_{\rm m}$, the curvature parameter Ω_k, and the contributions from the NMDC model variables x, y, and s.

F.2 Autonomous system

To construct the autonomous system, we analyze the dynamics of the dimensionless parameters with respect to the logarithm of the scale factor, $\ln a$. Taking the derivative of y with respect to $N = \ln a$, we obtain

$$\begin{aligned}
y' &= \frac{1}{H}\frac{\mathrm{d}}{\mathrm{d}t}\left(\frac{8\pi G_{\rm eff}V_0\phi^n}{3H^2}\right),\\
&= \frac{1}{H}\frac{\mathrm{d}}{\mathrm{d}t}\left(\frac{8\pi GV_0\phi^n}{3H^2(1-8\pi G\xi\phi^2)}\right),\\
&= \frac{8\pi GV_0}{3H}\left[\frac{H^2(1-8\pi G\xi\phi^2)n\phi^{n-1}\dot\phi-\phi^n 2H\dot H(1-8\pi G\xi\phi^2)-\phi^n H^2(-8\pi G\xi 2\phi\dot\phi)}{H^4(1-8\pi G\xi\phi^2)^2}\right],\\
&= \frac{8\pi G_{\rm eff}V_0\phi^n n\dot\phi}{3H^3\phi}-\frac{8\pi G_{\rm eff}V_0\phi^n}{3H^2}\left[\frac{2\dot H}{H^2}-\frac{8\pi G_{\rm eff}\xi 2\phi\dot\phi}{H}\right],\\
&= ny\frac{\dot\phi}{H\phi}-2y\frac{\dot H}{H^2}+ys\,,\\
&= \frac{12n\xi xy}{s}+2y\epsilon+ys\,,\\
&= sy+\frac{nsy}{2A}+2y\epsilon\,.
\end{aligned} \tag{F.6}$$

In the last equation, we use the relation

$$\begin{aligned}
\frac{x}{s} &= \frac{8\pi G_{\rm eff}\dot\phi^2}{6H^2}\times\frac{H}{16\pi G_{\rm eff}\xi\phi\dot\phi} \;=\; \frac{\dot\phi}{12H\xi\phi},\\
\frac{\dot\phi}{H\phi} &= \frac{12\xi x}{s},
\end{aligned} \tag{F.7}$$

and apply a constraint equation relating x, s, and A as follows

$$\begin{aligned} A &= 8\pi G_{\text{eff}}\xi\phi^2 = \frac{s^2}{24\xi x}, \\ x &= \frac{s^2}{24\xi A}. \end{aligned} \tag{F.8}$$

Taking the derivative of s with respect to $N = \ln a$, we obtain

$$\begin{aligned} s' &= \frac{8\pi G2\xi}{H}\frac{\mathrm{d}}{\mathrm{d}t}\left(\frac{\phi\dot{\phi}}{H(1-8\pi G\xi\phi^2)}\right), \\ &= \frac{8\pi G2\xi}{H}\left\{\frac{H(1-8\pi G\xi\phi^2)(\phi\ddot{\phi}+\dot{\phi}^2)-\phi\dot{\phi}[\dot{H}(1-8\pi G\xi\phi^2)+H(-8\pi G\xi 2\phi\dot{\phi})]}{H^2(1-8\pi G\xi\phi^2)^2}\right\}, \\ &= \frac{8\pi G2\xi(\phi\ddot{\phi}+\dot{\phi}^2)}{H^2(1-8\pi G\xi\phi^2)} - \frac{8\pi G2\xi\phi\dot{\phi}[\dot{H}(1-8\pi G\xi\phi^2)+H(-8\pi G\xi 2\phi\dot{\phi})]}{H^3(1-8\pi G\xi\phi^2)^2}, \\ &= \frac{8\pi G2\xi\phi\ddot{\phi}}{H^2(1-8\pi G\xi\phi^2)} + \frac{8\pi G2\xi\dot{\phi}^2}{H^2(1-8\pi G\xi\phi^2)} \\ &\quad - \frac{8\pi G2\xi\phi\dot{\phi}[\dot{H}(1-8\pi G\xi\phi^2)+H(-8\pi G\xi 2\phi\dot{\phi})]}{H^3(1-8\pi G\xi\phi^2)^2}, \\ &= \frac{16\pi G\xi\phi\ddot{\phi}}{H^2(1-8\pi G\xi\phi^2)} + 12x\xi - s\frac{\dot{H}}{H^2} + s^2, \\ &= \frac{16\pi G\xi\phi[-3H\dot{\phi} - nV_0\frac{\phi^n}{\phi} - 6\xi\phi H^2(2+\frac{\dot{H}}{H^2}+\frac{k}{a^2H^2})]}{H^2(1-8\pi G\xi\phi^2)} + 12x\xi + s\epsilon + s^2, \\ &= -3s - \frac{16\pi G_{\text{eff}}\xi nV_0\phi^n}{H^2} - (12\xi)8\pi G_{\text{eff}}\xi\phi^2(2+\frac{\dot{H}}{H^2}+\frac{k}{a^2H^2}) + 12x\xi + s\epsilon + s^2, \\ &= -3s - 6n\xi y - \frac{s^2}{2x}(2-\epsilon-\Omega_k) + 12x\xi + s\epsilon + s^2, \\ &= s^2 + \frac{s^2}{2A} + s(\epsilon-3) - 6ny\xi + 12A\xi(\epsilon-2+\Omega_k). \end{aligned} \tag{F.9}$$

Taking the derivative of Ω_k with respect to $N = \ln a$, we obtain

$$\begin{aligned} \Omega_k' &= -\frac{k}{H}\frac{\mathrm{d}}{\mathrm{d}t}\left(\frac{1}{a^2H^2}\right), \\ &= \frac{2k}{H}\left(\frac{\dot{H}}{a^2H^3}+\frac{\dot{a}}{a^3H^2}\right), \\ &= \frac{2k}{a^2H^2}\left(\frac{\dot{H}}{H^2}+1\right), \\ &= -2\Omega_k(1-\epsilon). \end{aligned} \tag{F.10}$$

Taking the derivative of A with respect to $N = \ln a$, we obtain

$$\begin{aligned} A' &= \frac{1}{H}\frac{\mathrm{d}}{\mathrm{d}t}\left(8\pi G_{\text{eff}}\xi\phi^2\right), \\ &= \frac{1}{H}\frac{\mathrm{d}}{\mathrm{d}t}\left(\frac{8\pi G\xi\phi^2}{1-8\pi G\xi\phi^2}\right), \\ &= 8\pi G\xi\left[\frac{(1-8\pi G\xi\phi^2)2\phi\dot{\phi}-\phi^2(-8\pi G\xi 2\phi\dot{\phi})}{(1-8\pi G\xi\phi^2)^2}\right], \\ &= \frac{16\pi G\xi\phi\dot{\phi}}{(1-8\pi G\xi\phi^2)}-\frac{8\pi G\xi\phi^2(-16\pi G\xi\phi\dot{\phi})}{(1-8\pi G\xi\phi^2)^2}, \\ &= 16\pi G_{\text{eff}}\xi\phi\dot{\phi}-8\pi G_{\text{eff}}\xi\phi^2(-16\pi G_{\text{eff}}\xi\phi\dot{\phi}), \\ &= s+sA. \end{aligned} \tag{F.11}$$

The variable $\epsilon = -\dot{H}/H^2$ can be expressed in terms of dimensionless variables by considering the second Friedmann equation. This gives

$$\begin{aligned} 2\dot{H}+3H^2+\frac{k}{a^2} &= -8\pi G_{\text{eff}}\Big(\frac{\dot{\phi}^2}{2}-4\xi H\phi\dot{\phi}-2\xi H\phi\ddot{\phi}-2\xi\dot{\phi}^2-\frac{1}{2}V_0\phi^n \\ &\quad +P_{\text{m}}+P_\Lambda\Big), \\ \frac{2\dot{H}}{3H^2}+1+\frac{k}{3a^2H^2} &= -\frac{8\pi G_{\text{eff}}\dot{\phi}^2}{6H^2}+\frac{2}{3}\frac{16\pi G_{\text{eff}}\xi\phi\dot{\phi}}{H}+\frac{16\pi G_{\text{eff}}\xi\phi\ddot{\phi}}{H}+4\xi\frac{8\pi G_{\text{eff}}\dot{\phi}^2}{6H^2} \\ &\quad +\frac{8\pi G_{\text{eff}}V_0\phi^n}{6H^2}-w_{\text{m}}\frac{8\pi G_{\text{eff}}\rho_{\text{m}}}{3H^2}-w_\Lambda\frac{8\pi G_{\text{eff}}\rho_\Lambda}{3H^2}, \\ -\frac{2\epsilon}{3}+1-\frac{\Omega_k}{3} &= -x+y+\frac{2}{3}s+\frac{s^2}{36x\xi}\frac{\ddot{\phi}}{H^2\phi}+4\xi x-w_{\text{m}}\Omega_{\text{m}}-w_\Lambda\Omega_\Lambda . \end{aligned} \tag{F.12}$$

To eliminate the $\ddot{\phi}$ term, we use the Klein-Gordon equation, which is expressed as

$$\begin{aligned} \frac{\ddot{\phi}}{H^2\phi} &= -3\frac{\dot{\phi}}{H\phi}-\frac{n}{2}\frac{V_0\phi^n}{H^2\phi^2}-6\xi\left(2+\frac{\dot{H}}{H^2}+\frac{k}{a^2H^2}\right), \\ &= -\frac{36\xi x}{s}-\frac{72n\xi^2yx}{s^2}-6\xi\left(2+\frac{\dot{H}}{H^2}+\frac{k}{a^2H^2}\right). \end{aligned} \tag{F.13}$$

This allows us to substitute $\ddot{\phi}$ in the relevant equations and proceed without second-order derivatives of the scalar field. Hence, the Friedmann equation (F.12) is expressed as

$$\begin{aligned} -\frac{2\epsilon}{3}+1-\frac{\Omega_k}{3} &= -x+y+\frac{2}{3}s-s-2n\xi y-\frac{s^2}{6x}(2-\epsilon-\Omega_k)+4\xi x-w_{\text{m}}\Omega_{\text{m}} \\ &\quad -w_\Lambda\Omega_\Lambda . \end{aligned} \tag{F.14}$$

According to the continuity equation of holographic dark energy, the equation of state is given by

$$\begin{aligned}
\dot{\rho}_\Lambda + 3H\rho_\Lambda(1+w_\Lambda) &= 0, \\
\frac{3c^2}{8\pi G}\left[(1-8\pi G\xi\phi^2)(2H\dot{H}-\frac{2k\dot{a}}{a^3}) - (8\pi G\xi 2\phi\dot{\phi})(H^2+\frac{k}{a^2})\right] + 3H\rho_\Lambda(1+w_\Lambda) &= 0, \\
\frac{3c^2(1-8\pi G\xi\phi^2)(H^2+\frac{k}{a^2})}{8\pi G}\left[\frac{(2H\dot{H}-2\frac{kH}{a^2})}{(H^2+\frac{k}{a^2})} - \frac{8\pi G\xi 2\phi\dot{\phi}}{1-8\pi G\xi\phi^2}\right] + 3H\rho_\Lambda(1+w_\Lambda) &= 0, \\
\rho_\Lambda H\left[\frac{2(\frac{\dot{H}}{H^2}-\frac{k}{a^2H^2})}{(1+\frac{k}{a^2H^2})} - \frac{8\pi G\xi 2\phi\dot{\phi}}{H(1-8\pi G\xi\phi^2)}\right] + 3H\rho_\Lambda(1+w_\Lambda) &= 0, \\
\left[\frac{2(\frac{\dot{H}}{H^2}+\Omega_k)}{1-\Omega_k} - s\right] + 3(1+w_\Lambda) &= 0.
\end{aligned} \tag{F.15}$$

Hence, the equation of state for holographic vacuum energy is

$$w_\Lambda = -1 + \frac{s}{3} + \frac{2}{3}\left(\frac{\epsilon-\Omega_k}{1-\Omega_k}\right), \tag{F.16}$$

Using constraint equation (F.4), (F.8), (F.16) and dust equation of state parameter $w_{\rm m}=0$, we obtain

$$\begin{aligned}
\epsilon = &\left\{s^2(1-4\xi) + 8As\xi\left[1+c^2\left(1-\Omega_k\right)\right] - 8A\xi\left[-3+3y-24A\xi-6ny\xi\right.\right. \\
&\left.\left.+c^2\left(3-\Omega_k\right)+\Omega_k+12A\xi\Omega_k\right]\right\} \Big/ \left[16A\xi\left(1-c^2+6A\xi\right)\right].
\end{aligned} \tag{F.17}$$

Using the Friedmann equations (6.7), effective equation of state parameter can be expressed as

$$\begin{aligned}
w_{\rm eff} &= \frac{P_{\rm tot}}{\rho_{\rm tot}}, \\
&= \frac{-2\dot{H}-3H^2-\frac{k}{a^2}}{3H^2+\frac{3k}{a^2}}, \\
&= \frac{-1-\frac{2\dot{H}}{3H^2}-\frac{k}{3a^2H^2}}{1+\frac{k}{a^2H^2}}, \\
&= \frac{-1+\frac{2}{3}\epsilon+\frac{\Omega_k}{3}}{1-\Omega_k}.
\end{aligned} \tag{F.18}$$

where $P_{\rm tot}$ and $\rho_{\rm tot}$ are total pressure.